UNIVERSIDADE DA BEIRA INTERIOR

FACULDADE DE CIÊNCIAS DA SAÚDE

Master Degree Thesis in Biomedical Sciences

DEVELOPMENT OF A NEW DRUG DELIVERY SYSTEM FOR FUTURE APPLICATION IN CANCER THERAPY

Vítor Manuel Abreu Gaspar

June 2010

DESENVOLVIMENTO DE UM NOVO SISTEMA DE ENTREGA DE DNA PLASMÍDICO PARA FUTURA APLICAÇÃO NA TERAPIA DO CANCRO

DEVELOPMENT OF A NEW DRUG DELIVERY SYSTEM FOR FUTURE APPLICATION IN CANCER THERAPY

Supervisors:

Professor Dr. Ilídio Joaquim Sobreira Correia

Professor Dr. Fani Pereira de Sousa

The content of the present work is of the exclusive responsibility of the author:

_____

Vítor Manuel Abreu Gaspar

“Failure is the preamble to success. Most first efforts don’t work. If you persist, you’ll eventually figure it out”

-***Thomas Fogarty***

Acknowledgments

First and foremost, I would like to thank my supervisors Professor Fani de Sousa and Professor Ilídio Correia for their invaluable support during my master studies, for their continuous guidance and help, for the immense expertise and constructive discussions that were crucial for the success of this work. It has been a privilege.

I would also like to acknowledge the Dean of the Universidade da Beira Interior Professor João António de Sampaio Rodrigues Queiroz for making possible the development of this investigation project. For that I am most grateful.

I also thank Eng. Ana Paula from the Optics department of Universidade da Beira Interior for all her help in getting the scanning electron microscopy images of the nanoparticles.

Moreover, I would like to express my gratitude to all the persons involved in the Centro de Investigação em Ciências da Saúde of University of Beira Interior with a special acknowledge to Dr. Angela Sousa and Dr. Ana Martinho and the persons in the Biotechnology research group for all their help.

I thank my family for all their love, support and care in the most difficult times during my academic formation.

Finally, a very special thanks to my girlfriend for all her love and support throughout all the days of intensive work. For her advices and most specially for supporting our dreams.

RESUMO

Durante as últimas décadas a terapia génica tornou-se uma alternativa promissora no tratamento de muitas doenças incuráveis, como é o caso cancro. Esta doença extremamente complexa possui características que fazem com que os tratamentos geralmente administrados sejam ineficazes. O trabalho de investigação apresentado nesta tese pretende tirar partido das novas abordagens terapêuticas baseadas no DNA plasmídico e em nanossistemas. A conjugação destas tecnologias pode conter a chave para o desenvolvimento de pacientes com cancro. Tendo por base este pressuposto, um vector de expressão plasmídico que codifica para uma proteína supressora de tumores, a p53 foi produzido em organismos recombinantes. Subsequentemente, as diferentes isoformas do plasmídeo foram isoladas e a isoforma superenrolada, a que possui actividade biológica e com melhor eficiência de transfecção, foi purificada por cromatografia de afinidade. Após esta purificação e recolha promoveu-se o desenvolvimento de novos nanossistemas que fossem capazes de entregar o DNA exógeno nas células cancerígenas. Os nanossistemas produzidos com quitosano apresentam gamas de tamanho pequenas e propriedades adequadas para a encapsulação do DNA plasmídico. Adicionalmente, a transfecção de células eucarióticas neoplásicas, revelou a potencialidade da aplicação destes nanossistemas como novos veículos de transporte de vectores que expressem a p53 até aos tumores.

Palavras chave: cancro, terapia génica, DNA plasmídico, nanossistemas

ABSTRACT

During the past few decades gene therapy has become a promising alternative for the treatment of many incurable diseases such as cancer. This extremely complex disease possesses characteristics that make most of the generally used treatments rather ineffective. The research work presented in this thesis attempts to take advantage of novel non-viral gene therapeutic approaches based on plasmidic DNA and nanoparticulated systems that might provide the foundation for the development of a novel therapeutic treatment from the production to a real application in the everyday life of cancer patients. Hence the production of an expression vector that encodes for a tumor suppressor, p53 was promoted in recombinant organisms. Subsequently the different plasmid DNA isoforms were isolated and the supercoiled isoform, the one biologically active and with enhanced transfection efficiency was purified by affinity chromatography. Following this purification and recovery the development of novel nanoparticle systems that could deliver the exogenous DNA into the malignant cells was promoted. Nanoparticulated systems produced with chitosan demonstrated small size ranges and suitable properties for the encapsulation of plasmidic DNA. Additionally, transfection of eukaryotic neoplastic cells revealed the suitability of the nanocarrier as a novel delivery system of p53 expression vectors to cancer.

Keywords: cancer, gene therapy, plasmid DNA, nanoparticle, p53

LIST OF ABREVIATURES

AEX - Anion exchange chromatography

Arg-G - Arginine-guanine

CS - Chitosan

CSCs - Cancer stem cells

CS-TPP – chitosan-TPP blank nanospheres

DD - Deacetilation degree

DMF - Dimethyl- formamide

dsDNA - Double strand DNA

***E.coli* -** *Escherichia coli*

EE - Encapsulation efficiency

EMEA - European Agency for the Evaluation of Medical Products

EPR - Enhanced permeability retention

FBS - Fetal Bovine serum

FDA - Food and Drug Administration

FITC - Fluorescein isothiociantate isomer I

H-bond - Hydrogen bond

HIC - Hydrophobic interaction chromatography

LC - Loading capacity

pDNA - plasmid DNA

PEG - Polyethilene glycol

PEI - Polyethylenimine

PLGA - poly (lactid-co-glycolic acid)

RES - Reticuloendothelial system

Sc - Supercoiled

SEC - Size exclusion chromatography

TPP - Pentassodium tripolyphosphate

XRD - X-ray diffraction

Wt-p53 – Wild type p53

LIST OF FIGURES

Section I - Introduction *Page*

Chatper I

Figure 1.Cancer evolutive model. **6**
Figure 2. Tumor progression based on the CSC model. **7**
Figure 3. Hallmarks of cancer. **9**
Figure 4. Apoptotic pathways. **10**
Figure 5. Structure of the p53 protein and three dimensional structure of the DNA binding domain. **11**
Figure 6. A multitude of stress signals can activate the tumor suppressor p53. ..... **12**
Figure 7. p53 mediation of tumor suppression. **13**

Chatper II

Figure 8. Stages from production to application of pDNA in gene therapy based treatments. **17**
Figure 9. Interaction between the affinity ligand and the target biomolecules.. ..... **19**
Figure 10. Nanocarrier targeting to tumors cells. **21**
Figure 11. Different barriers impacting gene delivery. **22**
Figure 12. DNA unpacking. **23**
Figure 13. Types of nanocarrier systems for gene delivery. **25**
Figure. 14 Chitosan chemical structure. **26**
Figure 15. Different chitosan DNA nanoparticles. **26**

Section II – Materials and Methods

Figure 1. Plasmid pcDNA3-FLAG-p53 backbone. **30**
Figure 2. Schematics of the amino-acid based matrix. **31**
Figure 3. 1DUVS *N*-acetyl-D-glucosamine spectra and reference curve. **34**

Section III – Results and Discussion

Figure 1. Growth profile of *E.coli* DH5α harboring the plasmid pcDNA3-FLAG-p53. ..... **40**
Figure 2. Electrophoresis of *E.coli* cell lisates. **41**
Figure 3. Amino acid base pair interactions. **44**
Figure 4. Chromatographic profile showing the purification of different plasmid isoforms by arginine affinity chromatography. **45**
Figure 5. Geometric dynamic fluctuations of the plasmid DNA supercoiling. **46**
Figure 6. Chromatogram depicting the elution of sc pDNA from the arginine affinity support. **47**

Figure 7. Effect of temperature on the retention of the different plasmid isoforms in arginine. **48**
Figure. 8. Phase diagram of nanoparticle formation for commercial chitosan. **50**
Figure 9. Morphology of the nanoparticles obtained from commercial chitosan flakes visualized by SEM. **52**
Figure 10. Morphology of the nanoparticles obtained from deacetilated chitosan visualized by SEM. **53**
Figure 11. Morphology of the nanoparticles obtained from acetilated chitosan visualized by SEM. **54**
Figure 12. XRD spectra of different chitosan samples. **56**
Figure 13. Nanocapsules obtained from commercial chitosan flakes visualized by scanning SEM. **58**
Figure. 14. Nanocapsules synthesized from deacetilated chitosan visualized by SEM. **58**
Figure. 15. Nanocapsules synthesized from acetilated chitosan visualized by SEM. **59**
Figure 16. Agarose gel electrophoresis of the nanocapsules following incubation with DNAse I. **62**
Figure 17. Agarose gel electrophoresis of the nanocapsule protection of pDNA following incubation with serum-supplemented Ham's F12K. **63**
Figure 18. Agarose gel electrophoresis of the nanocapsule protection of pDNA following incubation with lyzosyme for 1h and 3h. **64**
Figure 19. Agarose gel electrophoresis of the nanocapsule protection of pDNA following incubation with lyzosyme for 12h and 24h. **64**
Figure 20. Immunofluorescence of A549 Lipofectamine^{2000} – pDNA complexes transfected cells. **65**
Figure 21. Immunofluorescence of A549 nanocapsule transfected cells. **66**

LIST OF TABLES

Section I - Introduction *Page*

Chatper I

Table 1. Normal stem cell properties and cancer stem cells. **6**

Chatper II

Table 2. Summary of the most important formulation parameters in the design of nanoparticulated systems based on chitosan. **27**

Section III – Results and Discussion

Table 1. Summary of the retention/elution profiles for the different plasmid isoforms. **42**

Table 2. Nanosphere size distribution. **55**

Table 3 Degree of Deacetilation of the different chitosan samples as measured by 1DUVS. **56**

Table 4. Comparison between the different particle sizes obtained for variable formulations of CS-TPP-pDNA nanocapsules. **59**

Table 5. Encapsulation efficiency of the nanocapsules obtained from different chitosan materials. **60**

Table 6. Loading capacity of the nanocapsules obtained from different chitosan materials. **61**

Table of Contents

	Page
Acknowledgments	**i**
Abstract	**ii**
Resumo	**iii**
List of Figures	**iv**
List of Tables	**v**
List of Abbreviations	**vi**
Section I	
Introduction	**1**
Chapter I – Cancer and the tumor suppressor p53	**4**
1.1. Cancer - Development models and hallmarks	**5**
1.2. The Tumor Supressor p53	**11**
Chapter II – Non-viral cancer gene therapy	**15**
2.1. Plasmid DNA expression vectors for non-viral gene therapy	**17**
2.2. Amino acid-DNA affinity chromatography for sc pDNA purification	**18**
2.3. Non-viral nanocarrier mediated gene delivery	**20**
2.4. Non-viral polymeric nanoparticles for gene delivery	**24**
Section II	
Materials and Methods	**29**
2.1. Materials	**30**
2.1.1. Plasmid DNA	**30**
2.1.2. Chitosan	**30**
2.2. Methods	**31**
2.2.1. Bacterial growth conditions and plasmid recovery	**31**
2.2.2. Affinity chromatography	**31**
2.2.3. Agarose gel electrophoresis	**32**
2.2.4. Synthesis of deacetilated and reacetilated chitosan	**32**
2.2.5. First derivative ultraviolet spectrophotometry	**33**
2.2.6. X-ray diffraction (XRD)	**35**
2.2.7. Production of chitosan nanoparticles	**35**
2.2.8. Particle morphology	**35**
2.2.9. Encapsulation and loading capacity of pDNA	**36**
2.2.10. Protection and release of encapsulated pDNA	**36**
2.2.11. FITC fluorescent labeling of pDNA	**37**
2.2.12. Cell culture and *in vitro* transfection	**37**
2.2.13. Immunofluorescence	**38**
2.2.14. Statistical analysis	**38**
Section III	
Results and discussion	**29**
3.1. Plasmid amplification in recombinant *E.coli*	**40**

3.2. Purification of sc pDNA by arginine – agarose affinity chromatography	**42**
3.3. Formulation of chitosan-TPP nanoparticles	**49**
3.4. Morphology and characterization of CS-TPP blank nanoparticles	**52**
3.5. Synthesis of pDNA loaded nanoparticles - Nanocapsules	**57**
3.6. Nanocapsule encapsulation efficiency and loading capacity	**60**
3.7. Protection and *in vitro* release of pDNA	**62**
3.8. *In vitro* transfection	**65**
Section IV	
Conclusions and future perspectives	**68**
Section V	
Bibliography	**71**
Section VI	
Appendices	**76**

SECTION I

INTRODUCTION

Cancer is a major health issue of our time, it is estimated that approximately nine million new cases appear each year (Pelengaris and Khan, 2006) and the World Health Organization predicts that by 2030 twelve million of all deaths worldwide will occur due to cancer (Bode and Dong, 2009). The invasive and aggressive profile that characterizes this illness renders most of the conventional treatments such as surgery and radiotherapy ineffective in many cases. Thereof, the development of new cancer therapeutic strategies is an urgent requirement.

Gene therapy arises as one of the most powerful and promising alternatives. In fact the possibility of treating cancer by introducing genetic information that can inhibit or eradicate cancer has led to an ever growing interest in the scientific community (Cao et al., 2009).

The revolutionary concept of gene therapy appeared in 1963, when Joshua Lederberg commented the future of medicine, hypothesizing that the ultimate application of molecular biology would be to direct the control of nucleotide sequences in human chromosomes, coupled with selection and integration of the desired genes (Lederberg, 1963). In 1967, Edward Tatum expanded the idea by being optimistic about the possibility of a therapy based on the introduction of new genes into defective cells (Tatum, 1967). In fact, in 1980 Tatum and Lederberg's idea was devised when Anderson accomplished the first transfer of two functional genes into mammalian cells (Anderson et al., 1980).

Later in 1991 and with the development of viral gene delivery systems, gene therapy for cancer became a reality and the first clinical trial using a retroviral carrier for the treatment of cancer was carried out (Huber et al., 1991). Despite that, few years later the inherent risk of using these delivery systems was highlighted when it culminated with the death of one patient (Christof von Kalle et al., 2003).

Meanwhile non-viral cancer gene therapy has surpassed viral based therapies due to its improved safety features (Glover et al., 2005). Plasmid DNA (pDNA) expression vectors are essential to non-viral gene therapy and thus there is an increasing demand for the production of highly stable and purified pDNA (Gill et al., 2009).

Nowadays with the recent advent of nanomedicine and the continuous development of biotechnology new cancer gene therapy approaches are being developed in order to enhance production, purification and especially delivery, revolutionizing the way that genetic material is transported towards and into the cell (Qiao et al., 2010). Nanocarrier systems possess unique physical and biological characteristics that renders them ideal vehicles for gene delivery (Cao et al., 2009). Recently, Chen et al., 2010 demonstrated that nanoparticles conjugated with tumor targeting sequences that can successfully reach cancer cells and deliver gene silencing material that can inhibit tumor growth

(Chen et al., 2010). In addition to these findings the use of tumor suppressor genes that induce cell cycle arrest or trigger apoptosis of malignant cells is also becoming a very attractive alternative and recently raised new prospects in the field of cancer gene therapy (Tu et al., 2010).

Taking this into account this MsC work attempts to integrate several key factors of the development of a non-viral delivery system from production of pDNA to its application. The specific aims of this work include:

- Biosynthesis in recombinant organisms of a plasmid expression vector containing a sequence of the tumor suppressor p53;
- Implementation of an affinity purification strategy based on a chromatographic support with immobilized arginine amino acids;
- Development and characterization of nanoparticulated systems based on a biocompatible polymer;
- Evaluation of the carrier for the encapsulation potential, protection and release of biomolecules;
- Evaluate the feasibility of the developed nanocarrier systems as vehicles for gene delivery into malignant cells.

The hypotheses used in this work comprise:

- *Escherichia coli* recombinant organisms are adequate for production of plasmid expression vectors;
- Affinity chromatography based on immobilized amino acids is a technique that can purify the plasmid biologically active isoform;
- Biocompatible biopolymers with suitable properties can be used for the development of nanoparticulated systems that can incorporate and release biomolecules like pDNA;
- Nanoparticles based on chitosan can transpose the multitude of biological barriers and enter into the intracellular compartment of neoplastic cells.

Hence the work described in this thesis may be divided in three main stages: i.) The first comprises the production of the vector and the implementation of an affinity purification strategy with immobilized arginine amino acids to purify the supercoiled pDNA isoform (sc); ii.) The second stage consists of the development and characterization of the nanocarrier system, iii.) The final research topic integrates the former stages in order to promote the delivery of p53 coding sc pDNA to carcinogenic eukaryotic cells *in vitro*.

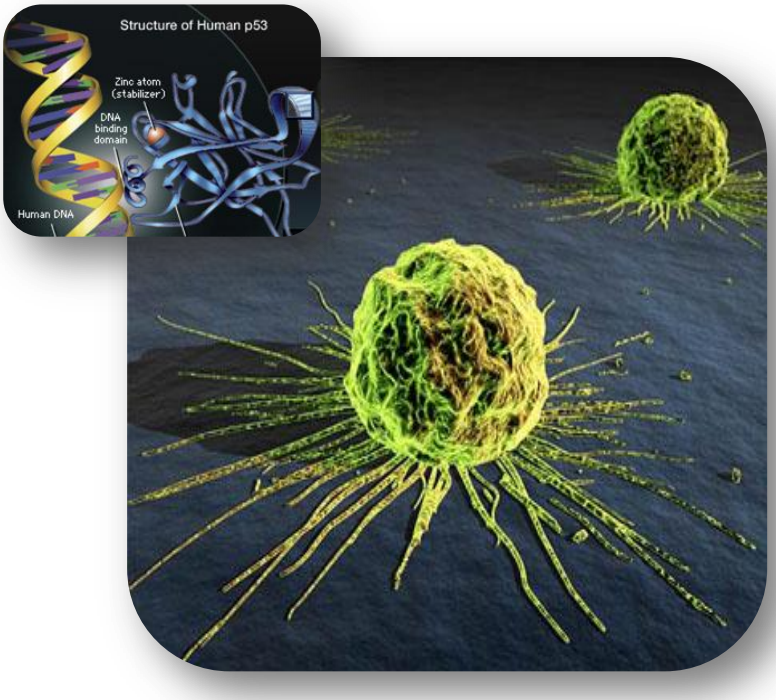

CHAPTER I

CANCER AND THE TUMOR SUPRESSOR P53

1.1. Cancer - Development Models and Hallmarks

Cancer is a complex genetic disease that arises as a result of a multistep mutagenic process that disrupts the normal cellular regulatory pathways (Hahn and Weinberg, 2002). Tumor development is associated with different cellular stresses promoted by the surrounding environment (radiation and chemicals), lifestyle behaviors (diet and smoking), or by inherited predispositions (Pelengaris and Khan, 2006). These different stress inducing factors are responsible for random genetic and epigenetic mutations in multiple genes that have highly diverse biochemical functions (Weinstein and Joe, 2006). The aforementioned mutations are the driving force of cancer and their accumulation can bring forth the malignant phenotype (Evan and Vousden, 2001).

The tumorigenic process is characterized by a profound cellular heterogeneity promoted not only by the ongoing mutagenesis but also by the aberrant differentiation of cancer cells (Reya et al., 2001). In an attempt to describe and account for these heterogeneous features and the tumor proliferation capacity of neoplastic cells two models have been proposed: the clonal evolution model and the cancer stem cell model (Visvader and Lindeman, 2008).

The clonal evolution model hypothesizes that cancer development can be characterized as a clonal disease in which proliferation occurs according to an evolutionary perspective in which natural selection acts upon the various somatic clones, favoring the expansion of those that carry gainful characteristics (Evan and Vousden, 2001). According to this model all of the cells have similar tumorigenic capacity and the development of a tumor begins with a single somatic cell in which an initial mutation leads to cell division and cell differentiation, culminating with the production of a genetically homogeneous clone. At this stage and although altered at the DNA level the cell is phenotypically normal (Macdonald et al., 2004).

The subsequent mutations that will occur in this neoplastic clone will be those responsible to give rise to an heterogeneous population of genetically and epigenetically unstable cells, the neoplasm, where natural selection takes place, as presented in figure 1 (Merlo et al., 2006). The selection process will benefit the clones that possess advantageous characteristics such as those that enable proliferation and autonomous survival, tissue invasion and metastasis (Stratton et al., 2009).

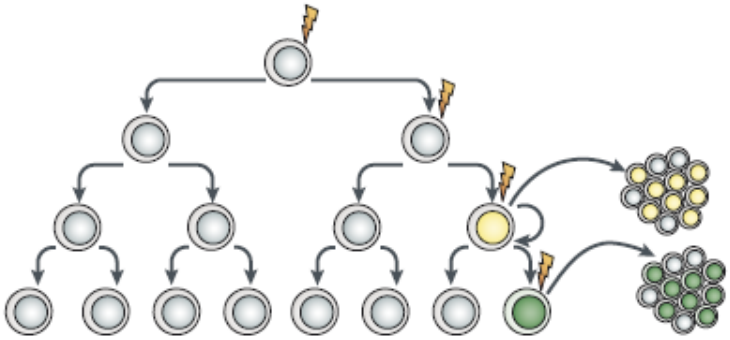

Figure 1.Cancer evolutive model. A cell that suffers a genetic mutation produces clones that in time are selected due to their growth advantages. All of the cells that make up the dominant population have similar potential to generate tumor growth (Adapted from Visvader and Linderman, 2008).

Contrariwise to the evolutionary model in which any cell can trigger tumorigenesis, the cancer stem-cell model suggests that only some cells are tumorigenic and that there is evidence of a hierarchical organization within a solid tumor (Reya et al., 2001). This hierarchy is governed by a population of stem-like cells (Visvader and Lindeman, 2008). Stem cells are unique cells that possess special characteristics like the capacity for self-renewal and potential for differentiation that distinguishes them from normal tissue cells (Rothenberg and Clarke, 2009). Cancer stem cells (CSCs) are phenotypically and functionally simillar to tissue stem cells, sharing a common set of properties with them, although with markedly differences (Table 1).

Table 1. Normal stem cell properties and cancer stem cells (Adapted from (Jordan et al., 2006, Mendelsohn et al., 2008)).

Normal Somatic Stem Cells	Cancer Stem Cells
Extensive but limited self-renewal capacity	Extensive and indefinite self-renewal capacity
Organogenic capacity	Tumorigenic capacity
Capacity to generate differentiated lineages with limited proliferative potential, often phenotypically diverse	Capacity to generate abnormal lineages with limited proliferative potential, often phenotypically diverse
Highly regulated self-renewal and differentiation	Highly deregulated self-renewal and differentiation
Rare in normal adult tissues	Infrequent or rare within tumors
Quiescent most of the time	Less mitotically active than other cancer cells

CSCs may arise from the oncogenic transformation of normal stem cells (Figure 2), a process closely related with their role in tissue homeostasis (Jordan et al., 2006). Stem cells are responsible for self-renewal of the distinctly differentiated cells that compose each tissue, however, the process of regeneration involves proliferation and

differentiation, the two stages where stem cells become more prone to malignant transformations (Rothenberg and Clarke, 2009).

In fact the same pathways that coordinate renewal and proliferation are likely to cause neoplasia when deregulated, among these the Wnt, Notch and Hedgehog pathways are the ones mostly responsible for CSCs generation and hyperproliferation (Visvader and Lindeman, 2008).

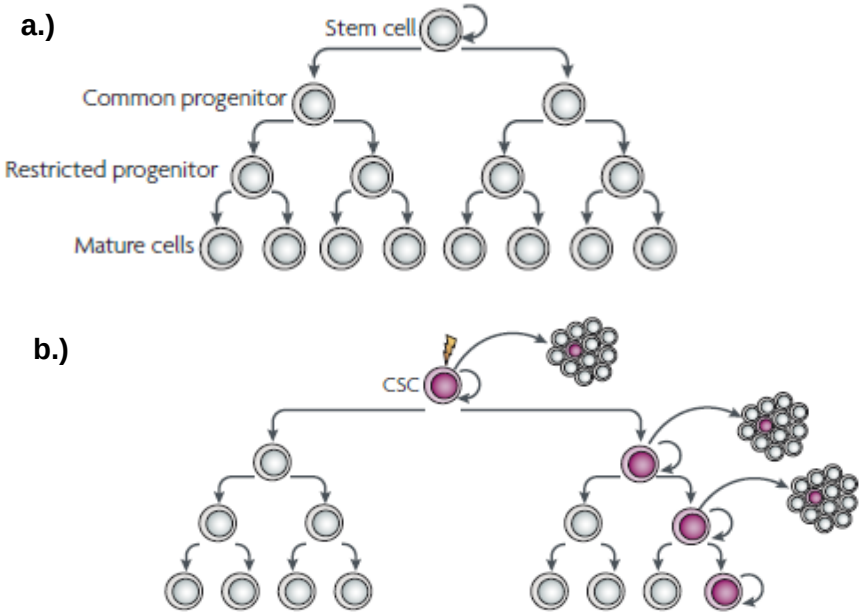

Figure 2. Tumor progression based on the CSC model. a.) A normal cellular hierarchy governed by stem cells generates a more restricted progeny that ultimately originates the heterogeneous mature cell types that constitute a particular tissue. b.) Cancer stem cell model where only a CSC due to its extensive proliferative capacity has the ability of triggering and sustaining tumorigenesis (Adapted from Visvader and Linderman, 2008).

It becomes therefore clear that CSCs alone can drive the continued expansion of the malignant cell population due to their substantial replicative capacity. Furthermore, to support this idea several evidences of the existence of these exceptionally tumorigenic cells have been identified in different types of malignancies, like acute myelogeneous leukemia, breast and pancreatic carcinomas, among others (Jordan et al., 2006, Visvader and Lindeman, 2008). Albeit, it is important to point out that CSCs can also arise from downstream progenitors or differentiated cells. Indeed, the existence of mutational events may confer a deregulated ability of self-renewal and other stem-like properties to these cell types, thus giving rise to CSCs (Mendelsohn et al., 2008). Even though the latter is true, it is more likely that CSCs are predominantly formed by stem cells due to their mitotic potential and preemptive activated self-renewal pathways (Mendelsohn et al., 2008).

In a global perspective and despite that CSC model is different from the evolutionary one they share mutual resemblances since the existence of malignant cells and genomic instability are marked characteristics of tumors (Rothenberg and Clarke, 2009). As a matter of fact CSCs themselves can undergo clonal evolution and the resulting progeny may be even more dominant and aggressive (Visvader and Lindeman, 2008).

Regardless of the model that best describes tumor development, to achieve a malignant phenotype a cell must, at some time, undergo genetic changes that are responsible for the deregulation of the normal cellular regulatory pathways (Hanahan and Weinberg, 2000). The majority of the genes that are mutated in cancer are classified as oncogenes and as tumor suppressor genes (Vogelstein and Kinzler, 2004).

Oncogenes are mutated versions of normal cellular genes (proto-oncogenes) being continuously active, or are active under the conditions where the wild type genes are dormant (Vogelstein and Kinzler, 2004). Oncogenes are responsible for accelerating cell division, growth and they are likely to play a key role in the loss of differentiation and cell motility, contributing to neoplasia (Pelengaris and Khan, 2006). On the contrary tumor suppressor genes act as guardians against DNA mutations. Tumor suppressor genes commonly supervise critical checkpoints including the mitotic cycle, transcription, differentiation and apoptosis (Pelengaris and Khan, 2006, Mendelsohn et al., 2008). Moreover, tumor suppressors also act as powerful negative regulators of oncogenes and their deactivation creates instability in proliferation and cell death, thus favoring tumorigenesis (Vogelstein and Kinzler, 2004). Furthermore and despite the controversy that surrounds the number of genetic changes required to generate malignancies (Hahn and Weinberg, 2002) point mutations in cancer genomes also need to be accounted because they foster potential to drive tumorigenesis and are responsible for an increase in cancer heterogeneity with more than 100 000 point mutations reported in some cancers (Stratton et al., 2009).

Comprehensibly the complexity of these modifications has profound impact in cancer treatment approaches. Therefore knowing the compilation of the common characteristics of cancer cells is mandatory for the development of new therapeutic approaches. At the time that a malignant transformation takes place, cancer cells collectively share a set of hallmarks, and although these are not the ones responsible for initiating tumorigenesis they are characteristic of innumerous tumor types (Figure 3) (Luo et al., 2009).

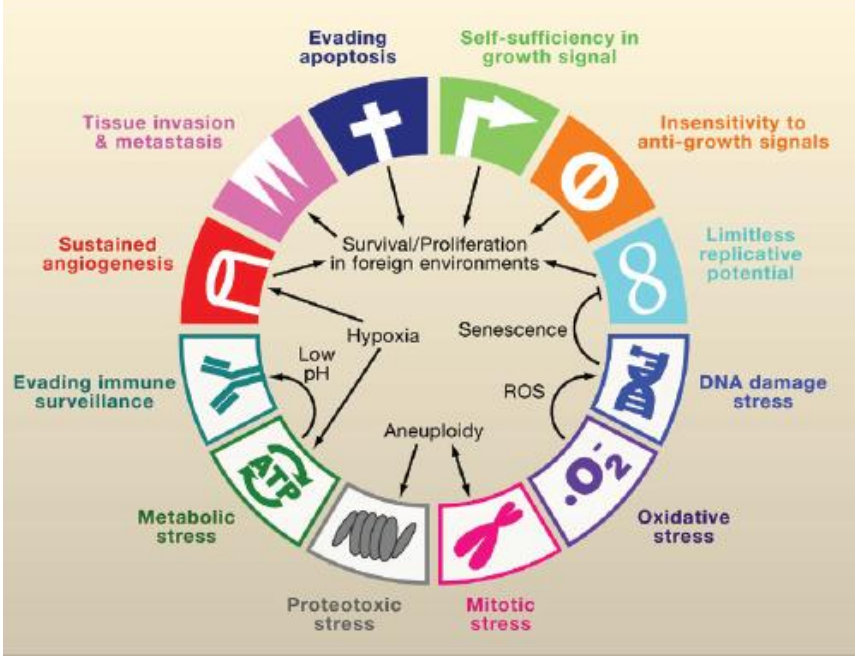

Figure 3. Hallmarks of cancer. Including the stress phenotypes of cancer: metabolic stress, proteo-toxic stress, mitotic stress, oxidative stress and DNA damage stress. Interrelationships between the different hallmarks promote the tumorigenic state (Adapted from Luo et al., 2009).

One of the major goals of anticancer therapy is to counteract the hallmarks depicted in figure 3, exploiting their vulnerabilities (Luo et al., 2009). Among all the phenotypic traits, the evasion of apoptosis is one of the most noteworthy, since it assures the continuous survival of the malignant cells in circumstances that otherwise would be deleterious (Evan and Vousden, 2001).

Apoptosis or programmed cell death plays a central role in the intricate balance that exists between cell survival, differentiation and death. This process is responsible for the elimination of unnecessary or dangerous cells (Melino and Vaux, 2010). The two major pathways that trigger apoptosis are the extrinsic or death-receptor mediated pathway and the intrinsic or mitochondrial mediated pathway (Melino and Vaux, 2010). The extrinsic pathway is activated whenever an extracellular signal is received by cell-surface death receptors (TNF superfamily), that in turn communicate with downstream signaling cascades. Whereas the intrinsic pathway is incited by different stresses like DNA damage, inducing the release of pro-death factors from the mitochondria (Zhivotovsky and Orrenius, 2003). Despite the pathway that is activated, both of them rely on caspases that are in charge of the effective execution of the apoptotic program (Figure 4). Caspases are proteases involved in the signaling cascade exercising their activity by cleaving several intracellular substrates that ultimately lead to cell death (Evan and Vousden, 2001).

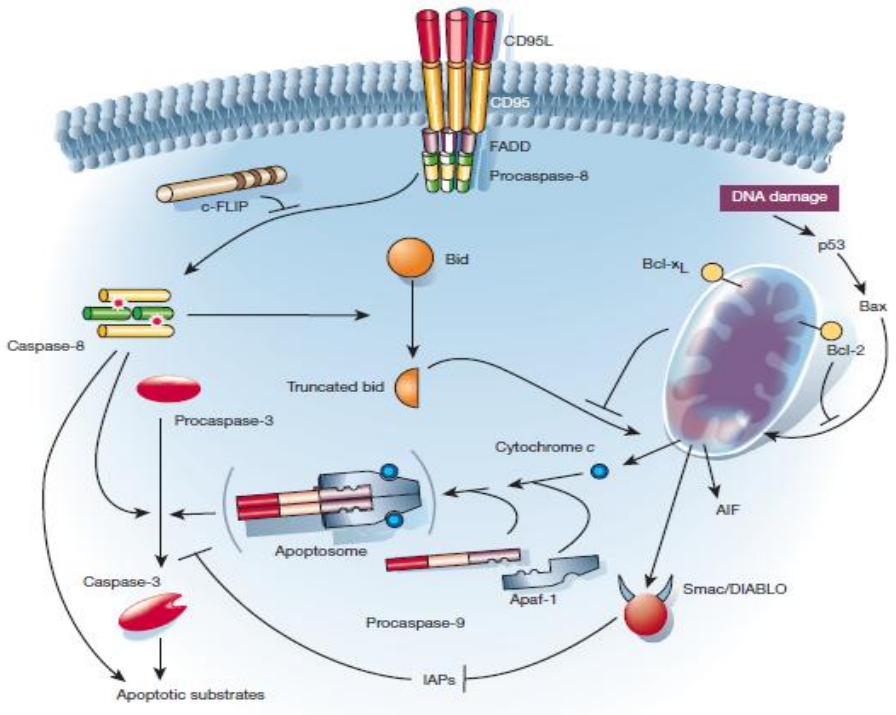

Figure 4. Apoptotic pathways. The extrinsic pathway (left) is triggered by the death receptor superfamily resulting in the activation of caspases-8. The intrinsic pathway (right) is activated in response to intracellular cues like DNA damage. In the mitochondria the pro-apoptotic members of the family Bcl-2 (including Bax, Bad, Bid and Bim) compete with other anti-apoptotic Bcl-2 family members, if the pro-apoptotic cues prevail the apoptossome is formed and apoptosis continues. The extrinsic and intrinsic pathways converge at the level of caspase-3 activation. Downstream of this caspases the apoptotic program continues and results in the dismantling and removal of the cell (Adapted from Hengartner, 2000).

It is clear that apoptosis requires the combination of a multitude of cellular programs and that this process acts as a potent control mechanism. Cancer cells acquire their outstanding resistance to programmed cell death by modification of these effector pathways (Melino and Vaux, 2010). In fact malignant cells are able to rewire several key points in the apoptotic cascade and thus sustain their survival. Identified mutations in the signaling pathways of malignant cells, include deficiencies in central executioners like caspase-8, accomplished through deletions and point mutations, inactivating the caspase cascade (Zhivotovsky and Orrenius, 2003). Additional dysfunctions in the mitochondrial pathway also play a significant role in the evasion from apoptosis and among those, described the DNA damage response mediated by the protein p53 is the most critical one. The loss of function of this tumor suppressor promotes cancer proliferation (Olivier et al., 2008).

Taking into account that the absence of apoptosis is a key point in the origin of tumor development it is evident that there is an immense potential in its exploitation. Actually most of the therapeutic intervention in cancer aims to stimulate or restore programmed cell death and the creation of novel and effective therapeutics is becoming a reality (Luo et al., 2009). In the midst of these emerging approaches gene therapy for cancer is clearly one of the most promising, and the use expression vectors that encode genes that restart apoptosis (for instance the tumor suppressor p53) is becoming an ever growing reality (Lane et al., 2010, Tu et al., 2010).

1.2. The Tumor Suppressor p53

One of the most common dysfunctions found in cancer is the inactivation of the tumor suppressor p53, in fact, it is estimated that the p53 gene is mutated in nearly 50% of all known cancers (Melino and Vaux, 2010). P53 is a unique transcription factor and it is generally considered as the “guardian of the genome” an alias that reflects its most important feature, the ability to efficiently inhibit cell proliferation (Bouchet et al., 2006).

The human p53, or TP53 is a nuclear phosphoprotein composed of 393 amino acids and 5 structural and functional domains (Bouchet et al., 2006) (Figure 5). Amidst those, the DNA binding domain is the most important not only due to the fact that it is the most mutated region in cancer pathologies but also because it is important to trigger apoptosis (Zambetti, 2005, Bouchet et al., 2006)

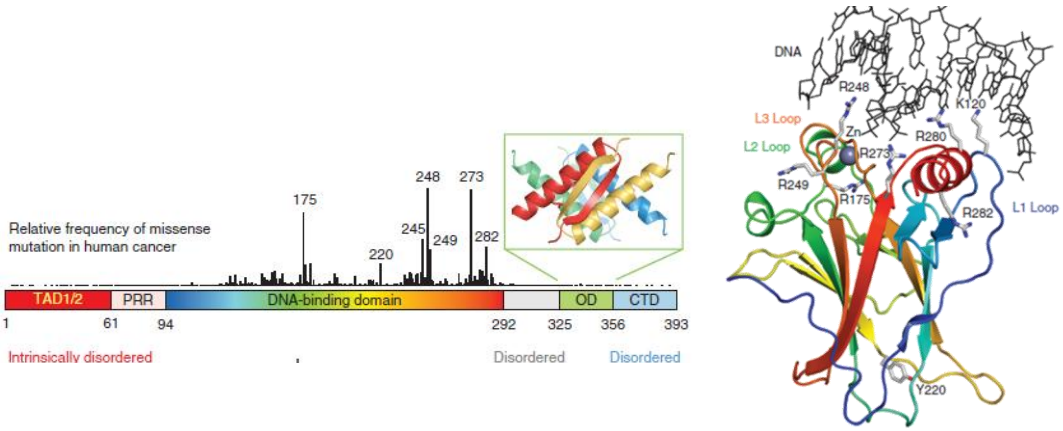

Figure 5. Structure of the p53 protein and three dimensional structure of the DNA binding domain. The p53 protein can be divided in five functional domains, the transactivation domain, a proline rich region, the DNA-binding domain, the oligomerization domain and the regulatory domain. (Adapted from Joerger and Fersht, 2010).

The success of the tumor suppression mediated by p53 relies on the proper and consistent activation of the p53 pathways (Vousden and Prives, 2009). The activation of this tumor suppressor protein is triggered by a wide variety of stress events that include genotoxic stress (DNA damage), oncogene activation, loss of normal cell adhesion contacts and hypoxia (Vousden and Prives, 2009). Although this activation depends on various factors such as the intensity of the cellular stress, cell type and microenvironment (Melino and Vaux, 2010), hence it is not surprising that the loss of p53 function has such a profound influence on cancer development (Figure 6).

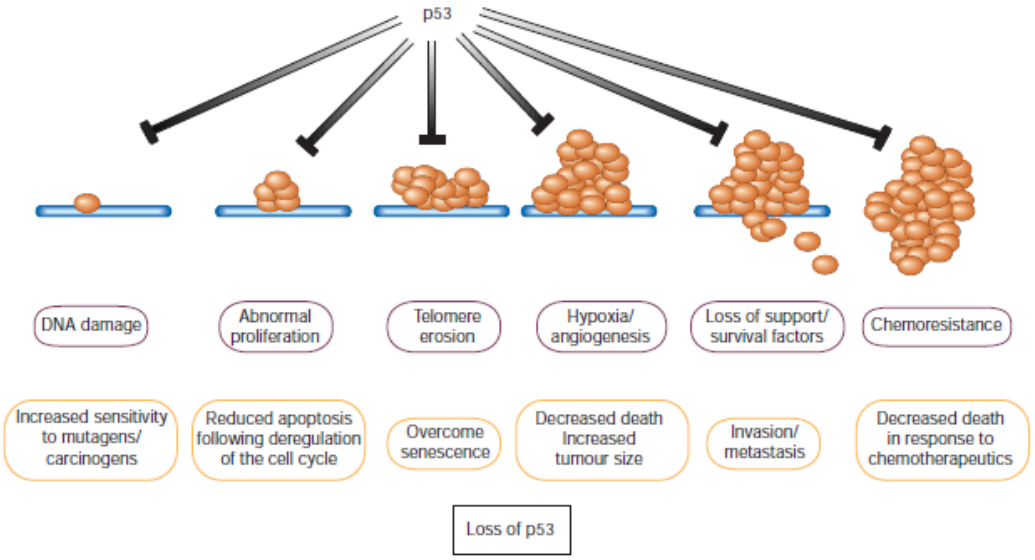

Figure 6. A multitude of stress signals can activate the tumor suppressor p53. The loss of function of this protein has a considerable influence in cancer development since it endows the capacity of cell survival under deleterious conditions, promotes tumor progression and metastasis (Adapted from Evan and Vousden, 2001).

Indeed the failure to activate the p53 dependent cascade in response to the stress signals that arise during the early stages of cancer development may be enough to consent the formation of pre-neoplastic lesions (Evan and Vousden, 2001). Additionally there is also the idea that the loss of p53 function may preemptively endow immediate selective disadvantages upon the modified cell in respect to normal ones, that if not overcomed may trigger proliferation (Evan and Vousden, 2001).

Despite these factors, once activated the tumor suppressor p53 can set off a series of pathways that ultimately lead either to cell cycle arrest, senescence or apoptosis which account for its tumor suppressor activity, as represented in figure 7 (Melino and Vaux, 2010).

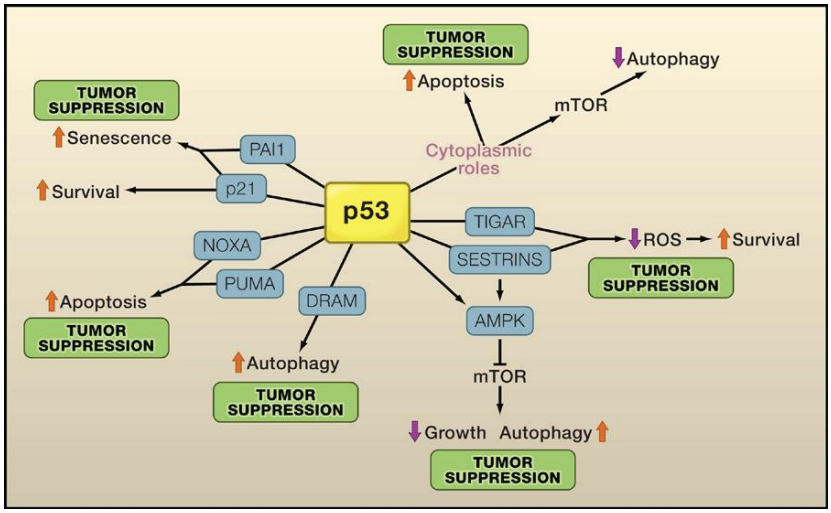

Figure 7. p53 mediation of tumor suppression. The control of proliferation, cell survival and death by p53 is regulated by the expression of p53 target genes (blue boxes). Most of these responses contribute to tumor suppression (Adapted from Vousden and Prives, 2009).

Although p53 triggers several processes that lead to tumor suppression, it is important to underline that apoptosis is the most well established mechanism to hinder tumorigenesis, since it attacks one of the most important hallmarks of cancer (Melino and Vaux, 2010). Moreover, p53 is so versatile that it can activate both the extrinsic and intrinsic apoptotic pathways, providing a rapid response when activated, and thus effectively affect malignant cells (Melino and Vaux, 2010).

Taking into account the issues regarding cancer evasion from apoptosis and the role of p53, it seems comprehensible that targeting this unique protein as an approach to cancer therapy is a promising alternative to the generally applied treatments.

Actually several approaches that target the reactivation of p53 are showing promising results. These include the use of drugs that can influence the wild type p53 (wt-p53) or its controlling mechanisms like the case of Nutlins, small molecules that inhibit the formation of a complex between p53 and its known negative regulator MDM2 showing good results in pre-clinical models (Lane et al., 2010).

However, the most promising outcomes arise from gene therapy based therapeutics. The approaches developed so far rely on the assumption that the inclusion of a wild type p53 gene into malignant cells induces apoptosis or growth inhibition.

The majority of these approaches are based on viral delivery systems, mainly adenoviruses that are responsible for delivering the wt-p53 gene into the neoplastic cells. In fact, the first commercialized p53 cancer based therapy is an adenovirus based strategy named Gendicine, developed in China (Lane et al., 2010).

Nonetheless, this drug is not yet been approved by the international regulatory agencies such as the US Food and Drug Administration (FDA) due to known issues regarding the use of adenoviral vectors (Lane et al., 2010). Among those the need to deliver continuous systemic doses that may stimulate the host immune system to produce antibodies is probably the one that hinders its approval (Lane et al., 2010).

Taking this into account it becomes clear that novel therapies with safer delivery vehicles, that are capable of surpassing these issues, are a requirement and their outcome will be probably responsible for the advent of a universal cancer gene based therapy.

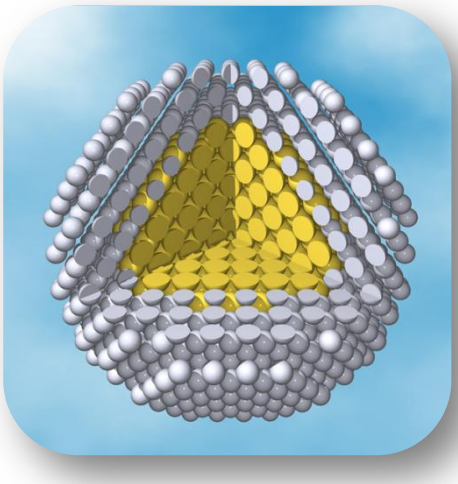

CHAPTER II

NON-VIRAL CANCER GENE THERAPY

Gene therapy possesses the potential to treat a wide variety of acquired or inherited diseases that nowadays are considered incurable, such as diabetes, haemophilia or cancer, as previously described in the literature (Grigsby and Leong, 2010).

The concept of this therapeutic strategy is based on the delivery of genetic material that encodes a desired gene into the cell nucleus where it will be expressed and subsequently trigger a therapeutic effect (Glover et al., 2005, Grigsby and Leong, 2010). However, this approach presents some bottlenecks regarding the sustained expression of the vector and its delivery into the intracellular environment (Grigsby and Leong, 2010). In fact, it is important to underline that often the concept of gene therapy is mostly referred as gene delivery, since the entry of the vector in the cell is the key factor that as hindered the translation of this technique into a clinical application (Grigsby and Leong, 2010).

Concerning this issue two major systems are usually used for the delivery of the genetic material into the cell: viral and non-viral systems (Glover et al., 2005). The first ones are viral systems derived from naturally occurring viruses, and they show promising results as described earlier (Glover et al., 2005). These are a consequence of the higher transfection efficiency, i.e. the ability to deliver the gene into the cell, a inherent capacity that virus possess, since to infect the host cells they need to express the virulent genome (Glover et al., 2005). Despite this fact, the use of these delivery vehicles is mostly restrained due to manufacture, structure, and safety associated limitations, such as immunogenicity and cytotoxicity, low transgene size loading and high cost (Morille et al., 2008).

Hence, as an alternative, non-viral based systems mainly cationic lipids and cationic polymers like chitosan, are now widely investigated as vehicles for gene delivery in cancer cells (Morille et al., 2008). However their outcome as the leading gene delivery vehicles is impaired due to their poor levels of transfection when compared to their viral counterparts (Morille et al., 2008, Grigsby and Leong, 2010). Nonetheless, they possess unique properties that renders them ideal carriers for DNA, as it will be further discussed. Moreover, the expansion of novel materials with nano-scale dimensions and tailored properties, could improve these carrier systems (Morille et al., 2008), making them certainly promising vehicles for use in cancer therapy in a near future.

From this viewpoint it becomes clear that non-viral gene delivery approaches are the most suitable for cancer therapy. Therefore in order to develop novel therapeutic approaches using this technique it is imperative to control and understand the whole process from the production of the expression vector and delivery system to their simultaneous application in cancer cells.

2.1. Plasmid DNA expression vectors for non-viral gene therapy

Plasmids are self-sufficient replicative entities that can be found in all bacterial species possessing variable sizes that range from 1 kb to 200 kb (Schleef, 2001). One of the major advantages of these molecules is the possibility of using them as cloning vectors into which foreign DNA can be inserted and replicated (Schleef, 2001). In fact pDNA vectors are fundamental in gene delivery therapies since these double-stranded DNA (ds DNA) biomolecules encode the proteins (for example p53) that are meant to trigger the therapeutic response in the host malignant cells (Ferreira et al., 2000, Williams et al., 2009). Plasmid vectors are usually over expressed in *Escherichia coli (E.coli)* bacteria before their delivery (Schleef, 2001). An integrative overview of the process of production to application in gene therapy is presented in Fig. 8.

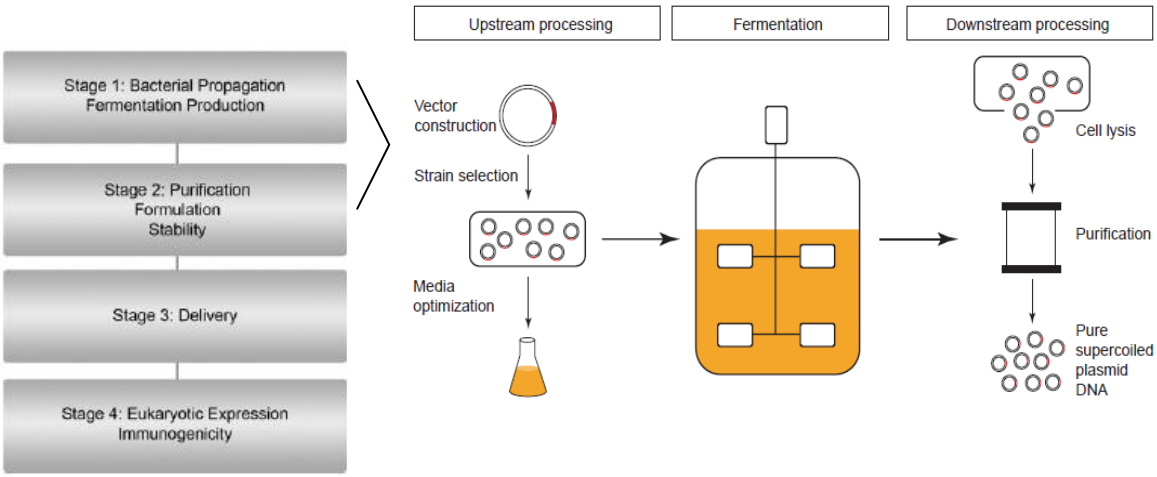

Figure 8. Stages from production to application of pDNA in gene therapy based treatments. In stage 1 (upstream processing) the plasmid vector is chosen and the construct designed to bear the transgene of interest a process followed by selection and optimization of the *E.coli* bacterial growth conditions and consequently fermentation. Stage 2 (downstream processing) comprises the final isolation of the expression vector and its purification. Stage 3 and 4 will be further addressed since there are key factors that hinder these stages before the ultimately therapeutic (Adapted from Ferreira et al, 2000; Williams et al., 2009).

As figure 8 depicts there are two key stages before the delivery of the expression vector into the malignant cells: the upstream and downstream stage. The first one can be summarized as the tailoring of conditions that allow the expression of large amounts of pDNA (Ferreira et al., 2000). Whereas the latter comprises the processing operations that aim to eliminate impurities, contaminants and recover the supercoiled plasmid DNA (sc pDNA) isoform (Ferreira et al., 2000).

This downstream stage is crucial since it is responsible for the removal of impurities such as endotoxins, RNA and genomic DNA that can cause serious side effects if delivered to the host (Ferreira et al., 2000). Furthermore, it is also at this stand point that the purification of the different plasmid isoforms takes place.

Plasmid DNA is considered to be a stable biomolecule, although during its production and recovery process it can undergo several stresses that may lead to its degradation (Quaak et al., 2009). This phenomenon mainly affects the sc isoform, the only plasmid isoform considered intact and undamaged (Quaak et al., 2009). Nonetheless, it is of most importance to point out that this isoform is also considered the one that possess the highest transfection efficiency and therefore it is the most appropriate one for cancer gene therapy approaches (Quaak et al., 2009). Taking this into account, it seems comprehensible that there is a growing demand for the recovery and purification of this isoform in the downstream process (Urthaler et al., 2005). In this subject, chromatography plays a central role either in the purification in large scale, or as an analytic technique used in the monitoring of the overall process. This is a key parameter, since pDNA products intended for gene therapy applications must comply to strict guidelines published by regulatory agencies such as FDA and the European Agency for the Evaluation of Medical Products (EMEA) (Diogo et al., 2005).

2.2. Amino acid-DNA affinity chromatography for sc pDNA purification

Among the different chromatographic approaches to purify sc pDNA such as size-exclusion chromatography (SEC), hydrophobic interaction chromatography (HIC), anion-exchange (AEX) and others, affinity chromatography has shown outstanding results in the purification of pDNA intended for gene therapy (Sousa et al., 2008b).

Affinity chromatography is a unique technique that relies on a specific binding ligand to purify biomolecules taking into account their biological functions and distinct chemical structures (Sousa et al., 2008a, Mondal and Gupta, 2006). The use of this methodology presents remarkable advantages since not only it abolishes unnecessary extra processing steps to purify pDNA, but also increases the yield of the recovered nucleic acids (Sousa et al., 2008a).

This purification approach separates biomolecules relying on a reversible interaction that occurs between the target molecule and the ligand (Figure 9).

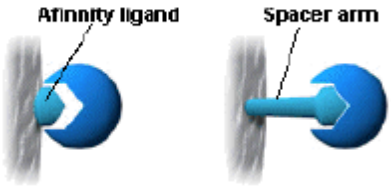

Figure 9. Interaction between the affinity ligand and the target biomolecules. The presence of a spacer arm assures the accessibility of the ligand (Adapted from Healthcare).

The specific interactions described above involve a multitude of complex physico-chemical interactions including electrostatic, hydrophobic, van der Walls forces and/or hydrogen bonds (Sousa et al., 2008a). Moreover, the selection of the matrix and the used conditions need to account not only for these interactions but also for the molecular properties of the biomolecules. (Sousa et al., 2008a). Once the sample is loaded into the column their selective capture is promoted by the ligand if the conditions are suitable, hence if that is the case the biomolecules stand bound onto the matrix (Mondal and Gupta, 2006). Subsequently, elution steps can be performed either specifically (with competitive ligands) or non-specifically by changing conditions like pH, ionic strength or polarity depend mostly on the features of the different biomolecules (Sousa et al., 2008a). In general this affinity purification strategy can purify pDNA in a single purification step that, as described earlier, is crucial to further promote the stability of the most biologically active isoform. Although it is important to underline that this unique feature is mostly dependent on the type of the affinity ligand.

Regarding this issue, the use of small amino acid ligands termed pseudobio affinity ligands has proven to be a promising strategy to efficiently isolate sc pDNA with high yield and purity (Sousa et al., 2008a). In fact histidine has been used to purify the sc pDNA isoform successfully although with low yield and using high salt concentrations (Sousa et al., 2008a). To overcome the aforementioned issue, novel arginine supports have been designed, taking advantage of the fact that protein-DNA structures are mostly dependent on arginine-based interactions to purify pDNA. In fact Sousa et al., 2008, demonstrated that these supports have unmatched selectivity to the different pDNA isoforms, being capable of separating the sc pDNA isoform with high yield, stability and purity (Sousa et al., 2008b), most certainly meeting the regulatory requirements for further application in gene therapy.

Despite the fact that this has been a major breakthrough, efficient gene expression can only be attained if the pDNA can reach the nucleus in a structurally intact form. Hence it is crucial to assure the transport of the genetic material in a safe and efficient way.

2.3. Non-viral nanocarrier mediated gene delivery

A major challenge for cancer gene therapy is the delivery of the pDNA that contains the transgene of interest into the cell (Glover et al., 2005).

Nanoparticulated delivery systems arise nowadays as the most promising candidates for the delivery of pDNA into the intracellular compartment and ultimately into the nucleus of malignant cells (Gullotti and Yeo, 2009). These nanocarriers are exceptional delivery systems due to their unique nanoscopic size characteristics, generally situated in the range of 1 to 1000 nm (Ferrari, 2005). Furthermore, they are not only able to enter the cell but they also possess unmatched release characteristics that are responsible for the release of their payload. Such property is very important for their use as gene delivery system for cancer (Gullotti and Yeo, 2009).

However, it is important to first address the challenges of targeting these carrier systems into malignant cells. Comprehensibly, there is a pre-requisite to understand the underling concepts that the tumor biology presents to efficient gene delivery and combine them with the optimized design of nanoparticulated systems (Peer et al., 2007).

One of the most interesting features of tumors is their leaky vasculature that allows the nanoparticles to diffuse freely into tumor cells (Peer et al., 2007). This mechanism is called enhance retention and permeability effect (EPR), and is often characterized as a passive targeting strategy to deliver nanoparticles into the tumor microenvironment (Gullotti and Yeo, 2009). EPR is based on the assumption that the blood vessels surrounding tumors acquire increased permeability with fenestrations ranging from 100 to 600nm and deregulated lymphatic drainage (Gullotti and Yeo, 2009). Therefore, the passive targeting of the nanoparticulated systems is achieved due to their accumulation in the vasculature that surrounds the tumor (Figure 10).

Although, to take advantage of this effect it is crucial that the non-viral nanocarriers are able to evade the immune surveillance system and circulate for long periods of time in the bloodstream (Gullotti and Yeo, 2009). In fact, the nanoparticles must avoid the reticuloendothelial system (RES), the one responsible for their opsonization and consequent phagocytosis (Gullotti and Yeo, 2009).

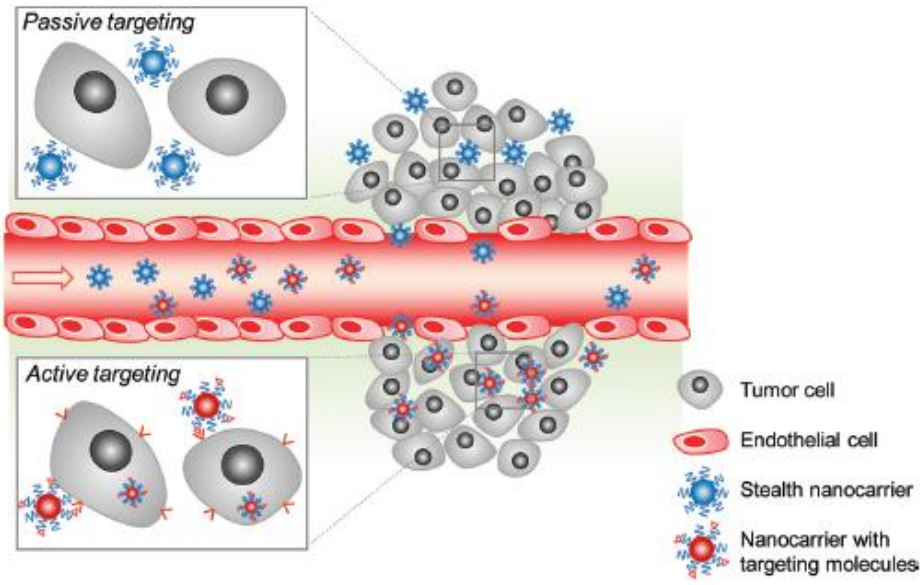

Figure 10. Nanocarrier targeting to tumors cells. The nanocarrier systems can reach the tumor by different targeting mechanisms: passive targeting and active targeting. Upon arrival at the tumor microenvironment, nanoparticles with specifically adsorbed or conjugated molecules can bind to tumor cells, on the contrary normal carrier systems are less effective in interacting with tumor cells, although they also enter into the cellular compartment (Adapted from Gullotti and Yeo, 2009).

In addition to the EPR effect another targeting approach may also be used as depicted in figure 10. This methodology is named active targeting and involves the adsorption or chemical conjugation of specific molecules on the surface of the nanocarrier systems. In turn, these molecules are recognized by malignant cells and internalization is mediated by this specific interaction (Gullotti and Yeo, 2009). In spite of the fact that several reports describe the potential of this approach to enhance transfection efficiency and consequently the anticancer effect, it is important to underline that an ideal nanocarrier should attain delivery both relying of the EPR effect and on active targeting, thus exponentially increasing their tumor distribution (Gullotti and Yeo, 2009). At this point, another barrier to gene transfection arises since the tumor matrix that consists of collagen and other proteins obstruct the nanoparticle systems, in such a way that it limits their mobility (Morille et al., 2008).

Notwithstanding, in addition to these targeting issues, once they are located in the tumor microenvironment the non-viral nanocarriers systems face the most challenging obstacles that hinders their entry into the cell (Figure 11).

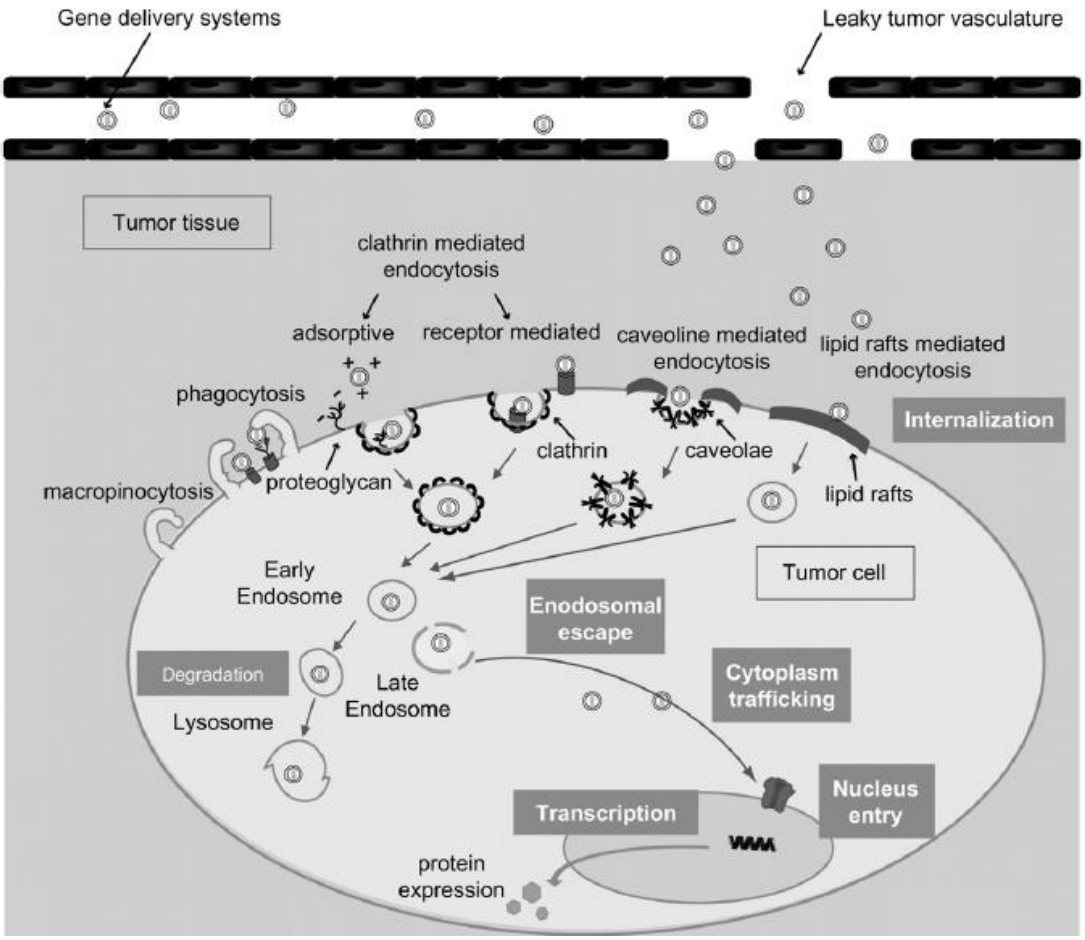

Figure 11. Different barriers impacting gene delivery through nanoparticulated systems before and after entering the cell (Adapted from Morille et al, 2008).

Following the arrival at the tumor site the first contact with the tumor cells is determinant, since the nanocarrier must be able to transpose the extracellular membrane (Morille et al., 2008). As figure 11 shows there are a multitude of entering pathways, although the predominant way that nanocarriers use to enter in the intracellular compartment seems to be the easier, i.e. the one that relies on non-specific endocytosis, followed by the clathrin-coated mechanism (Morille et al., 2008). Nonetheless, it is important to state that the contribution of each pathway to the internalization of the carriers is not yet defined due to their different compositions. Among the factors that may set of the entry into the cell trough one mechanism in detriment of other are the size of the carriers and their surface charge (Morille et al., 2008). Following endocytosis, the nanocarrier vectors remain captured in the vesicles, which presents itself as a major drawback to efficient transfection, since if the nanoparticle carrier stays for indeterminate time in the vesicle it will most likely be degraded by lyzossomes (Morille et al., 2008). Taking this into account, the nanocarrier

system must possess well defined characteristics that will ultimately allow its release into the cytoplasm a process that is thought to be mediated by a mechanism know as proton sponge effect (Pathak et al., 2009).

The proton sponge effect is a consequence of the increase in osmotic pressure promoted by the positive charge of the nanocarrier systems (Pathak et al., 2009), a crucial characteristic that determines the chosen materials for their synthesis, as it shall be seen further ahead (Mao et al., 2009).

When the nanocarrier is released into the cytoplasm two critical stages that will ultimately dictate the efficiency of the process arise, the nanocarrier unpacking of pDNA and the entry of the expression vector into the nucleus. The first one depends mostly on the properties of the nanocarrier systems and are one of those that prove most difficult to engineer (Grigsby and Leong, 2010).

It is comprehensible that the carrier systems must dissociate from their pDNA cargo so the genetic material can be translated in to the protein of interest by the cell machinery. Although the question arises, when is the best moment for this event to take place. Reports in the literature are quite opposite in what comes to this matter and some show that it occurs in the cytoplasm, well others report it happens in the nucleus (Grigsby and Leong, 2010). From this stand point it is only important to underline that these findings are only dependent on the tailoring characteristics of the carriers and they need to be carefully engineered to optimize transfection (Grigsby and Leong, 2010). Schematics of the ideal protection/release characteristics of the carriers are presented in Fig. 12.

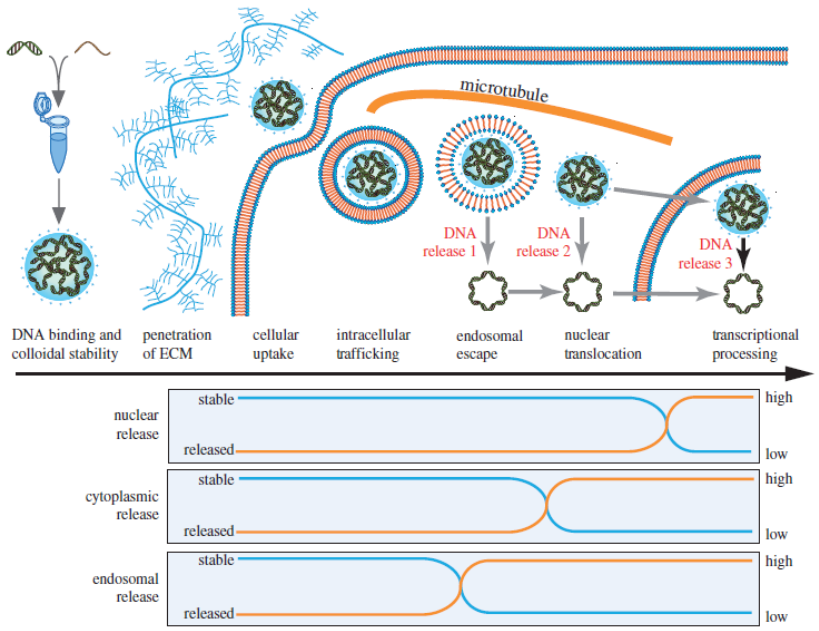

Figure 12. DNA unpacking. After entering the cell the nanocarrier must be able to release its genetic content (Adapted from Grisby and Leong 2010).

As depicted in figure 12 the release of the pDNA cargo from the nanocarrier systems may occur in three distinct stages: i.) inside the endossomal vesicle; ii.) in the cytoplasm; iii.) in the nucleus (Grigsby and Leong, 2010). Ideally the carrier should protect DNA from nuclease mediated degradation, but at the same time it should be able to release it (Pathak et al., 2009). If these binding/release states will not occur in the nucleus the expression vector must also transpose this barrier until it is ultimately expressed. The nuclear uptake of the pDNA vectors may occur by two distinct routes. The first one during the cell division stage and the second one through the nuclear pore complex, a process mediated by the cell import machinery which depends on small proteins named caryopherins (Pathak et al., 2009).

From this stance it is comprehensible that at some time in the non-viral transfection process the nanocarrier intrinsic characteristics play a decisive role in the overall yield of the process, hence the type and material that composes the nano delivery system must be chosen wisely.

2.4. Non-viral polymeric nanoparticles for gene delivery

The majority of non-viral gene delivery systems comprise a wide number of polycations including cationic lipossomes, branched and linear polyethylenimine (PEI), polyamidoamine dendrimers and chitosan among others (Hart, 2010). These polycations posses unique advantages that distinguish them from viral vectors, such as low immunogenicity, easy to manufacture and no limitations in what regards the transport of genetic material (Park et al., 2006). Moreover, their positive charge allows them to condense DNA and form sub-micron ranged particles frequently referred as nanoparticles (Hart, 2010). In fact, due to their size, nanoparticles can achieve higher intracellular uptake when compared to other systems (Mosqueira et al., 2001). This structural characteristic gains special importance given the fact that until the pDNA reaches the nucleus of the cell, an adverse environment acts upon the carrier and the vector, as describer earlier.

These nanoparticulated delivery systems can be defined as solid colloids that collectively include nanospheres, nanocapsules, lipossomes and polymeric micelles as shown in figure 13.

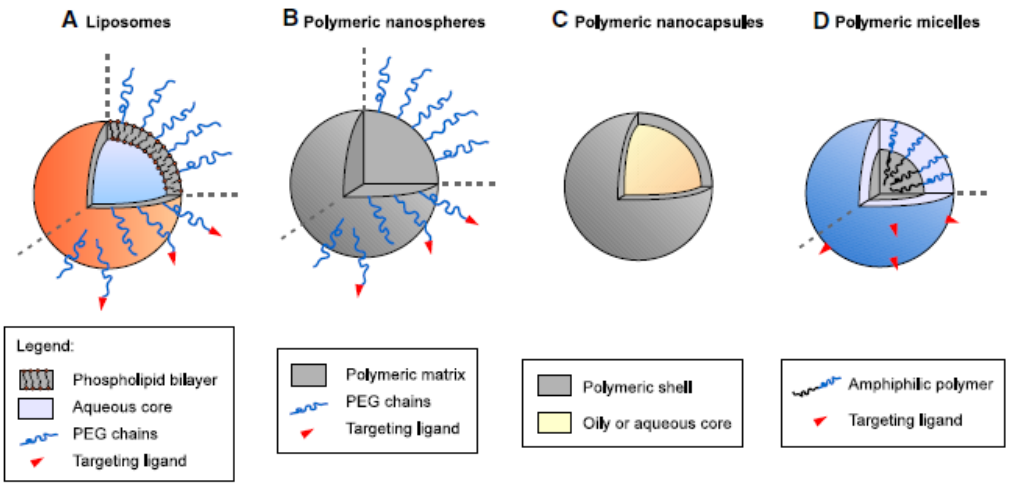

Figure 13. Types of nanocarrier systems for gene delivery. A.) Lipossomes are formed by phospholipid bilayers (one or more) surrounding an aqueous core, they can be modified in their surface by PEGylation or with targeting ligands. B) Polymeric nanospheres are formed by biodegradable polymers. C.) Polymeric nanocapsules are formed by a thin polymeric membrane (with the same material as the nanospheres), that surrounds an aqueous or oil core. D.) Polymeric micelles are composed of amphiphilic polymers (Adapted from Hillaireau and Couvreur, 2009).

Among the delivery systems depicted in figure 13 nanocapsules are one of the most important ones. They are vesicle like polymer carriers composed of an aqueous core involved by a polymeric envelope that exhibits a typical core-shell structure in which pDNA can be entrapped (Parveen and Sahoo, 2008). Several reports exist in the literature regarding the use of nanoparticulated polymeric materials (nanoparticles and nanocapsules) for gene delivery systems such as those based on PEI (Dall'Era et al., 2008), or PEI poly (lactic-co-glycolic acid) (PLGA) polymer conjugates, polyethylene glycol (PEG) (Olga et al., 2008) or alginate (Reis et al., 2006).

Despite the diversity of materials at the disposal for synthesis of nanoparticulated systems chitosan-based nanocarriers have been gaining an exponential interest as non-viral gene delivery systems, mainly due to its undoubtedly unique properties (Mao et al., 2009).

Chitosan is synthesized from the deacetilation of chitin, which is a part of the exoskeletal structure of crustaceans (shrimp, crabs, etc). Chitosan is a biodegradable polysaccharide consisting of repeting D-glucosamine and *N*-acetil-D-glucosamine monomers, linked via β1-4 glycosidic bonds (Figure 14) (Mao et al., 2009). Chitosan contains a primary amine group in each deacetilated unit with a pKa of 6.5 rendering it soluble only in acidic media and insoluble in neutral or basic medium (Mao et al., 2009).

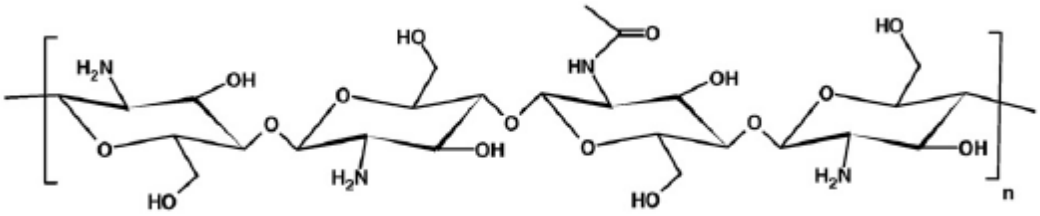

Figure 14. Chitosan chemical structure (Adapted from Mao et al, 2009).

In the physiological environment chitosan can be degraded by lysozymes or by chitinases which can be produced in the human intestinal flora or be present in the blood (Mao et al., 2009).

The main feature of chitosan that accounts for its potential as a gene delivery vehicle is its cationic nature (Borchard, 2001). Curiously, chitosan most important characteristic is due to the primary amine groups present in its backbone, since below the pKa they become positively charged (Mao et al., 2009). These amine groups are the ones responsible for the reaction with DNA molecules since they interact via electrostatic forces (Borchard, 2001). This contact between the positively charged chitosan molecule and the negatively charged DNA backbone (due to its phosphate groups) is responsible for the spontaneous formation of chitosan-DNA nano-complexes, also known as polyplexes, (Figure 15) which only takes place at a suitable nitrogen to phosphate ratio (N:P ratio) (Köping-Höggård et al., 2004, Mao et al., 2009).

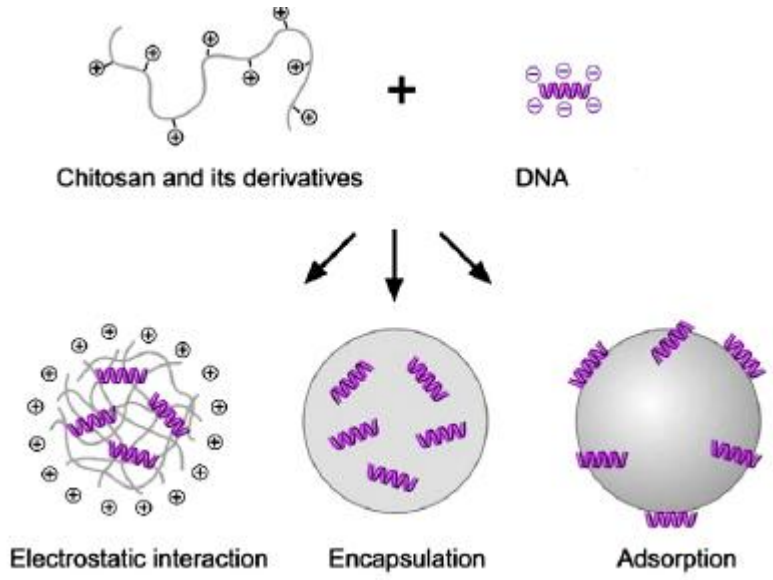

Figure 15. Different chitosan DNA nanoparticles formulated by different synthesis mechanisms (Adapted from Mao et al., 2009).

As presented in figure 15 different nanoparticles can be formed with chitosan and DNA depending on the processing method, this is an issue of most importance since

the formulation of chitosan polyplexes yields rather unstable and morphologically undefined particles when compared to those obtained using cross-linking agents (Csaba et al., 2009).

Taking into account what was earlier described, chitosan as a lot of properties and some of them need to be summarized and addressed in order to understand what effect their manipulation would have in the final nanoparticle formulations for gene delivery. Chitosan can be characterized by its molecular weight, viscosity, crystallinity and most importantly its degree of deacetilation the one to be studied most thoroughly, due to the fact that it not only influences crucial nanoparticle formulation parameters but also because it plays a fundamental role in polymer degradation and transfection efficiency (Mao et al., 2009). Some of the most important formulation parameters for the synthesis of chitosan-based delivery systems are summarized in table 2.

Table 2. Summary of the most important formulation parameters in the design of nanoparticulated systems based on chitosan.

Properties	Characteristics	Influences	References
Deacetilation Degree	Percentage of primary amine groups in the polymer backbone (determines the positive charge density)	Higher degrees results in increased DNA binding, cellular uptake, longer degradation time and smaller particle size	(Kiang et al., 2004);
pDNA concentration	Amount of pDNA that is incorporated in the cationic polymer	Higher concentrations enhance transfection until a saturation point	(Zhao et al., 2006)
Molecular weight	Particle size, cell uptake, transfection efficiency	Decrease in size with decrease in molecular weight	(Huang et al., 2005)
Cross-linker agents	Encapsulation of pDNA, modification of the particle physicochemical properties	Higher transfection efficiency, higher stability, formation of nanocapsules	(Csaba et al., 2009);(Bao et al., 2008)
Polymer Concentration	Amount of positive charges in solution	Higher concentration increased particle size	(Gan et al., 2005)
pH	Amount of primary protonated amines	Particle size increase at pH 6.0	(Gan et al., 2005)

It is clear that chitosan is a polymer with immense potential for gene delivery applications. Recently some advances in respect to nano-encapsulation of pDNA (Csaba et al., 2009) inside its particle core and the results regarding gene therapy delivery systems for cancer (Hee-Dong et al., 2010) make this polymer a valuable option for gene therapy applications.

SECTION II

MATERIALS AND METHODS

2.1. Materials

Arginine Sepharose 4B gel was obtained from Amersham Biosciences (Uppsala, Sweden). Pentasodium tripolyphosphate (TPP), ethidium bromide (purity 95%), *N*-acetyl-D-glucosamine, Sodium nitrate ($NaNO_2$), Fluorescein isothiocyanate isomer I (FITC), Anti-VE-Cadherin antibody (anti-rabbit), paraformaldehyde,Triton X-100, Tween 20, bacterial and cell culture reagents were all obtained from Sigma–Aldrich (St. Loius, MO, USA). 2-(4-aminophenyl ethylamine) was purchased from Acros Organics (Geel, Belgium). One kbp DNA ladder was obtained from Vivantis Technologies (Oceanside, CA, USA.). A549 non-small lung carcinoma cell line was purchased from ATCC (Middlesex, UK). All transfection reagents and Hoesht 33342 (trihydrochloride, trihydrate), were obtained from Invitrogen (Carlsbad, CA, USA). All used salts used in this research were of analytical grade.

2.1.1. Plasmid DNA

The 6.7 kbp pcDNA3-FLAG-p53 plasmid was purchased from Addgene (Cambridge, MA, USA). The vector encodes for the human p53 protein conjugated with a FLAG tag. The vector contains the SV40 virus mammalian expression promoter and the ampicillin resistance gene.

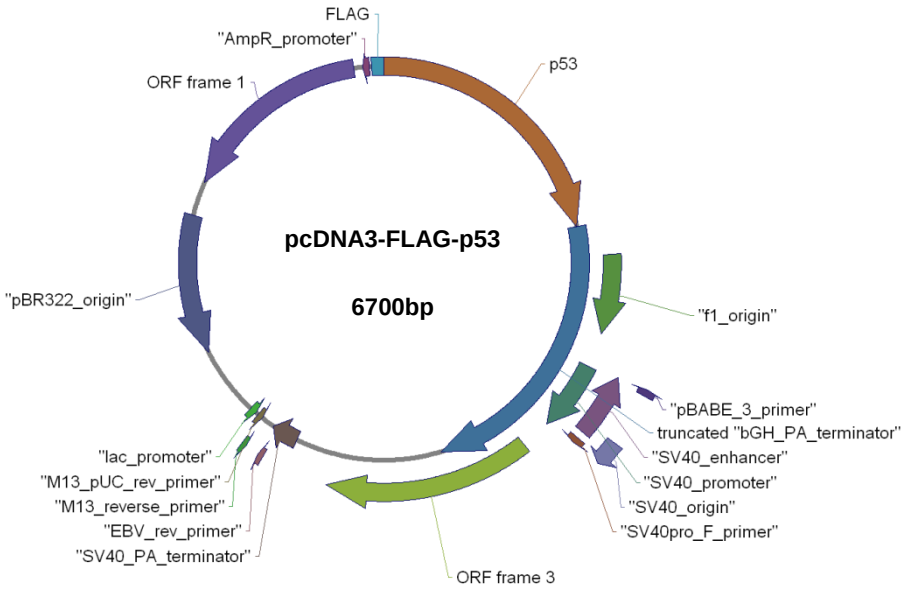

Figure 1. Plasmid pcDNA3-FLAG-p53 backbone (Vector drawn using the Redasoft Visual Cloning 3.2 ™ software).

2.1.2. Chitosan

Chitosan (low molecular weight (LMW)), from crab shells was purchased from Sigma-Aldrich (St. Loius, MO, USA). Chitosan molecular weight (MW) ranged between 50 and

190 kDa, and the degree of deacetilation ranged from 75% to 85%, as provided by the manufacturer. The chitosan flakes used for the production of the nanoparticulated systems were those commercially available. Moreover, batches from the purchased product were also submitted to previous modification procedures such as deacetilation and reacetilation.

2.2. Methods

2.2.1. Bacterial growth conditions and plasmid recovery

The 6.7 kbp pcDNA3-FLAG-p53 plasmid (Addgene, Cambridge, MA, USA) used for the experiments was produced by a cell culture of *Escherichia coli (E.coli)* DH5α. Growth was carried out at 37ºC, and with and agitation of 250 rpm in a 1L Erlenmeyer with 250 mL of complex Terrific Broth medium (20 g/L of tryptone, 24 g/L of yeast extract, 4 ml/l of glycerol, 0.017 M KH_2PO_4, 0.072 M K_2HPO_4) supplemented with 20μL of ampicillin. Growth was suspended at late log phase ($OD_{600nm} \approx 9$). Cells were recovered by centrifugation and the plasmid purified by the Qiagen Plasmid Maxi Kit (Quiagen, CA, USA) according to the supplier's protocol. This procedure was used to remove contaminants such as cellular debris, genomic DNA and RNA, thus purifying pDNA. Subsequently these pDNA samples were submitted to a chromatographic isolation step to separate the different isoforms.

2.2.2. Affinity Chromatography

Chromatography was carried out in a fast protein liquid chromatography system (FPLC) (Amersham Biosciences). A standard 16 x 100mm column (corresponding to approximately 20mL) was packed with an arginine-Sepharose 4B gel. The gel matrix was a 4% agarose bead cross-linked with a 12 carbon atom spacer arm (Figure 2). The experiments were performed at 4ºC and the temperature was controlled by using a circulating water bath, alternatively experiments at room temperature were also performed to determine the influence of the temperature conditions on the retention/elution of the different pDNA isoforms from the column.

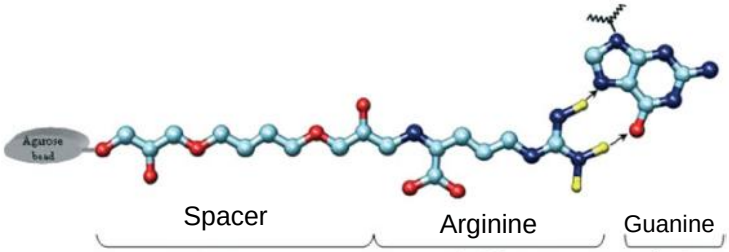

Figure 2. Representation of the aminoacid based matrix interacting with a guanine nucleotide through 'bidentate' interactions based on hydrogen bonds (Adapted from Sousa et al., 2008b).

The experiment was prepared using two solutions: (i) 10mM Tris.HCl buffer (pH 8.0) solution; (ii) 300 mM NaCl solution in 10mM Tris.HCl buffer (pH 8.0), that were pumped into two different compartments (A and B) of the FPLC system. The column was then equilibrated with 37.3 % of the 300mM NaCl solution present in compartment A, together with the 10mM Tris.HCl buffer (pH 8.0) solution present in compartment B, at a flow rate of 1mL/min. The solutions were ice cooled or at room temperature, according to each experiment. Afterwards partially purified pDNA obtained after recovery from the Qiagen Plasmid Maxi Kit was loaded onto the column using a 200µL loop at the same flow rate. The absorbance of the eluate was continuously monitored at 280nm. After the elution of the weakly bound species the ionic strength of the buffer was increased to 300mM NaCl in 10mM Tris.HCl buffer (pH 8.0). Fractions were collected according to the chromatograms obtained and stored (at -80ºC) for further analysis. After all of the chromatographic runs, the column and the FPLC system were rinsed with three volumes of ultrapure water.

2.2.3. Agarose gel electrophoresis

Electrophoresis is a technique that uses an electric field applied to a gel matrix. Gel electrophoresis is usually made in an agarose gel. This technique is used to separate and estimate the size of nucleic acid fractions. The migration of double stranded DNA fragments towards the positive pole, is size dependent since the gel matrix act as porous network. The conformation of the pDNA also affects its migration along the gel, hence more compacted forms migrate faster towards the positive pole.

The electrophoresis experiments were carried out with the preparation of a 1% agarose gel (Hoefer San Francisco, CA, USA), stained with ethidium bromide (0.5µg/mL). Electrophoresis was carried out at 90V for 55 minutes with TAE buffer (40mM Tris base, 20mM acetic acid and 1mM EDTA pH 8.0). The gels were visualized under UV light in a Vilber Loumat system (ILC Lda, Lisbon, Portugal).

2.2.4. Synthesis of deacetilated and reacetilated chitosan

To address the influence of the presence of primary amine groups in the polymer chain, the chitosan material was deacetilated like previously described in the literature with slight modifications (Gan et al., 2005). Briefly, the chitosan flakes were dispersed in a NaOH solution. 500 mg of chitosan were mixed with 10mL of 1 M NaOH. The mixture was then heated at 50ºC under magnetic stirring for 3h and then filtered with a 0.44µm filter in a Buchner funnel. The remaining material was washed extensively until the pH was the same of ultrapure water and then dried at 40ºC overnight. The chitosan

recovered material was dissolved in 1M acetic acid solution. A solution of 1M NaOH was used to adjust the pH to 7, which precipitated the chitosan material. The product was then centrifuged at 4500*rpm* (Sigma 3K18C centrifuge), this procedure was repeated 3 times and finally the recovered pellet was lyophilized for 1 day. Chitosan with lower deacetilation degree (DD) was also synthesized. Briefly, 750mg of chitosan were flush mixed with 1.2g of acetic in 80mL of solvent (0.38% CH_3COOH/31.25% methanol) at room temperature overnight, the chitosan was then recovered as previously described.

2.2.5. First derivative ultraviolet spectrophotometry

The first derivative ultraviolet spectrophotometry (*1DUVS*) is a technique used for determination of the DD of chitosan samples in acidic solutions. The *1DUVS* is based on the measurement of the height (H) of the maximum absorbance value of *N*-acetyl-D-glucosamine residues in the polymer backbone to address the percentage of the primary amine groups. Although, chitosan is only soluble in dilute acids, usually acetic acid, and therefore the contribution of the solvent to the absorbance values needs to be addressed in order to avoid overestimations.

The determination of the DD degree and the acetic acid solution spectra was performed as previously described (Tan et al., 1998) with some modifications. Briefly, the spectra of acetic acid solutions with different concentrations from 0.01M to 0.03M were obtained using a Shimadzu 1700 Uv-vis spectrophotometer (Shimadzu Corporation, Kyoto, Japan) in the range of 240-190nm. The first derivative spectra demonstrated the existence of a common point at 203nm, denoted as the zero crossing point (ZCP). Afterwards a sequence of *N*-acetyl-D-glucosamine standard solutions of 0.005 – 0.050 mg/mL in a 0.01M acetic acid were prepared and their first derivative spectra registered as denoted in figure 3a. The superimposition of the ZCP spectra and the *N*-acetyl-D-glucosamine allowed the measurement of the maximum H value at 203nm. A linear calibration curve was consequently obtained by plotting the H_{203} values versus the corresponding *N*-acetyl concentration as depicted in figure 3b.

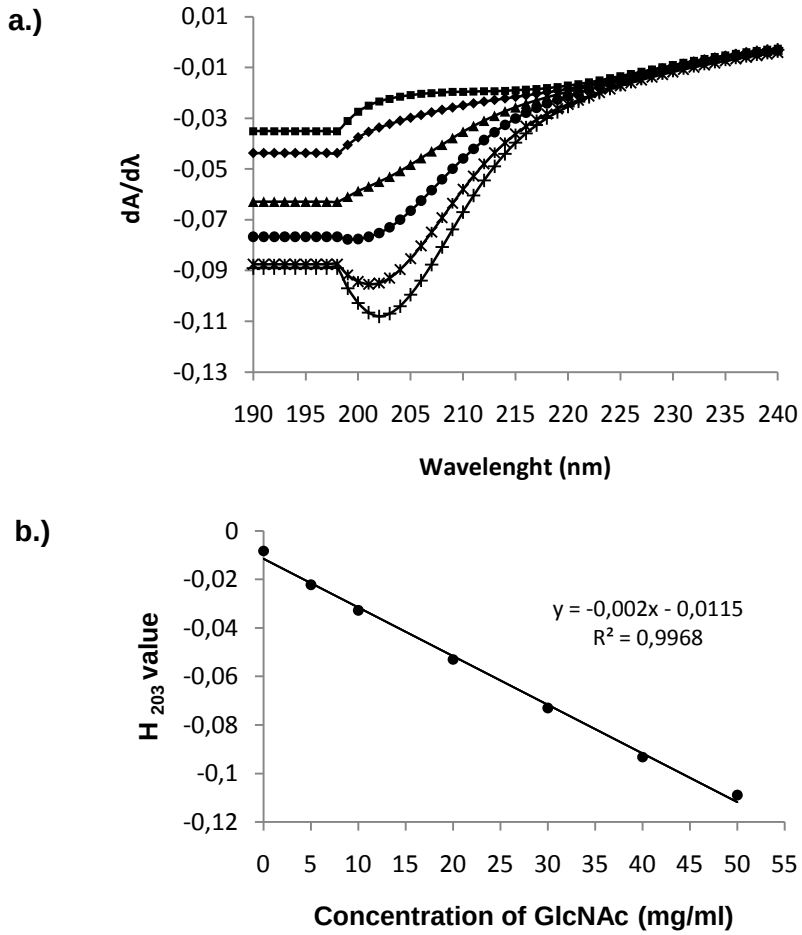

Figure 3. 1DUVS *N*-acetyl-D-glucosamine spectra and reference curve. a.) First derivative spectra of the of *N*-acetyl-D-glucosamine solutions (■- 0.005 mg/mL; ♦ - 0.01 mg/mL; ▲ – 0.02mg/mL; ● – 0.03mg/mL; ***** - 0.04mg/mL; + - 0.05mg/mL); b.) Reference curve *N*-acetyl-D-glucosamine.

To determine the DD, 0.01mg of chitosan samples were dissolved in 10mL of 0.01M acetic acid and diluted in 90mL of ultrapure water as described by Tan and colaborators, 1998. The first derivative spectra of the chitosan materials were recorded and the H_{203} value was measured. The DD of the different samples was determined as follows:

$$DD\ (\%) = \left[1 - \left(\frac{A}{\frac{((10 \times W) - 204\ A)}{161} + A}\right)\right] \times 100 \qquad (1)$$

204 – Molecular weight of *N*-acetyl-D-glucosamine

161 – Molecular weight of D-glucosamine

A – Amount of *N*-acetyl-D-glucosamine

W – Mass of the chitosan sam«ple

2.2.6. X-ray diffraction (XRD)

X-ray diffraction analysis was used to determine the physical form (amorphous or crystalline) of the different lyophilized chitosan samples. The experiments were performed over the range from 2θ from 1º to 50º, using a Rigaku Geigger Flex D-max III/c diffractometer (Rigaku Americas Corporation, USA) with a copper ray tube operated at 30kV and 20mA. The powder samples were mounted in silica supports using a double sided adhesive tape and then analyzed.

2.2.7. Production of chitosan nanoparticles

Chitosan nanoparticles were formulated using the ionotropic gelation technique. The ionotropic gelation is based on formation of inter- and intramolecular linkages between cationic polymers and negatively charged polyanions like pentasodium tripolyphosphate (TPP). The positively charged polymer has the ability to gel instantly when in contact with the counter anion TPP under stirring, leading to the formation of nanoparticulated systems.

Before the encapsulation of pDNA, preliminary experiments were performed to identify the concentration zone were the nanoparticles were formed. Briefly, chitosan (0.02 – 0.1 g; pH 4.9) was dissolved in 100ml of ultrapure water in the presence of 1M HCl under stirring. TPP solution (0.02 – 0.1 g; pH 5.5) was dissolved in 100mL of ultrapure water. 1 mL of TPP was then added drop wise to 4mL of chitosan under mild magnetic stirring conditions (300 ± 50 rpm). The particle formation zone was further explored by mixing different chitosan:TPP (v/v) ratios (1:1, 5:1 and 6:1). The nanoparticles formed upon the addition of TPP were recovered by centrifugation at 17000 g (Hermle Z323K centrifuge) for 30min at 25ºC in a 10µL glycerol bead. The final pH of all the solutions was between 5.2 and 5.3.

2.2.8. Particle Morphology

The morphological characterization of the nanoparticles was analyzed using a scanning electron microscope (SEM) (Hitachi S-2700, Tokyo, Japan), operated at an accelerating voltage of 20 kV with variable magnifications. The nanoparticle samples were resuspended in 100 µL of ultrapure water; one drop was then added to 16mm cover glasses and mounted in aluminum boards using a double-sided adhesive tape. The samples were sputter coated with gold using an Emitech K550 sputter coater (London, England). All the particle samples were analyzed immediately after synthesis. Nanoparticle size was measured with the Roentgen SEM acquisition software version 1.3.

2.2.9. Encapsulation and loading capacity of pDNA

The pDNA encapsulation efficiency and loading capacity are two important parameters to be determined during the encapsulation of biomolecules in the nanoparticulated systems. It is important to clarify these notions since they both establish a relation of the pDNA weight loaded into the nanoparticles as denoted in equations 2.1 and 2.2.

In order to promote the encapsulation, pDNA was added to the TPP solution to assure that no interaction would occur between the negatively charged DNA and positively charged chitosan, prior to nanoparticle formation. The concentration of 13 µg/mL of pDNA used for nanocapsules formation was constant at all times.

Chitosan polyplexes were also synthesized and used as a control. The complexes were formed at a N:P ratio of 4:1 as previously described (Köping-Höggård et al., 2002). Briefly, polyplexes were formed by adding pDNA in Tris.HCl buffer (pH 8.0) to the chitosan solution under intense stirring on a vortex mixer for 60 seconds. The pDNA concentration for the formation of the polyplexes was the same used for particle preparation.

The encapsulation efficiency (EE) of the pDNA inside the nanocapsules was determined after isolation by centrifugation (10000 g, 30min, 25ºC) and recovery of the supernatant that contained the unbound pDNA. The amount of unencapsulated pDNA was determined by Uv-vis analysis at 260 nm (Shimadzu Uv-vis 1700 spectrophotometer). The loading capacity (LC) was determined by weighing blank tubes before the experiment and after the recovery of nanoparticles as described above. The encapsulation efficiency and loading capacity was calculated as follows:

$$EE\ (\%) = \frac{Amount\ Total\ pDNA - Amount\ of\ unbound\ pDNA}{Amount\ of\ Total\ DNA} \times 100 \qquad (2.1)$$

$$LC\ (\%) = \frac{Amount\ Total\ pDNA - Amount\ of\ unbound\ pDNA}{Nanoparticle\ weight} \times 100 \qquad (2.2)$$

2.2.10. Protection and release of encapsulated pDNA

The protection and release profile of the encapsulated pDNA was addressed by agarose gel electrophoresis. The protection experiments were carried out by incubation of 25 µL of chitosan nanocapsules with 5µL of DNAse I solution (10mg/mL) or with 5µL of Dulbecco's modified eagle's medium/Nutrient mixture F-12 Ham (Ham's F12K) medium supplemented with 10 % fetal bovine serum (FBS).

To characterize the release of the encapsulated pDNA, the nanoparticle samples were incubated, during different time frames, with 5µL of lysozyme solution (10 mg/mL, pH 6.2) was performed at different time frames.

2.2.11. FITC fluorescent labeling of pDNA

The preparation of fluorescently labeled pDNA was performed with some modifications of the method previously described (Ishii et al., 2000) with some modifications. Briefly FITC (10 mg) was activated overnight with 2-(4-aminophenyl)-ethylamine in 150 µL of dimethyl-formamide (DMF) under stirring, at room temperature. Afterwards, FITC-aniline conjugate was reacted with $NaNO_2$ (110 µmol) in 0.5M HCl at 0ºC under stirring, for 5 min. The reaction was stopped by adding 100 µL of 1M NaOH solution. FITC-diazonium salt was further mixed with the pcDNA3-FLAG-p53 plasmid solution in Tris.HCl buffer (pH 8.0) at room temperature, under stirring, for 25 min. The FITC labeled plasmid was recovered by precipitation at 16000 g using 0.7 volumes of ice cold isopropanol.

2.2.12. Cell culture and in vitro transfection

The cell culture experiments were performed with a A549 non-small lung carcinoma cell line cultured in Ham's F12K medium supplemented with 10% v/v heat activated FBS and antibiotic-antimycotic (penicillin G (100 U/mL); streptomycin G(100 µg/mL)) at 37ºC, under a 5% CO_2 atmosphere. Cells were seeded in 25 cm^3 T-flasks until confluence. Following confluence the cells were sub-cultivated by incubation on 0.18%% trypsin (1:250) with 5mM EDTA.

The *in vitro* transfection experiments were carried out by seeding the cells in 24 well-plates at a density of 3×10^4 cells/well in 1mL of Ham's F12K complete medium and incubated for 24h. Afterwards, the complete medium was replaced by 500 µL of medium supplemented with 10% FBS and without antibiotic, in order to promote transfection. The transfection of pDNA was then performed with a commercially available transfection reagent, Lipofectamine^{2000} and nanoparticulated systems, previously produced in our lab. Briefly, the formulation of Lipofectamine-pDNA complexes was performed by mixing equal volumes (50 µL of Optimem medium) of FITC-pDNA and lipofectamine solutions, according to the supplier protocol. Before the complexation reaction Lipofectamine was incubated for 5 min at room temperature, the pDNA solution was then added and the mixture was incubated for an additional period of 20 min, at room temperature, to promote the synthesis of the complexes. Subsequently, 100 µL of the mixture was added to each well containing the cells and

the medium. The cells were consequently incubated for a period of 6h after which the medium was exchanged for Ham's F12 K complete medium. The formulation of FITC-pDNA loaded nanoparticles was the same as described in section 1.2.7. Particles were formed at a 4:1 ratio with deacetilated chitosan, and after recovery they were resuspended in 100 µL of Ham's F12K FBS supplemented medium. Then, 25 µL of nanoparticles (corresponding to 0.3 µg of pDNA) was added to each well. The cells were then incubated for 4h, after which the medium was exchanged as described for lipofectamine experiments. The different transfection approaches were then characterized by immunofluorescence.

2.2.13. Immunofluorescence

The immunofluorescence experiments were performed after *in vitro* transfection. Following the exchange of the medium transfected cells were fixed with 4% paraformaldehyde in PBS and incubated for 20 min. The cells were then permeabilized with 1% Triton X-100 and blocked with 10% FBS and 0.1% Tween 20 in PBS for 3h. Subsequently the cells were incubated in PBST - 1% FBS for 1h, at room temperature with rabbit monoclonal anti-VE cadherin antibody (6 µg/mL) and afterwards washed 10 times with PBST. Hoesht 33322 was then added and incubation proceeded for 15 min at room temperature, followed by 10 washing steps with PBST. Afterwards the cells were incubated with Alexa Fluor 546 goat anti rabbit IgG (1g/mL) for 1h, with further washing steps. The samples were then mounted with DAKO mounting medium and visualized using a Zeiss AX10 microscope and analyzed with the Axio Vision Real 4.6 software (Carl Zeiss SMT Inc., USA).

2.2.14. Statistical analysis

The experimental data is representative of replicate independent experiments with a sample size of three in each experiment. The results are represented as the mean and standard deviation (mean ± SD) and analyzed by one-way ANOVA with the post-hoc Dunnet's test, using the trial version of the GraphPad Prism software (GraphPad Software Inc., CA, USA).

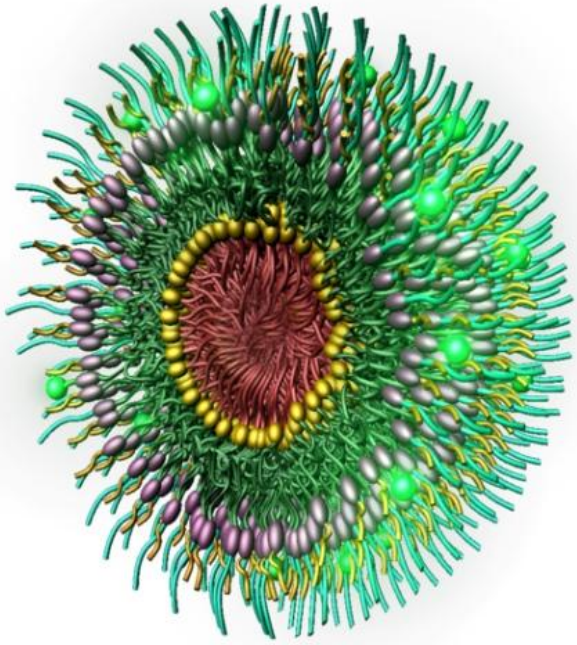

SECTION III

RESULTS AND DISCUSSION

In this work the biosynthesis and purification of pDNA conjugated with the formulation of customized nanoparticulated systems provided the basis for a novel cancer gene therapy approach, integrated from its production to application. Results regarding plasmid amplification in *E.coli* revealed high levels of production of the pcDNA3-FLAG-p53 expression vector. Furthermore, purification by an arginine affinity chromatography support promoted the recovery of the sc pDNA isoform with high yield, purity and structural stability. Carrier systems intended for the transport of the sc pDNA were formulated by the ionotropic gelation technique, forming stable colloids with sub-cellular sizes (<1μm). These nanoparticulated systems also demonstrated the ability to condense and entrap pDNA inside their core (≈ 75 % yield for sc isoform at 4:1 ratio). Additionally, nanoparticles were also proficient in *in vitro* transfection of malignant cells, since a high degree of transfection was obtained.

3.1. Plasmid amplification in recombinant E.coli

Plasmid DNA expression vectors are fundamental for non-viral based gene therapy applications. Hence, there is a demand for efficient manufacturing processes that can provide the production of large quantities of genetic material for *in vitro* and *in vivo* transgene expression. *E.coli* recombinant strains shown to be efficient vessels for pDNA production not only yielding high amounts of the vector but also maintaining its integrity (Carnes et al., 2006). Therefore, pcDNA3-FLAG-p53 vector amplification was performed in *E.coli* DH5α strain in a batch-fermentation. The cell growth profiles for bacterial cell density, obtained by the measurement of the optical density at 600 nm, are depicted in Fig 1.

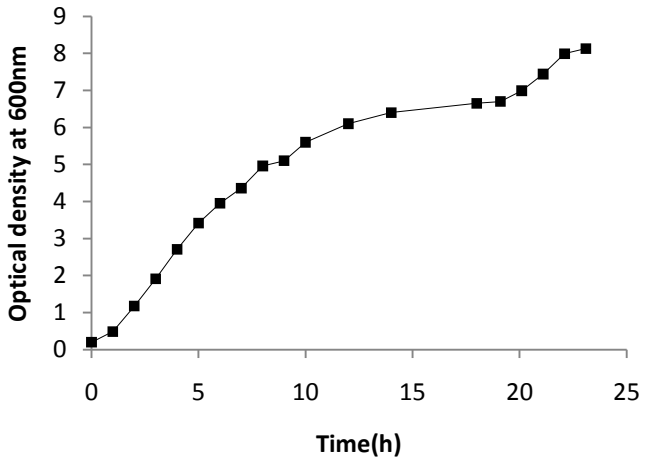

Figure 1. Growth profile of *E.coli* DH5α harboring the plasmid pcDNA3-FLAG-p53 performed at 37ºC with an agitation of 250 rpm.

As demonstrated in figure. the growth curve is time spanned and approximately 24h of fermentation are required to attain a high cell density. These findings are mostly related to an extended metabolic burden in *E.coli* cells due to the production of large pDNA copy numbers. Ow et al., 2006, previously reported that plasmid maintenance endows metabolic stress on host cells, resulting in a reduced cell density (Ow et al., 2006). In fact, it is also important to point out that a high-copy number plasmid like the pcDNA3-FLAG-p53 vector imposes further metabolic pressure that results in a downregulation of structural related bacterial genes (Ow et al., 2006).

However not only the quantity of pDNA produced in *E.coli* is important. As denoted by regulatory agencies such as FDA, pDNA must be mainly produced in its supercoiled isoform, since it is the biologically active one (Shamlou, 2003). As shown in figure 2. the pDNA amplification process in *E.coli* also yielded a higher concentration of the sc pDNA isoform in comparison to the oc form.

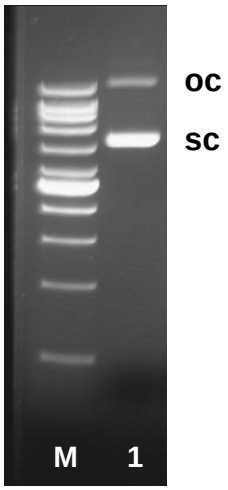

Figure 2. Electrophoresis of *E.coli* cell lisates. Lane M – Molecular weight marker; Lane 1 – pDNA produced by *E.coli* DH5α (sc pDNA and oc pDNA isoforms), purified by the Qiagen purification kit.

This fact is very important because as recently reported by Sousa et al., 2008, the transfection experiments conducted with the sc pDNA isoform demonstrate an improved transgene expression efficiency (Sousa et al., 2008b). In fact sc pDNA was able to transfect 62% of the cells, a much higher efficiency when compared to the one achieved with the oc isoform (16%) (Sousa et al., 2008b). Nevertheless, despite sc pDNA is produced in *E.coli* further purification of this isoform is critical for gene therapy applications.

3.2. Purification of sc pDNA by arginine - agarose affinity chromatography

A novel generation of chromatographic supports based on specific affinity interactions between amino acids and nucleic acids has proven to enhance downstream purification strategies (Sousa et al., 2008c), thus improving the global process from production to clinical application. This approach enables not only the efficient isolation of the sc pDNA isoform in a one step process, but also the removal of endotoxins present in *E.coli* extracts. Although, inherent particularities arise when these specific interactions are involved. For this reason, the adjustment of the conditions that promote binding/elution of the different plasmid bound species are essential to accomplish high resolution and selectivity profiles, parameters that most certainly influence the overall recovery yield.

From this stand point, several preliminary experiments were performed in order to establish the binding/elution conditions of the pcDNA3-FLAG-p53 vector onto the arginine affinity support.

Initially a first screen was performed to select the best salt concentration for binding/elution conditions with the aim to determine the concentration range were two distinctly resolved peaks (corresponding to the different pDNA isoforms) appeared in the chromatographic profile. The column was first equilibrated with Tris.HCl buffer (pH 8.0) at 4ºC using a flow rate of 1mL/min. Following plasmid injection the elution was promoted with NaCl in 10mM Tris.HCl buffer (pH 8.0), with variable concentrations as summarized in table 1.

Table 1. Summary of the retention/elution profiles for the different plasmid isoforms.

	Elution Step [NaCl] (mM)		
Sample loaded	**100 mM**	**200 mM**	**300 mM**
sc pDNA	Retention	Elution/Retention	Elution
oc pDNA	Retention	Elution	-

The findings presented in table 1 reveal distinct interactions between the arginine-agarose support and the different pDNA isoforms, that are reflected by the different binding/elution conditions. This fact is decisive since it suggests that the arginine matrix has the ability to discriminate and differentially interact with both plasmid isoforms.

Furthermore analyzing the results it is evident that a specific recognition with the sc isoform occurs, since it remains bound to the column when the oc form is totally eluted (table 1). These different affinities observed are in accordance to the results previously reported by Sousa et al., 2009, where it was described a similar retention behavior using similar conditions, although with a different plasmid vector (pVax1-LacZ) (Sousa et al., 2009).

Given the fact that the pcDNA3-FLAG-p53 and the pVax1-LacZ are two distinct plasmids in what regards their base constitution, it would be interesting to correlate the influence of the composition with the different affinities for the arginine matrix, although the full sequence of the p53 expression vector is not fully known. Despite this fact, it is of most importance the analysis of the interaction between pDNA and the chromatographic support in a molecular basis to understand the differences in isoform recognition.

It was reported by Seeman et al, 1976 that the majority of interactions between amino acids and DNA take place in the major groove atoms, particularly at positions where hydrogen bonding (H-bond) is promoted (Seeman et al., 1976). Moreover, the amino acids have more affinity for bases with enhanced donor/acceptor patterns like guanine, which is the nucleotide that shows the highest degree of contribution in H-bonds (Luscombe et al., 2001). Arginine is a unique amino acid since that it is capable of: (i) interacting in different conformations (single, bidentate, complex) ; (ii) has a side chain of easier access and finally it has the ability to promote H-bonding (Sousa et al., 2007). All of the former properties contribute for the specific recognition capacity of arginine towards a given pDNA isoform. The most determinant interaction that favors arginine-pDNA interactions is the formation of H-bonds (Luscombe et al., 2001). In fact Luscombe et al., 2001 demonstrated that although van der Wall forces and water mediated bonds are also present in amino acid – DNA interactions, H-bonds are the predominant forces that dictate their contact (Luscombe et al., 2001). Furthermore, Luscombe et al, 2001 also showed that a distinct pairing preference between amino acids and nucleotide bases takes place, particularly arginine-guanine (Arg-G) interactions, among others are privileged (Luscombe et al., 2001). The H-bond formation between Arg-G is mostly based on bidentate interactions (67%) in which there are two or more bonds with a base pair. Additionally, more complex bonds also occur, in these the amino acid is capable of interacting with more than one nucleotide base simultaneously (Luscombe et al., 2001).

These Arg-G interactions via H-bonding are the key factor responsible for the ability that the arginine matrix possesses to specifically recognize the different isoforms and are the basis of the affinity purification process.

However, for these interactions to take place the bases in the pDNA backbone must undergo a certain degree of exposure (Sousa et al., 2007). In as it can be seen in figure 3 the interactions between amino acids and base pairs use a simple steric and geometric criteria (Cheng et al., 2003).

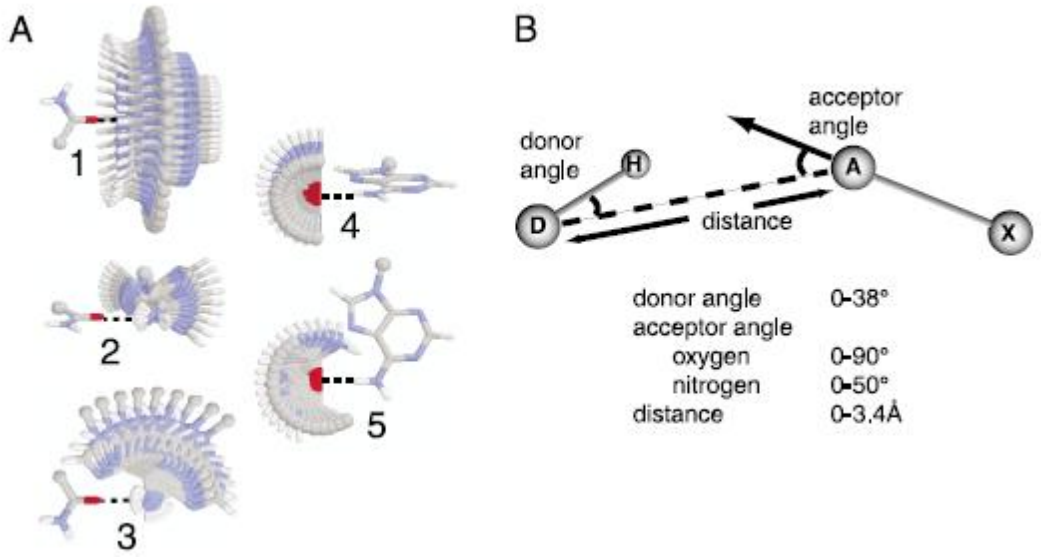

Figure 3. Amino acid base pair interactions. A.) 1 and 3 demonstrate rotations around the donor atom, 4 and 5 illustrate rotations about the acceptor atom. In a more perceptive example, the same has holding fixed the amino acid and rotating the nucleotide base (1-3) and then the contrary (4-5). B.) Three major parameters are involved in a H-bond: the acceptor angle, the donor angle and the distance between the two (Adapted from Cheng et al., 2003).

Based on these facts and correlating the torsional strain dependent deformations that are characteristic of the sc isoform, it seems comprehensible that the recognition of the sc isoform presented in table 1, arises from these molecular based interactions and with more strength when compared with the oc isoform.

Furthermore, these findings are supported by Vologdskii et al., 1992, which reported that the free energy associated with DNA supercoiling was responsible for a 100 fold higher protein association and folding in the sc DNA backbone, when compared to the oc form (Vologodskii et al., 1992).

Besides the H-bond interactions previously mentioned, it is also important to point out that the specific arginine-agarose matrix used for the experiments possesses a 12-carbon spacer arm that is responsible for another type of interactions, the hydrophobic ones.

The results in table 1 also depict the discovery of the concentration range were binding and total elution was promoted with reasonable peak resolution between the two isoforms. From this standpoint, further experiments were performed to find the exact conditions in which sc pDNA could be isolated. These tests were conducted as described earlier for the initial screening experiments, although with different salt concentrations in an attempt to narrow the range in which an efficient separation could be achieved. The chromatographic profile obtained in these circumstances is presented in Fig. 4.

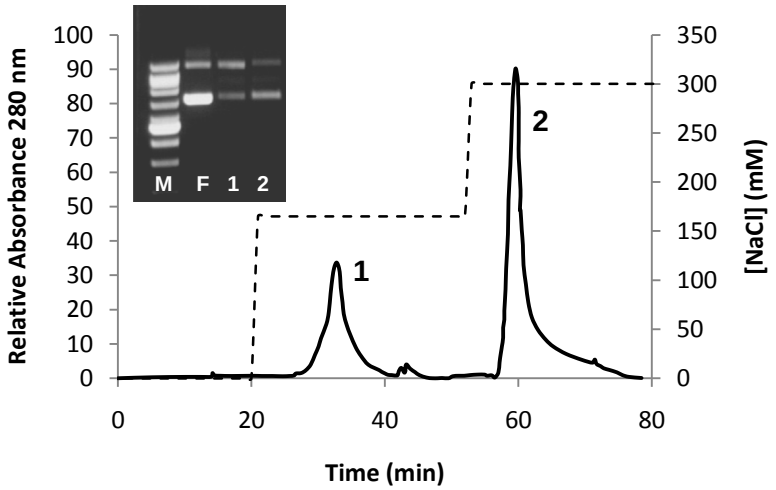

Figure 4. Chromatographic profile showing the purification of different plasmid isoforms by arginine affinity chromatography. Elution was performed at 1mL/min by stepwise increasing the NaCl concentration in the eluent, as represented by the dashed line. Agarose gel electrophoresis for the analysis of the collected fractions. Lane M: molecular weight marker; Lane F – pDNA feed sample injected onto the column (oc+sc); Lane 1 – pDNA recovered from peak 1; Lane 2 – pDNA recovered from peak 2.

Analyzing the chromatographic profile obtained under the described conditions it is clear the existence of two resolved peaks eluting at 165mM (peak 1) and 300mM (peak 2) as the figure demonstrates. In order to indentify the eluted species, peak fractions were recovered during elution and further analyzed by agarose gel electrophoresis. With respect to peak 1 it should be noted that it corresponds mostly to the oc eluted isoform, although, it is important to point out that a small fraction of sc pDNA was also eluted at this salt concentration (Fig. 4, lane 1). Alongside, analysis of the lane corresponding to the second peak higher amount of sc pDNA was recovered, however at the expense of a contamination with oc isoform. It is important to underline that although the salt concentration was optimized in order to promote the elution of the two

isoforms, an amount of sc or oc was always present in the samples whether the concentration of the first gradient was increased or decreased. These findings could be associated with the column equilibration step with Tris.HCl buffer since arginine is very effective in binding pDNA at low ionic strength (Sousa et al., 2007). The fact that the pDNA binds to the affinity support at these conditions suggests that a strong interaction between pDNA and arginine occurs as formerly described. Indeed, it is comprehensible that since pDNA is negatively charged, due to its phosphate groups in the backbone, constructive electrostatic interactions between these groups and the positively charge arginine ligands occur (Sousa et al., 2009). These interactions are present in numerous protein-DNA interactions and provide stability rather than specificity (Sousa et al., 2007), which is related to H-bond formation.

Despite, this does not totally explain the fact that some oc or sc isoforms are more tightly bound than others. A possible explanation may arise from the theory that van der Walls energy fluctuations as well as twisting fluctuations create intercrossed or semi-relaxed intermediate forms (Schlick et al., 2004) like the ones depicted in Fig. 5, and that these interact with the affinity support in different modes.

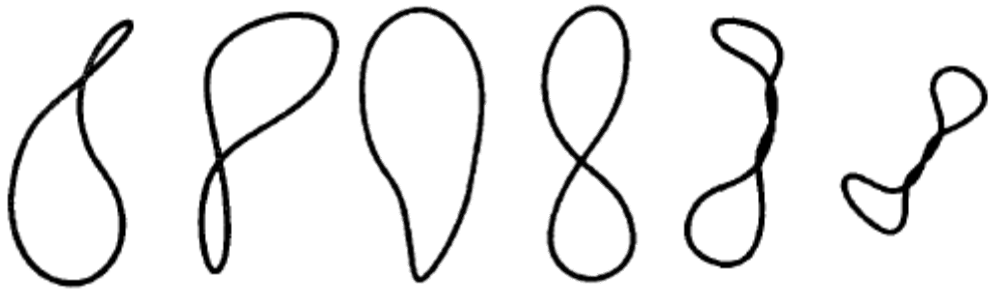

Figure 5. Geometric dynamic fluctuations of the plasmid DNA supercoiling. Denote the interconversion among forms in nearby structural families (Adapted from Schlick et al., 2004).

Hence, to solve this problem additional chromatographic runs with novel parameters were performed to assure the total elution of the oc and sc isoforms independently. These experiments were carried out by initially equilibrating the column not with Tris.HCl buffer, but with a low salt concentration of 112mM NaCl in 10mM Tris.HCl buffer (pH 8.0), at 4ºC, and using a flow rate of 1mL/min. Following the plasmid injection the chromatographic profile obtained is represented in Fig. 6.

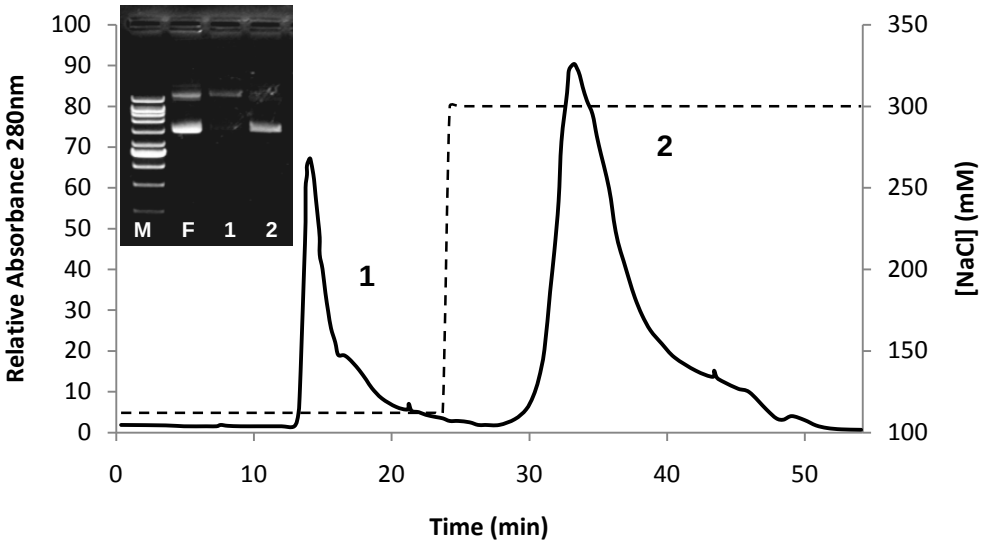

Figure 6. Chromatogram depicting the elution of sc pDNA from the arginine affinity support. Step wise elution was conducted by increasing NaCl concentration in the eluent from 112mM to 300mM (dashed line). Analysis by agarose gel electrophoresis of the collected samples. Lane M: molecular weight marker; Lane F: pDNA sample injected onto the column. Fractions corresponding to peaks (1) and (2) are shown in the corresponding lanes 1 and 2.

According to the binding/elution results obtained with initial low ionic strength conditions two eluted peaks at 112mM NaCl (peak 1) and 300mM (peak 2) were recorded. In order to establish a relationship between peak elution and the corresponding pDNA isoform/s agarose gel electrophoresis was carried out. The analysis of the results revealed that the first eluting peak at the lowest salt concentration corresponded to the elution of the oc pDNA isoform without any sc pDNA eluting from the column, thus further optimizing the results presented in table 1. Moreover, as illustrated in figure 6, lane 2 the sc isoform eluted in the second peak with 100% purity, high yield and structural stability. This result denotes that a stronger interaction and specific recognition by the arginine-agarose matrix takes place. In fact, the instant elution of the oc isoform after injection implies that its interaction with the support is not strong enough. These findings are correlated with those reported in the literature by Sousa et al., 2009.

Although, pDNA binding/elution is not only dependent on these parameters and the effect of temperature needs to be accounted for, since it might influence the interactions with the arginine support and consequently the reproducibility of the purification strategy. To address this influence an experiment at 25ºC temperature was performed. Initially the column was equilibrated with higher salt concentrations 170mM NaCl in Tris.HCL buffer (pH 8) due to the previously described results that showed that

higher temperatures increase retention. In fact, as it can be seen in figure 7, the resulting chromatographic profile presented an increase in pDNA isoform retention when the temperature was increased.

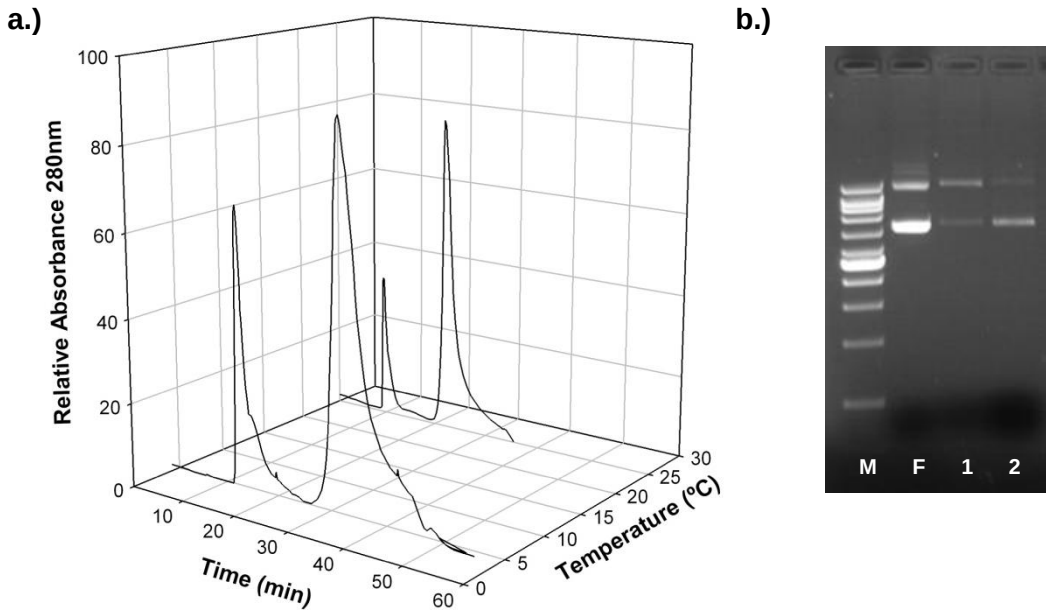

Figure 7. Effect of temperature on the retention of the different plasmid isoforms in arginine affinity chromatography 4ºC and 25ºC. a.) The elution was performed at 1mL/min by increasing NaCl concentration from 170mM to 300mM. b.) Agarose gel electrophoresis of the collected peak fractions. Lane M: molecular weight marker; Lane F: Feed pDNA sample; Lane 2: predominant oc isoform; Lane 3: predominant sc isoform.

As denoted in figure 7 the pDNA isoform retention increased with the increase in temperature. This fact affected the efficiency of the purification process since the recovered oc isoform that eluted at 170mM had some sc contamination (figure 7b, lane1). Moreover, the opposite is also evident in figure 7b (lane 2) since the collected sc fractions where approximately 98% pure because they contained residues of oc pDNA.

These results might be attributed to the multitude of interactions that where formerly described. This fact is supported by the results obtained by Müller, 1986 that demonstrated that the elution of dsDNA fragments needed higher salt concentrations whenever the temperature was risen (Müller, 1986). However, it is also important to underline that the binding of the pDNA into the chromatographic support occurs at low salt concentrations (<300mM), what is quite the opposite that occurs in HIC. However, since the retention was promoted by an increase in temperature, and since HIC is a thermodynamically driven process this suggests that hydrophobic interactions promoted by the 12 - carbon spacer arm might occur, as described by Sousa et al., 2007.

Overall the affinity purification approach was able to purify the sc pDNA isoform with 100% purity and stability. Additionally, it is also important to state that the whole purification process occurs at mild conditions, i.e low salt elution conditions, an issue of great importance which demonstrates the feasibility of this approach for its inclusion in an integrative gene based treatment, from production to application. Nonetheless these results reveal themselves quite interesting in the way that they can be extrapolated in to an industrial scale pDNA purification process for therapeutic applications. Hence, after recovery the highly purified sc pDNA samples are encapsulated in nanocarrier systems that will be responsible for their transport into the cellular compartment.

3.3. Formulation of chitosan-TPP nanoparticles

The delivery of genetic material to the intracellular compartment with intact structural stability is mandatory for the correct and sustained expression of the transgene of interest. Nanoparticles composed of cationic polymers arise as promising candidates for the delivery of the genetic material. However, a multitude of parameters influences the overall process of manufacture of the delivery systems, and ultimately the encapsulation of the DNA.

In order to address these issues and tailor the most beneficial characteristics that improve the different nanocarrier systems, the formulation parameters of nanoparticulated systems composed of chitosan-TPP blank nanospheres (CS-TPP) and chitosan-TPP-pDNA nanocapsules were formulated by the ionotropic gelation, a technique that promotes extremely mild encapsulation conditions.

The experiments were performed by the drop wise addition of TPP into the commercial chitosan solution at a CS-TPP volume ratio of 4:1 respectively, at variable concentrations. A phase diagram with the different behaviors observed is represented in figure 8.

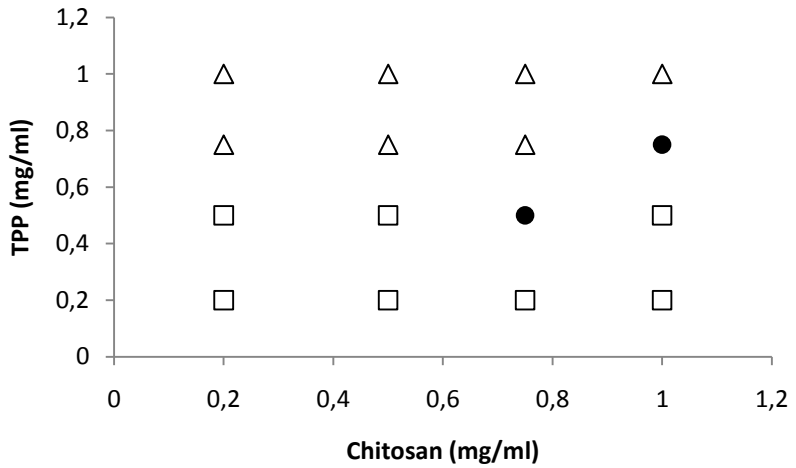

Figure. 8. Phase diagram of nanoparticle formation for commercial chitosan. (□) Concentrations not suitable for particle formation or too low for morphological analysis. (●) Concentrations leading to the formation of nanoparticles. (∆) Concentrations where particle aggregation takes place.

Analyzing the phase diagram in figure 8, it is clear that the formation of the nanoparticles took place only for specific concentrations. It is important to denote that if the polyanion concentration was too low no particle formation occurred and a clear solution was observed. Whereas, if the initial amount of TPP was too high particle aggregational events occurred and, in this case, the solution appeared as an opalescent suspension.

These findings are a consequence of the forces between the positively charged polymer chains and the negatively charged polyanion species. Indeed, Hayashi et al., 2002, using a screened Coulomb potential model, based on Monte Carlo simulations studied these electrostatic interactions between oppositely charged polyelectrolytes in solution. Hayashi and collaborators also reported that the nature of the formed complexes is dependent on the linear charge density of the chains, and that positively charged polyions undergo contraction when complexation with counterion species occurs (Hayashi et al., 2002). In fact, this was exactly the same behavior that promoted the controlled gelation of chitosan into well defined nanoparticulated systems when TPP was added to the polymer solution. Previously, it was also demonstrated that for shorter equilibrium bond lengths charged and well separate complexes were formed, whereas for longer equilibrium bond lengths larger and less defined clusters were obtained (Hayashi et al., 2002). The latter can explain why the formation of aggregates occurs in solution. Moreover, it was also reported that charged nanoparticles are likely to form aggregates when a sufficiently high concentration of a counterion is added to the solution (Richardi, 2009). The counterion is responsible for the disruption of the

particle-particle repulsion barrier that defines their stability as individual colloids, leading to aggregation (Richardi, 2009).

It becomes therefore clear that the formation of stable unaggregated nanoparticles occurs only at precise conditions as can be observed in figure 8.

In an attempt to further study other nanoparticle formation conditions, and once the concentration zone of smaller size particle formation was defined (CS – 0.75mg/mL; TPP – 0.5mg/mL), further experiments regarding other (v/v) ratios of chitosan and TPP solutions (5:1 and 6:1 respectively) were conducted, using the same conditions described for the experiments at the 4:1 ratio.

Notwithstanding, it is important to underscore that the results presented in figure 8 correspond to experiments performed with the commercially available chitosan material which contained some contaminants. This issue is of most importance since that any biomaterial used for gene delivery applications, projected to be included in an *in vivo* biological environment needs to be free of protein contaminants that may trigger a deleterious immune response from the host. Therefore, the removal of these contaminants is mandatory. Furthermore, it is also important to assure that the material used for the assembly of nanospheres and nanocapsules has the highest purity and integrity to assure the reproducibility of the process.

Taking this into account, the chitosan material was submitted to a thorough purification process described in section 2.2.3.

Simultaneously, the polymer was also deacetilated and reacetilated in an attempt to address the influence that the primary amine groups would have in particle formation. The several differences observed in the different experiments are addressed in the following section.

3.4. Morphology and characterization of CS-TPP blank nanoparticles

The morphological analyses of the nanoparticles formed for the differently processed chitosan materials and ratios, are presented in figures 9, 10, and 11.

Global results demonstrate that both for commercial deacetilated and reacetilated chitosan flakes nanoparticles are formed with well defined spherical shapes along the range of ratios. The spherical and compact morphology is a consequence of the chitosan controlled gelation promoted by TPP (Janes et al., 2001). These results correlate with the photographs of CS-TPP nanoparticles taken by Calvo and collaborators that exhibited round and solid structure (Calvo et al., 1998).

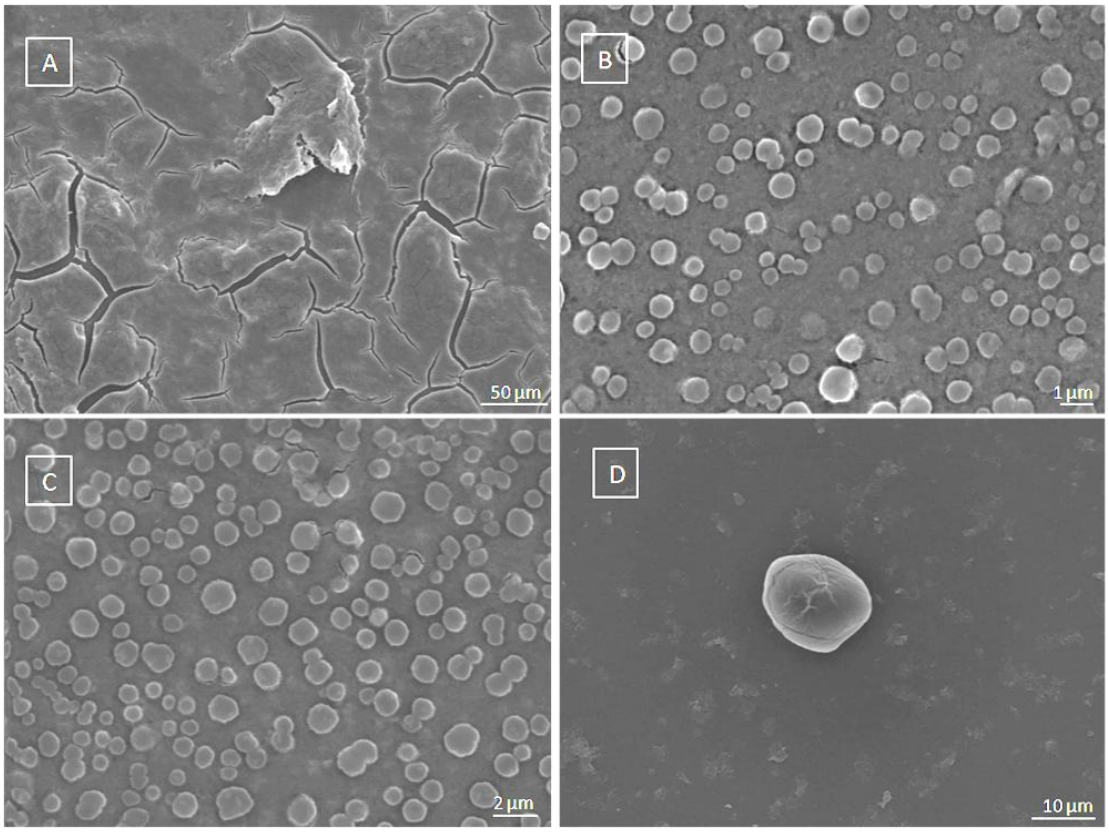

Figure 9. Morphology of the nanoparticles obtained from commercial chitosan flakes visualized by SEM. A.) Nanoparticle aggregation at 1:1 (v/v) ratio. B, C and D.) Particles formed at different ratios, 4:1; 5:1 and 6:1 respectively.

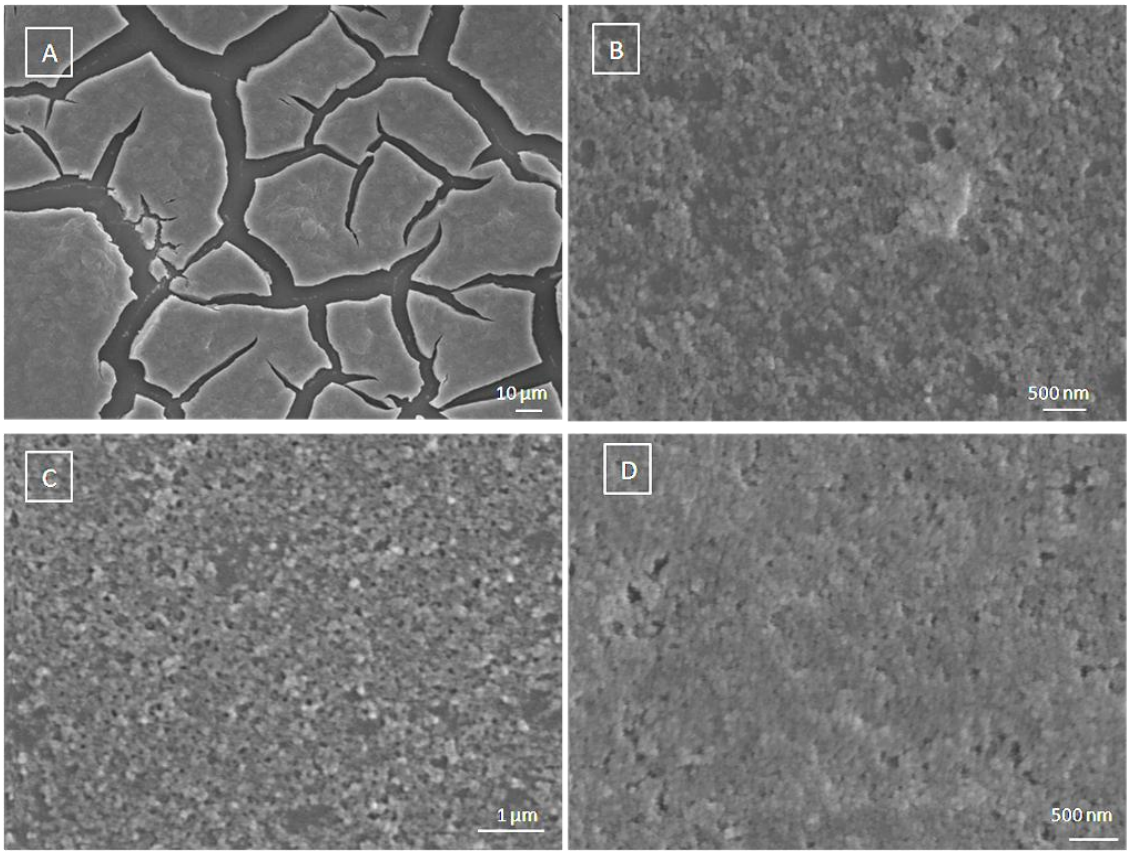

Figure. 10. Morphology of the nanoparticles obtained from deacetilated chitosan visualized by SEM. A.) A.) Nanoparticle aggregation at 1:1 (v/v) ratio. B, C and D.) Particles formed at different ratios, 4:1; 5:1 and 6:1 respectively.

Analyzing the figures 9a and 10a it should be noted that for CS-TPP ratio of 1:1 a chitosan film was formed instead of well defined nanoparticles, these findings are a consequence of the excess of the concentration of the polyanion in respect to that of the polycation, i.e. chitosan, resulting in a cross-linking degree so high that a gel-like structure was formed. With the respect to the figures 9, 10, b and c, nanoparticles with defined morphological characteristics were formed equally despite the chitosan material used. Although, it is important to underline that the experiment with the deacetilated polymer performed at a 6:1 ratio showed initial signs of particle aggregation as can be observed in figure. 10d. Moreover, it is also important to indicate that the experiment with the commercial chitosan material at the same ratio yielded nanoparticulated systems with far greater size. These two issues will be further discussed. The results regarding the experiments conducted with the reacetilated material are represented in figure 11.

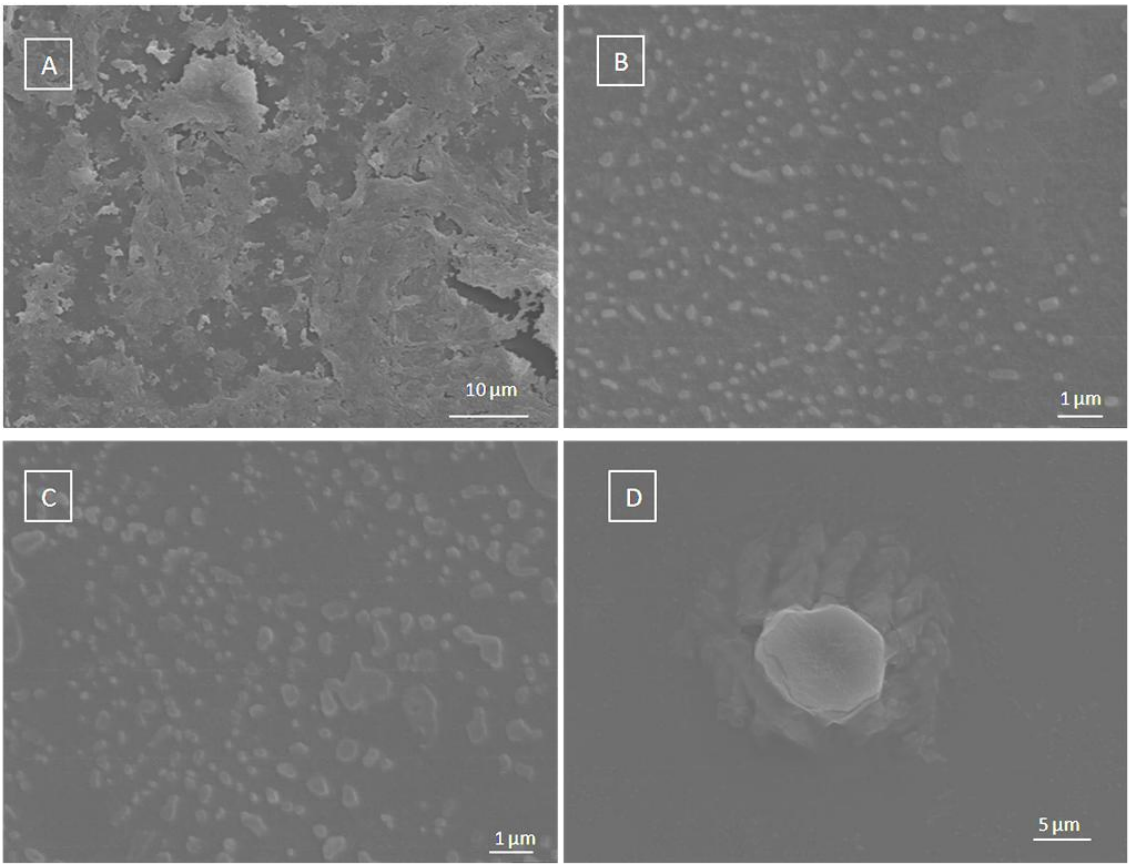

Figure 11. Morphology of the nanoparticles obtained from acetilated chitosan visualized by scanning electron microscopy (SEM). A.) Nanoparticle aggregation at a 1:1 ratio. B,C and D) Particles formed at different ratios, 4:1; 5:1 and 6:1 respectively.

Though the analysis of the results presented in figure 11 it is visible that a chitosan filmed was produced at the 1:1 ratio. This finding is in accordance with the previously results obtanined for the other tested materials. Although, when comparing the morphology of the particles obtained from reacetilated chitosan in the figures 11b and 11c with those from the other experiments it is clear that the nanoparticles formed using the commercial and deacetilated material were arranged in defined sphere-like structures, whereas those produced with the reacetilated polymer present toroid and rod- like morphologies. These are important results since it has been previously demonstrated that the shape of the nanoparticles largely influences its transfection efficiency (Chithrani and Chan, 2007). As demonstrated by Chithrani and Chan the nanoparticles with spherical shape had greater uptake that those with rod-like morphology. This intriguing phenomena was related with the time that the cell takes to engulf the different shaped particles, changing according to their volume-surface relationship (Chithrani and Chan, 2007).

Further characterization of the nanoparticulated systems, mainly concerning their size, was performed using the SEM image acquisition software and the results that were obtained for the different particles are presented in table 2.

Table 2. Nanosphere size distribution obtained from different chitosan materials at variable chitosan-TPP ratios measured by SEM image acquisition software

	Particle Size (nm)		
Ratio	**Reacetilated Chitosan**	**Commercial Chitosan**	**Deacetilated Chitosan**
4:1	242 – 348	573 - 890	66 – 73
5:1	636 – 515	765 - 1635	87 - 150
6:1	10190	18619	Aggregates

As table 2 shows, the particle size generally increased as the chitosan amount increased. These findings are consistent with the results obtained by (Gan et al., 2005). In respect to the lower CS-TPP ratio the smaller particle size obtained was a consequence of the cross-linking due to the higher presence of the polyanion (TPP) in the mixture, which in turn resulted in a more densely packed particle structure. The manipulation of the nanoparticle size is important because this characteristic plays an essential role in the delivery of the genetic material to the intracellular compartment as described earlier. The success of gene delivery using nanoparticles has shown to be very dependent on the size of these systems. Prabha et al, 2002 demonstrated that 27-fold higher transfection efficiency levels in COS-7 cells were attained when smaller-sized nanoparticles were used as an alternative to larger ones (Prabha et al., 2002).

The analysis of the results obtained for deacetilated chitosan in table 1 it is observed that considerably smaller particles were formed when compared to those synthesized from commercial or reacetilated chitosan samples. Moreover, not only the particle sizes were smaller but also the particle size distribution was narrower, a parameter that is also important for the release of the nanoparticle content and the transfection efficiency of these systems (Prabha et al., 2002, Zhang et al., 2004). Additionally, it is important to point out the results obtained for the reacetilated nanoparticles, since they possessed a smaller size than those synthesized with the commercial polymer. Despite the fact that these seem strange findings (since the polymer charge in the reacetilated material is less positive) and their exact nature is unknown they may be explained by the fewer amount of particles formed. Which suggests that TPP molecules react with a smaller amount of charged chains that undergo higher contraction.

It is therefore clear that the deacetilation/acetilation degree of chitosan influences the particle size and other characteristics like its encapsulation efficiency, an issue that will

be further discussed in the next section. Taking this into account, it is therefore important to determine the percentage of the primary amines, i.e. the DD of the different polymer samples. The determination of the DD was in accordance to the previously described parameters in section 2.2.4. The results of the performed experiments are represented in table 3.

Table 3 Degree of Deacetilation of the different chitosan samples as measured by 1DUVS (means ± SD., *n* =3).

Chitosan Sample	Nominal DD* (%)	Determined DD** (%)
Comercial	75-85	85,58 ± 0,81
Deacetilated		98,82 ± 0,01
Acetilated		76,72 ± 2,12

*Provided by the manufacturer

**Determined by 1DUVS

As table 3 implies, the deacetilation degree obtained for chitosan is above 98%, which means that almost all the primary amine groups along the chitosan polymer chain are positively charged and therefore ready to react not only with TPP but also with pDNA, as it will be demonstrated in the next sections.

A further study was performed in an attempt to analyze the influence that the modification of the DD would have on the polymer thermodynamic properties and crystalinity. Therefore, a series of experiments were conducted to determine the x-ray diffraction spectra of the different chitosan samples. The results obtained are presented in figure 12.

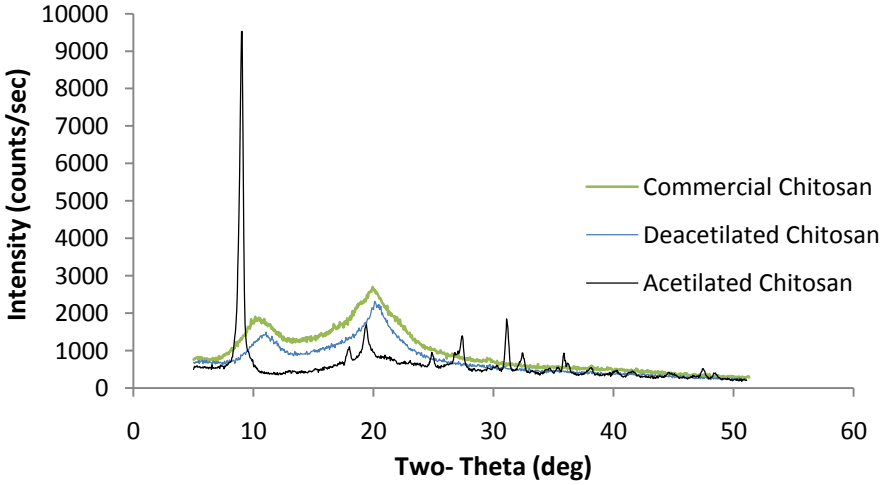

Figure 12. XRD spectra of different chitosan samples. (Yellow – commercial chitosan; Blue – deacetilated chitosan; Black – acetylated chitosan).

Analyzing the spectra for the different chitosan samples it can be observed that in the commercial chitosan sample which as the characteristic crystalline peaks of chitosan when compared with its theoretic key card (Check Appendices I). In respect to the deacetilated sample it can be observed that the peak at $2\theta = 10.15°$ and $2\theta = 20.55°$ shifted to the left to $2\theta = 11.05°$ and $2\theta = 20.45°$, this might be due to a polymoph structure change from the initial crystal form to an even most thermodynamically stable form (Yang et al., 2010). This fact is critical since it influences the characteristics of the delivery system in the organism. Regarding the acetylated sample a huge collapse in the crystalline structure is observed since the characteristic peaks of chitosan disappeared. Correlating this with the morphology of these particles the structure of the polymer chain may also therefore influence the formation of more stable and morphologically defined nanoparticles.

3.5. Synthesis of pDNA loaded nanoparticles - Nanocapsules

The entrapment of the pDNA inside the nanoparticles is a crucial step for further delivery into the cellular environment. Thereof several experiments were performed to promote the incorporation of the genetic material inside the particle core. The experiments were carried out by using the ionotropic gelation mechanism since it not only promotes the formation of the particle systems, as denoted earlier, but also favors the stability and entrapment of the pDNA, due to the mild conditions used (pH, stirring and temperature). The nanocapsules obtained from these experiments are represented in figure. 13, 14 and 15.

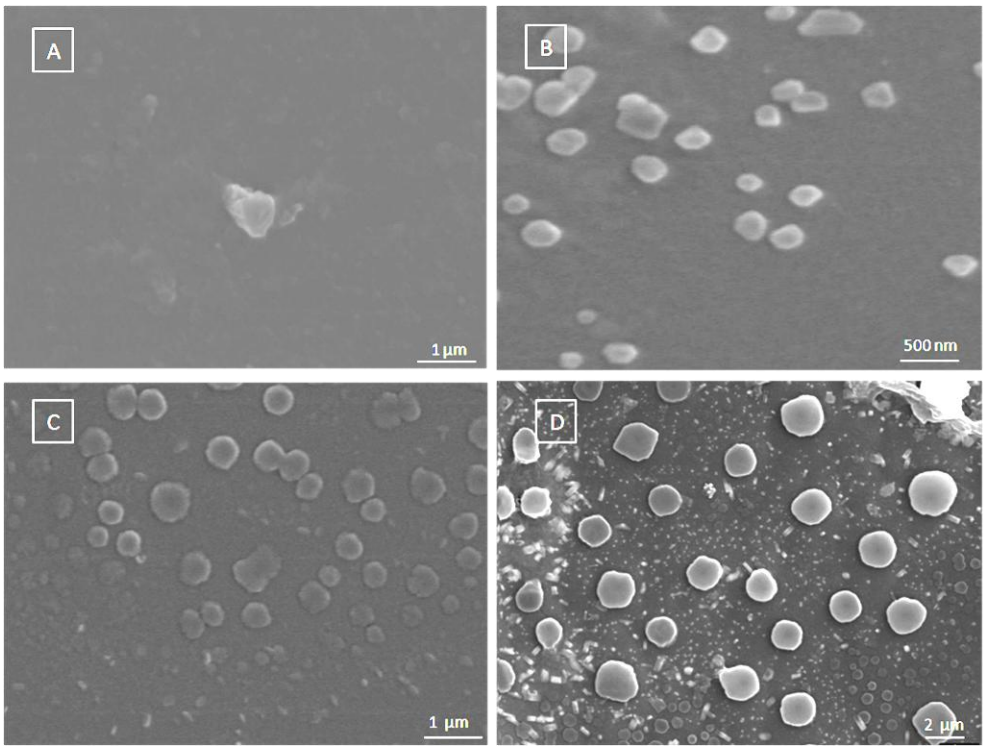

Figure 13. Nanocapsules obtained from commercial chitosan flakes visualized by SEM. A.) Polyplexes obtained from chitosan and pDNA at a 4:1 amine to phosphate ratio. B, C and D.) Nanocapsules loaded with pDNA (13µg/mL) formed at different CS-TPP ratios (4:1; 5:1 and 6:1 respectively).

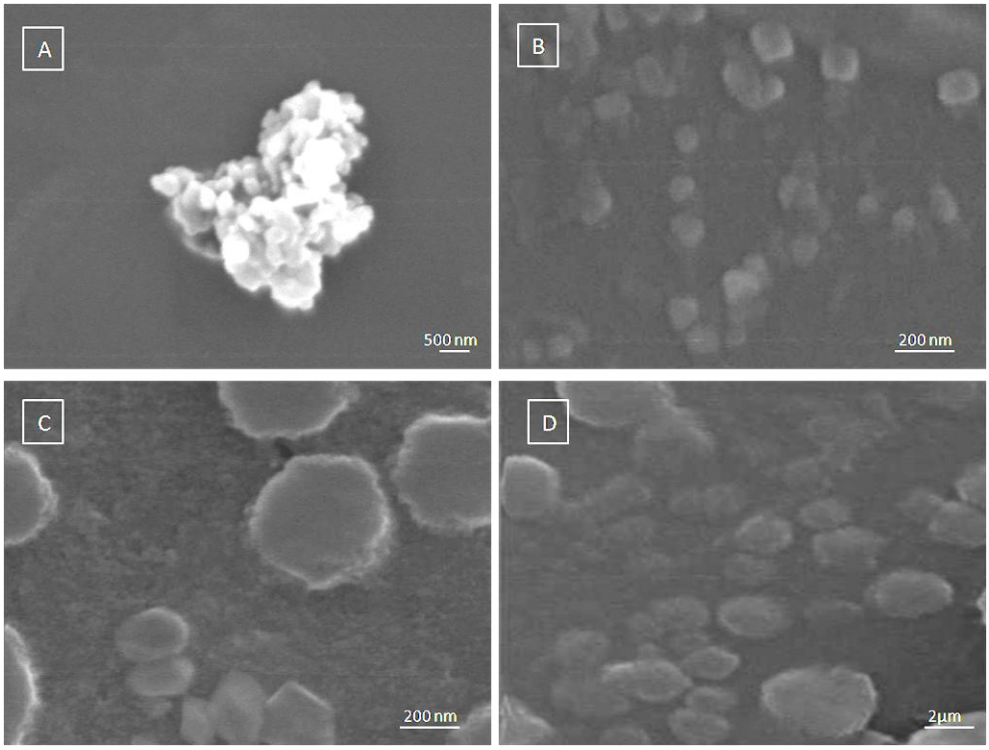

Figure. 14. Nanocapsules synthesized from deacetilated chitosan visualized by SEM. A.) Polyplexes obtained from chitosan and pDNA at a 4:1 amine to phosphate ratio. B, C and D.) Nanocapsules loaded with pDNA (13µg/mL) formed at different CS-TPP ratios (4:1; 5:1 and 6:1 respectively).

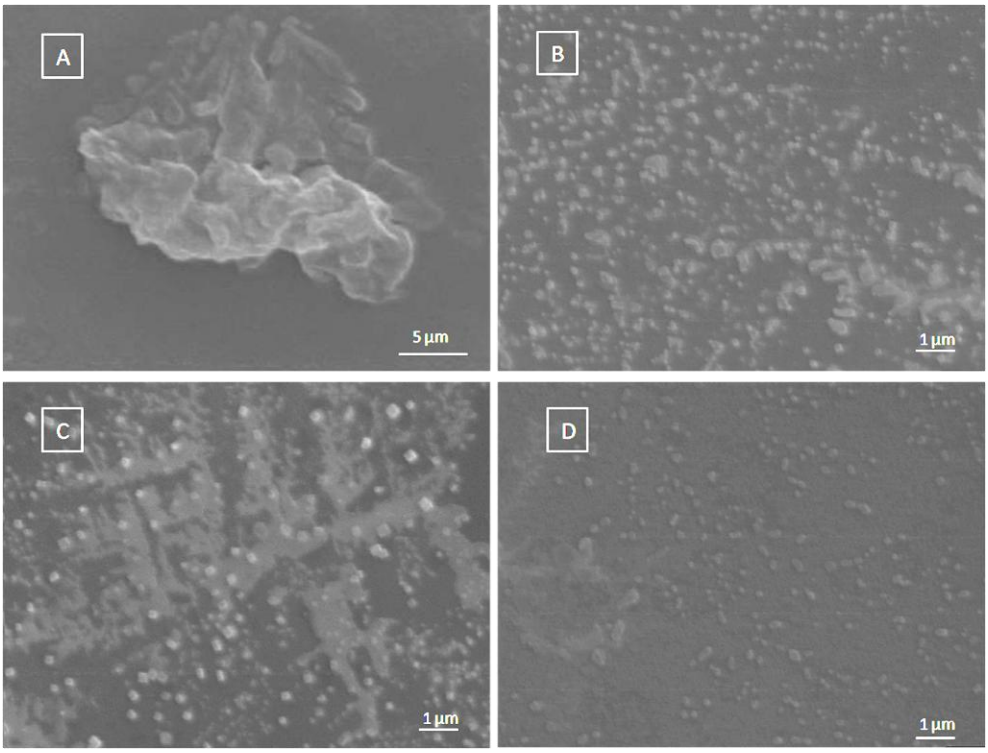

Figure. 15. Nanocapsules synthesized from acetilated chitosan visualized by SEM. A.) Polyplexes obtained from chitosan and pDNA at a 4:1 amine to phosphate ratio. B, C and D.) Nanocapsules loaded with pDNA (13µg/mL) formed at different CS-TPP ratios (4:1; 5:1 and 6:1 respectively).

A thorough analysis of the figures 13 to 15 reveals that the morphology was maintained for the three different samples in respect to their nanoparticle counterparts. It is also quite interesting to denote the morphological characteristics associated with polyplexes that showed an unorganized structure. This outcome reinforces the idea that the defined spherical shapes obtained are a consequence of the electrostatic interaction promoted by the counterion, TPP. The results concerning the nanospheres particle size are represented in table 4.

Table 4. Comparison between the different particle sizes obtained for variable formulations of CS-TPP-pDNA nanocapsules.

	Particle size (nm)		
Ratio	**Reacetilated**	**Commercial**	**Deacetilated**
4:1	154 - 226	191 - 303	113 - 197
5:1	278 – 424	354 - 722	295 - 622
6:1	293 - 817	1925 - 2637	1107 - 1885

Table 4 shows that the nanocapsules mean particle size is reduced (in comparison with those of table 3), with the addition of pDNA in the three different samples, suggesting that the presence of an additional negatively charged specie promotes the contraction of the positively charged polymer chain. In addition the neutralization degree of the charged amino groups is significantly improved originating a smaller net charge also responsible for the smaller particle size as reported by Liu and Gao, 2008 (Liu and Gao, 2008). The analysis of the size differences between the commercial (≈ 85% DD) and deacetilated (≈98%) chitosan nanocapsules shows that the mean particle size for the latter is smaller. However, it is also important to underline the size of the reacetilated (≈ 76%) nanocapsules which, once again, is smaller than the commercial ones. These results may be explained by the encapsulation of the pDNA and will be further discussed.

3.6. Nanocapsule encapsulation efficiency and loading capacity

The ability of the carrier system to encapsulate as much genetic material as possible is an important parameter to improve the delivery of the pDNA to the cells. Hence to address this characteristic, several experiments were performed to determine the encapsulation efficiency of the nanoparticulated systems. Moreover, additional experiments were conducted in an attempt to shed some light concerning the encapsulation efficiency of the different pDNA isoforms. The results that were obtained are presented in table 5.

Table 5. Encapsulation efficiency of the nanocapsules obtained from different chitosan materials (mean ± SD, *n*=3).

Encapsulation Efficiency (%)						
		Chitosan			Deacetilated Chitosan	
Ratio	**pDNA loading (µg/mL)**	**Reacetilated**	**Commercial**	**Deacetylated**	**Supercoiled (sc)**	**Open Circular (oc)**
4:1	13	31,11 ± 0,3	41,41 ± 0,4	54,10 ± 0,8	75,11 ± 0,1	22,94 ± 0,4
5:1	13	41,96 ± 0,2	44,35 ± 0,1	56,28 ± 0,5	-	-
6:1	13	53,57 ± 0,4	57,94 ± 0,3	75,89 ± 0,2	-	-

As the results in table 5 demonstrate, the encapsulation efficiency of the deacetilated nanocapsules is higher than that of the nanocapsules synthesized from commercial or acetylated chitosan flakes. In agreement with these results, Kiang et al, 2004, previously reported that the degree of deacetilation affects the DNA binding and hence *in vitro* and *in vivo* gene transfection efficiency (Kiang et al., 2004). Furthermore, these findings demonstrate that the amount of pDNA entrapped inside the nanocapsules increases with the CS-TPP ratio, suggesting that the encapsulation of the pDNA also depends on the amount of polymer or polymer charge that can react with the negatively charged phosphate groups present in the pDNA backbone. Regarding the results for encapsulation efficiency in reacetilated samples it is important to denote that pDNA is less entrapped in these systems possibly due to the lack of enough positively charged amines. This fact may also be responsible for their smaller size when compared with commercially synthesized nanocapsules.

With respect to the experiments with the different pDNA isoforms isolated using the arginine chromatography method, they were performed using the 4:1 ratio since it was the one that yielded smaller and narrower particle size ranges. The results in table 5 demonstrate that the sc isoform is encapsulated with far greater efficiency than the oc. These findings were quite surprising, suggesting that the compact structure of the sc isoform might play an important role also in encapsulation. Nonetheless, the encapsulation of the sc isoform in the nanoparticulated systems gains further importance due to the fact that sc pDNA yields far greater transfection efficiency as previously reported (Sousa et al., 2008b), and therefore enhances the therapeutic effect.

Additionally results regarding the pDNA partition, mainly the nanocapsule loading capacity ,were also performed and the results obtained are presented in table 6.

Table 6. Loading capacity of the nanocapsules obtained from different chitosan materials (mean ± SD, *n*=3).

		Loading capacity (%)		
Ratio	**pDNA loading (µg/ml)**	**Reacetilated**	**Comercial**	**Deacetylated**
4:1	13	*	41,41 ± 0,4	54,10 ± 0,8
5:1	13	*	44,35 ± 0,1	56,28 ± 0,5
6:1	13	*	57,94 ± 0,3	75,89 ± 0,2

*Too low for quantification

Examining the results in table 6 it is understood that the nanocapsules formulated by deacetilated chitosan possess higher loading capacity than the commercial formulations. In fact it is important to underline that for a 4:1 ratio approximately 54% of the nanocapsule is composed of pDNA. In contrast the loading capacity of the reacetilated nanocapsules was not determined due to the fact that the particles formed were too few to yield significant results.

3.7. Protection and in vitro release of pDNA

The development of nanocapsules that are stable in the extracellular environment is essential for the protection of the genetic material. In fact the serum nucleases are a major concern that affects pDNA stability and consequently its transfection efficiency. In this way, to address if a proper protection of pDNA was promoted by its encapsulation in the particles a stability study with the commercial and purified chitosan nanocapsules was performed using DNAse I and FBS. The results obtained for the endowed protection from DNase I activity are depicted in figure 16.

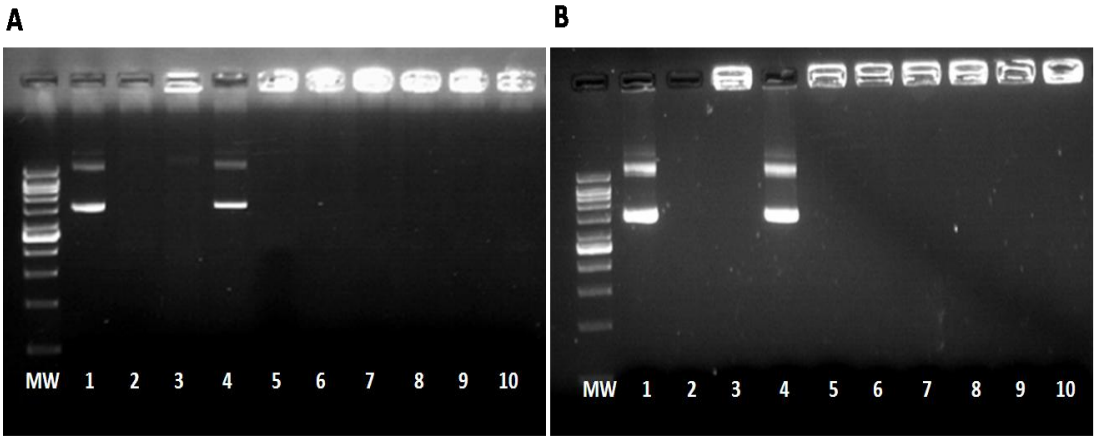

Figure 16. Agarose gel electrophoresis of the nanocapsules following incubation with DNAse I. A.) Comercial Chitosan. B.) Deacetilated Chitosan. MW –molecular weight marker, Lane 1 – pDNA; Lane 2 – pDNA + DNAse I (10µg/mL); Lane 3 – DNA polyplexes, (N-P ratio 4:1); Lane 4 – TPP + pDNA; Lane 5 – pDNA NC (4:1); Lane 6 – pDNA NC (5:1); Lane 7 – pDNA NC(6:1); Lane 8 - pDNA NC (4:1) + DNAse I; Lane 9 – pDNA NC (5:1) + DNAse I; Lane 10 – pDNA NC (6:1) + DNAse I.

Regarding the protection promoted from the nanoparticulated systems it should be noted that neither the pDNA in the nanocapsules produced with commercial chitosan, nor the pDNA in the nanocapsules obtained from deacetilated chitosan showed any signs of degradation when in contact with DNAse I. Whereas the naked pDNA was completely degraded after 1h of incubation (figure 16a and 16b, lane 2). Furthermore, to assure that no protection of the pDNA was promoted by the polyanion, but only from chitosan, a control with polyplexes and TPP was also performed (figure 16a and 16b,

lane 4). It can be denoted that the pDNA was not retained in the well and migrated in the agarose gel.

Similar results were obtained when the nanocapsules were incubated with serum-supplemented Ham's F12K (figure 17).

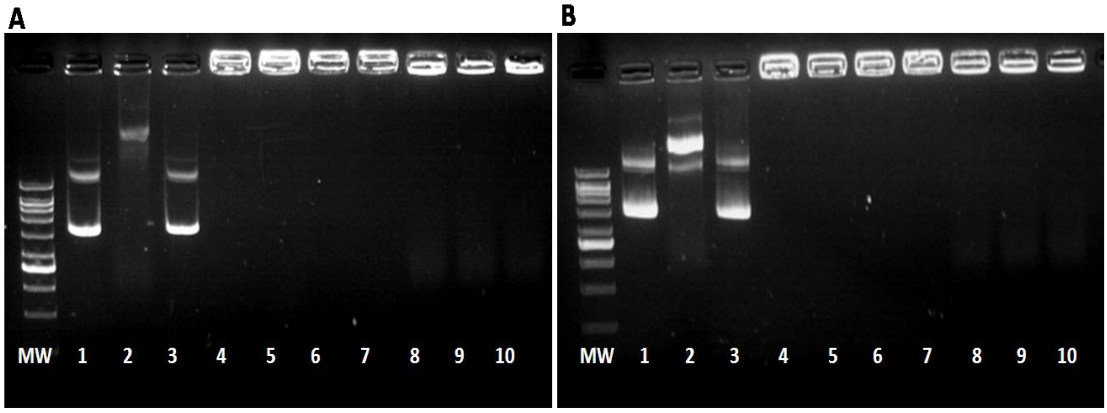

Figure 17. Agarose gel electrophoresis of the nanocapsule protection of pDNA following incubation with serum-supplemented Ham's F12K. A.) Commercial chitosan. B.) Deacetilated Chitosan. MW – molecular weight marker, Lane 1 – pDNA; Lane 2 – pDNA + FBS (10%); Lane 3 – DNA polyplexes, (N-P ratio 4:1); Lane 4 – TPP + pDNA; Lane 5 – pDNA NC (4:1); Lane 6 – pDNA NC (5:1); Lane 7 – pDNA NC(6:1) + FBS (10%); Lane 8 - pDNA NC (4:1) + FBS (10%); Lane 9 – pDNA NC (5:1) + FBS (10%); Lane 10 – pDNA NC (6:1) + FBS (10%).

Addressing the results in figure 17 no degradation of the nanocapsules occurred when in contact with FBS (figure 17a and 17b, lanes 5 to 10). On the contrary the pDNA incubated with FBS showed signs of degradation which implies that the serum nucleases are responsible for degradation of the vector structure (figure 17a and 17b, lane 2). Generally, both nanocapsule formulations were able to protect DNA against serum degradation thus suggesting that they are suitable delivery vehicles for gene delivery applications *in vivo*. Moreover, it should be noted that these results reinforce the idea that pDNA is located within the particles and protected by a shell structure.

In a further attempt to mimic the *in vivo* degradation environment pDNA loaded nanocapsules were incubated with lysozyme, an enzyme that is known to degrade chitosan *in vivo.* The experiments were conducted in different time frames (1, 3, 12 and 24h) to address whether the nanocapsules were promptly degraded *in vivo* or not, the results obtained are shown in figures 18 and 19.

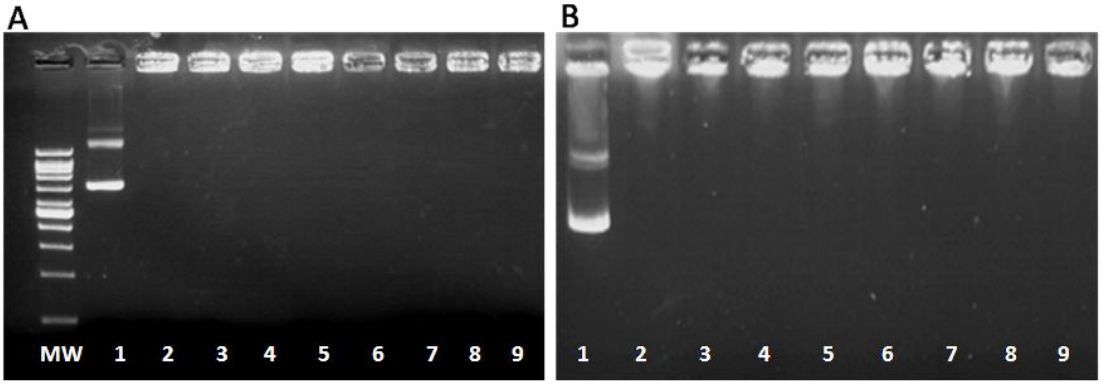

Figure 18. Agarose gel electrophoresis of the nanocapsule protection of pDNA following incubation with lysozyme (10mg/mL) for 1 and 3 h. A – commercial chitosan and B – deacetilated chitosan. MW – molecular weight marker; Lane 1 – pDNA; Lane 2 – DNA polyplexes (N:P ratio 4:1); Lane 3 – pDNA NC (4:1); Lane 4 – pDNA NC (5:1); Lane 5 – pDNA NC (6:1), 1h incubation time. Lane 6 – DNA polyplexes (N:P ratio 4:1); Lane 7 – pDNA NC(4:1); Lane 8 - pDNA NC (5:1); Lane 9 – pDNA NC (6:1), 3h incubation time.

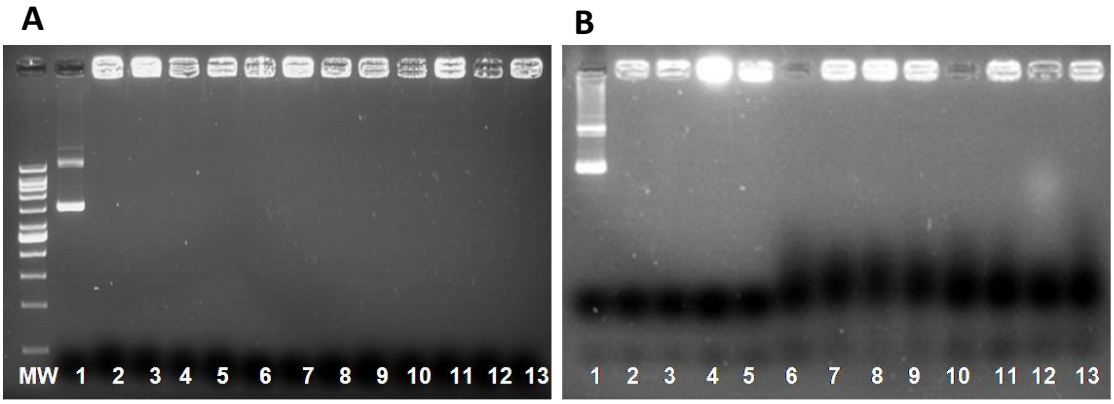

Figure 19. Agarose gel electrophoresis of the nanocapsule protection of pDNA following incubation with lysozyme (10mg/mL) for 12 and 24 h. A – commercial chitosan and B – deacetilated chitosan. MW – molecular weight marker; Lane 1 – pDNA; Lane 2 – DNA polyplexes (N:P ratio 4:1); Lane 3 – pDNA NC (4:1); Lane 4 – pDNA NC (5:1); Lane 5 – pDNA NC (6:1), controls incubated in PBS for 24h. Lane 6 – DNA polyplexes (N:P ratio 4:1); Lane 7 – pDNA NC (4:1); Lane 8 - pDNA NC (5:1); Lane 9 – pDNA NC (6:1), 12h incubation time; Lane 10 – DNA polyplexes (N:P ratio 4:1); Lane 11 – pDNA NC (4:1); Lane 12 - pDNA NC (5:1); Lane 13 – pDNA NC (6:1), 24h incubation time.

The results concerning the incubation with lysozyme for a period of 1 and 3 h demonstrate that the polymer matrix begins to degrade either for commercial (figure 18a) or deacetilated samples (figure 18b). However, it is important to point out that for the commercial chitosan the polymer matrix seemed to degrade more rapidly (figure 18, lanes 6 to 9). In respect to the 12 and 24h period the commercial polymeric matrixes denoted higher degradation, although when compared with their controls immersed in PBS they also showed some degradation (figure 19, lanes 2 to 5), which

suggests that the presence of saline solutions may also influence the release behavior of the nanocarriers. These results may be important to clarify that not only lysozyme is responsible for *in vivo* degradation.

3.8. In vitro transfection

The previous formulation of nanoparticulated systems was able to accomplish the entrapment and protection of the pDNA inside their core. Despite these achievements the nanocapsules must ultimately be able to transport their payload into the malignant, which is the main objective. Indeed, it is well known that a multitude of barriers arise and the whole formulation and optimization process is in check at this critical stage. Taking this into account experiments regarding the transfection of malignant cells *in vitro* were performed to address the viability of these systems as carriers for pDNA.

Initially a set of preparative pDNA delivery experiments were conducted with a commercially available transfection system to ascertain the transfection of the neoplastic cells. The results obtained are depicted in figure 20.

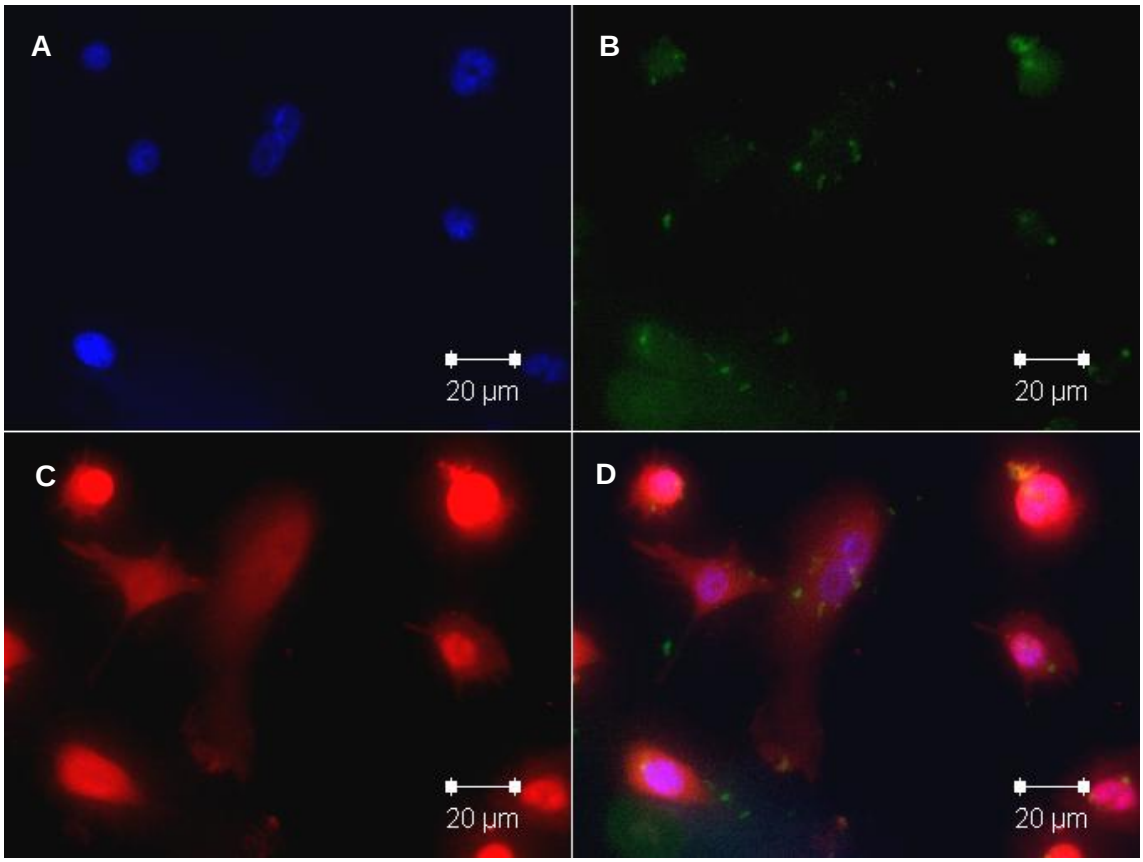

Figure 20. Immunofluorescence of A549 Lipofectamine^{2000} – pDNA transfected cells. A.) Nuclear staining with Hoesht 33322 (blue); B.) Lipofectamine-FITC labeled pDNA complexes (green); C.) Staining with Anti-VE cadherin antibody (red); D.) Merged image. The micrographs were obtained at 63x magnification.

The transfection trials presented in figure 20 showed that not only the A549 malignant cell line is prone to transfection, but also that FITC labeled pDNA when associated with cationic lipossomes is able to likely localize itself in the intracellular compartment (figure 20d).

Following these trials the experiments to examine the transfection efficiency of the chitosan nanocapsules were performed. The nanocapsules were formulated at a 4:1 ratio, with FITC labeled pDNA, since this was the one that yielded smaller particle sizes. The results from these studies are presented in Fig. 21.

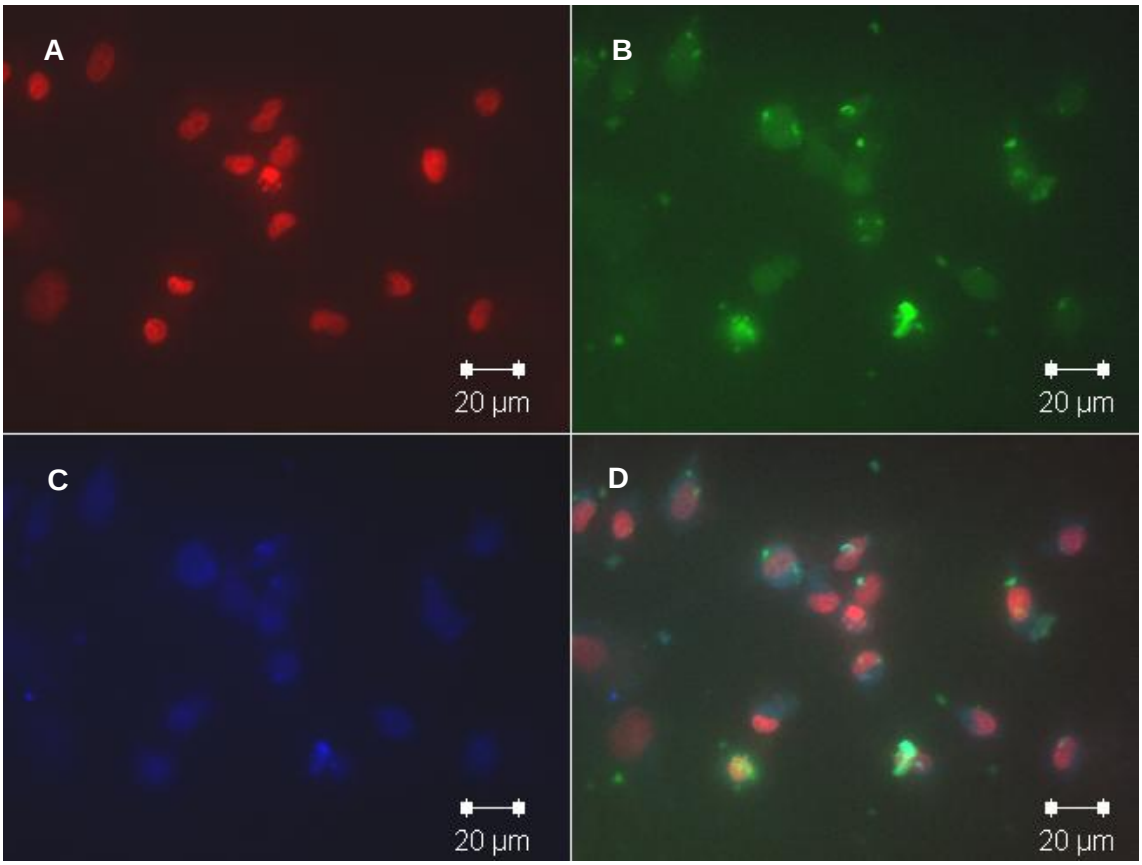

Figure 21. Immunofluorescence of A549 nanocapsule transfected cells. A.) Staining with Anti-VE cadherin antibody (red); B.) Lipofectamine-FITC labeled pDNA complexes (green); .C.) Nuclear staining with Hoesht 33322 (blue); D.) Merged image. The micrographs were obtained at 63x magnification.

Through the analysis of the above figure it is clear that the nanoparticulated systems that were developed are capable of transposing the barriers that hinder the delivery of the genetic material. Depicted in figure 21 d the green fluorescent dots (corresponding to the pDNA loaded nanoparticles) are most likely located inside the cell. Moreover examining the figure 21 b and c simultaneously it can be observed that the nanoparticles are largely located in the perinuclear space or in the cell nucleus. This fact is of extreme importance since the cytoplasmatic route is also a major concern due

to the fact that it hinders the transport of the expression vector to the cell nucleus where it will ultimately be expressed. Apart from this, a thorough observation of both images regarding transfection, provides the idea that the nanoparticulated systems are not only able to transfect most of the cells but also they do it with greater efficiency when compared to the transfection reagent (figure 20d and 21d).

It therefore becomes clear that the developed nanocarriers composed by chitosan possess intrinsic properties needed for an efficient transfection and thus they can be used in the near future as novel carrier systems for cancer gene based therapies.

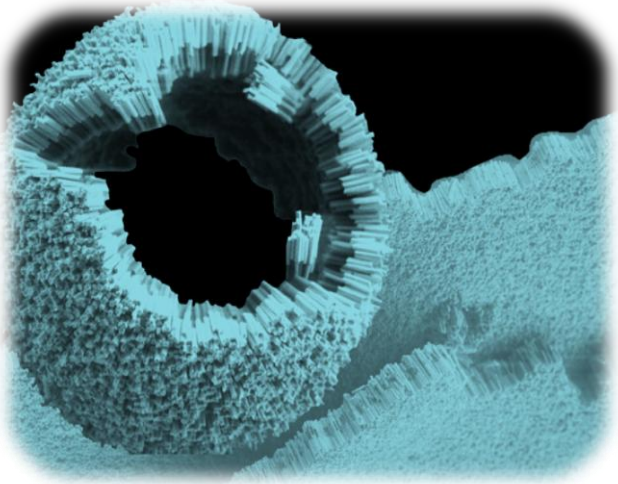

SECTION IV

CONCLUSIONS AND FUTURE PERSPECTIVES

The ever growing necessity of the outcome of most effective cancer therapeutics has promoted the cooperation of different areas of knowledge in an attempt to bring forth a promising alternative to the ever existing cancer treatments. Outstanding advances have been made so far, however such a complex disease as cancer needs a powerful suppressor therapy that dictates the extinction of the malignant phenotype for good.

This dissertation describes the development of an integrative non-viral therapeutic strategy from production to application. To accomplish this, the conjugation of plasmid production and purification techniques with the development of tailored nano-delivery systems was promoted. The production of pDNA expression vectors was prepared in *E.coli* bacterial extracts that produced the vector with high yield. Subsequently, several purification strategies based on affinity chromatography were applied to further purify the biologically active pDNA isoform. By changing the parameters that promoted the binding/elution of the pDNA isoforms in the affinity support the recovery of the sc isoform with high yield, stability and degree of purity, that reached 100%, was achieved. This purification strategy was a versatile and effective technique to be used in the purification of the expression vectors meant to cancer gene therapy applications.

Consequently the need for a specialized delivery system that could transpose the innumerous cellular barriers to transfection and alongside protect and deliver the sc pDNA isoform lead to the development and characterization of a group of different nanoparticulated systems formulated with a biocompatible biopolymer, namely chitosan. Several formulation parameters were addressed in order to determine the most suitable ones for transfection. The manipulation of the deacetilation degree of the polymer revealed itself has a crucial parameter in the overall synthesis of the nanoparticulated systems, since not only it lead to the formation of smaller nanoparticles, with size ranges between 113-197 nanometers but also to more defined and thermodynamically stable nanocapsules. Moreover the modulation of the deacetilation of the polymer originated a boost in encapsulation efficiency. Allied to this fact, surprisingly the encapsulation of the sc isoform was far greater that its oc counterpart, this finding was rather unexpected and certainly future encapsulation experiments and even simulations at the molecular dynamics level may shed some light into this issue.

Although a greater deacetilation degree of chitosan may seem beneficial, it is important to underline that the degradation kinetics of the nanoparticulated systems in the intracellular environment may greatly depend on this parameter and an equilibrium between size-protection-release is ought to be determined for future applications.

Nonetheless the nanoparticulated systems demonstrated that they could transpose the cellular barriers and enter the intracellular compartment and even the nucleus, as it

was observed in the transfection experiments. The majority of the cells were transfected, and when compared to its commercial counterpart the nanoparticulated systems showed a higher transfection efficiency.

However, it is important to denote that further experiments to tailor and bolster active targeting of these carriers may be attained. In fact, in the future these systems are so versatile that they can be functionalized with targeting molecules either on their surface or on the polymeric network. Apart from this, it is also important in a near future to address the feasibility of the action of wt-p53 since it may or may not lead to cancer annihilation. Further *in vivo* studies would also be fundamental to account for the capacity of the nanocapsules to evade and target the malignant cells within the host environment.

Overall the results of this thesis are promising foundations for the future development of a sustained, effective and widespread cancer therapy.

ANDERSON, W., KILLOS, L., SANDERS-HAIGH, L., KRETSCHMER, P. & DIACUMAKOS, E. 1980. Replication and expression of thymidine kinase and human globin genes microinjected into mouse fibroblasts. *Proceedings of the National Academy of Sciences,* 77**,** 5399.

BAO, H., LI, L. & ZHANG, H. 2008. Influence of cetyltrimethylammonium bromide on physicochemical properties and microstructures of chitosan-TPP nanoparticles in aqueous solutions. *Journal of colloid and interface science,* 328**,** 270-277.

BODE, A. M. & DONG, Z. 2009. Cancer prevention research then and now. *Nat Rev Cancer,* 9**,** 508-516.

BORCHARD, G. 2001. Chitosans for gene delivery. *Advanced Drug Delivery Reviews,* 52**,** 145-150.

BOUCHET, B., DE FROMENTEL, C., PUISIEUX, A. & GALMARINI, C. 2006. p53 as a target for anti-cancer drug development. *Critical reviews in oncology/hematology,* 58**,** 190-207.

CALVO, P., REMUNAN-LOPEZ, C., VILA-JATO, J. & ALONSO, M. 1998. Novel hydrophilic chitosan-polyethylene oxide nanoparticles as protein carriers. *Journal of Applied Polymer Science,* 63**,** 125-132.

CAO, S., CRIPPS, A. & WEI, M. 2009. New strategies for cancer gene therapy: Progress and opportunities. *Clinical and Experimental Pharmacology and Physiology,* 37**,** 108-114.

CARNES, A., HODGSON, C. & WILLIAMS, J. 2006. Inducible Escherichia coli fermentation for increased plasmid DNA production. *Biotechnology and applied biochemistry,* 45**,** 155-166.

CHEN, Y., WU, J. & HUANG, L. 2010. Nanoparticles Targeted With NGR Motif Deliver c-myc siRNA and Doxorubicin for Anticancer Therapy. *Molecular Therapy*.

CHENG, A., CHEN, W., FUHRMANN, C. & FRANKEL, A. 2003. Recognition of nucleic acid bases and base-pairs by hydrogen bonding to amino acid side-chains. *Journal of molecular biology,* 327**,** 781-796.

CHITHRANI, B. & CHAN, W. 2007. Elucidating the mechanism of cellular uptake and removal of protein-coated gold nanoparticles of different sizes and shapes. *Nano Lett,* 7**,** 1542-1550.

CHRISTOF VON KALLE, M., SCHMIDT, M. & FRANÇOISE LE DEIST, M. 2003. A Serious Adverse Event after Successful Gene Therapy for X-Linked Severe Combined Immunodeficiency. *New England Journal of Medicine,* 348**,** 255.

CSABA, N., KÖPING-HÖGGÅRD, M. & ALONSO, M. 2009. Ionically crosslinked chitosan/tripolyphosphate nanoparticles for oligonucleotide and plasmid DNA delivery. *International journal of pharmaceutics*.

DALL'ERA, J., MEACHAM, R., MILLS, J., KOUL, S., CARLSEN, S., MYERS, J. & KOUL, H. 2008. Vascular endothelial growth factor (VEGF) gene therapy using a nonviral gene delivery system improves erectile function in a diabetic rat model. *International journal of impotence research,* 20**,** 307-314.

DIOGO, M., QUEIROZ, J. & PRAZERES, D. 2005. Chromatography of plasmid DNA. *Journal of Chromatography A,* 1069**,** 3-22.

EVAN, G. & VOUSDEN, K. 2001. Proliferation, cell cycle and apoptosis in cancer. *Nature,* 411**,** 342-348.

FERRARI, M. 2005. Cancer nanotechnology: opportunities and challenges. *Nature Reviews Cancer,* 5**,** 161-171.

FERREIRA, G., MONTEIRO, G., PRAZERES, D. & CABRAL, J. 2000. Downstream processing of plasmid DNA for gene therapy and DNA vaccine applications. *Trends in Biotechnology,* 18**,** 380-388.

GAN, Q., WANG, T., COCHRANE, C. & MCCARRON, P. 2005. Modulation of surface charge, particle size and morphological properties of chitosan-TPP nanoparticles intended for gene delivery. *Colloids and Surfaces B: Biointerfaces,* 44**,** 65-73.

GILL, D., PRINGLE, I. & HYDE, S. 2009. Progress and prospects: the design and production of plasmid vectors. *Gene Therapy,* 16**,** 165-171.

GLOVER, D., LIPPS, H. & JANS, D. 2005. Towards safe, non-viral therapeutic gene expression in humans. *Nature Reviews Genetics,* 6**,** 299-310.

GRIGSBY, C. & LEONG, K. 2010. Balancing protection and release of DNA: tools to address a bottleneck of non-viral gene delivery. *Journal of the Royal Society Interface,* 7**,** S67.

GULLOTTI, E. & YEO, Y. 2009. Extracellularly activated nanocarriers: a new paradigm of tumor targeted drug delivery. *Molecular Pharmaceutics,* 6**,** 1041-1051.

HAHN, W. & WEINBERG, R. 2002. Modelling the molecular circuitry of cancer. *Nature Reviews Cancer,* 2**,** 331-341.

HANAHAN, D. & WEINBERG, R. A. 2000. The hallmarks of cancer. *Cell,* 100**,** 57-70.

HART, S. 2010. Multifunctional nanocomplexes for gene transfer and gene therapy. *Cell biology and toxicology,* 26**,** 69-81.

HAYASHI, Y., ULLNER, M. & LINSE, P. 2002. A Monte Carlo study of solutions of oppositely charged polyelectrolytes. *The Journal of Chemical Physics,* 116**,** 6836.

HEALTHCARE, G. *Affinity Chromatography Handbook: Principles and Methods*.

HEE-DONG, H., MANGALA, L., LEE, J., SHAHZAD, M., KIM, H., SHEN, D., NAM, E., MORA, E., STONE, R. & LU, C. 2010. Targeted Gene Silencing Using RGD-Labeled Chitosan Nanoparticles. *Clinical Cancer Research*.

HILLAIREAU, H. & COUVREUR, P. 2009. Nanocarriers' entry into the cell: relevance to drug delivery. *Cellular and molecular life sciences,* 66**,** 2873-2896.

HUANG, M., FONG, C., KHOR, E. & LIM, L. 2005. Transfection efficiency of chitosan vectors: effect of polymer molecular weight and degree of deacetylation. *Journal of Controlled Release,* 106**,** 391-406.

HUBER, B., RICHARDS, C. & KRENITSKY, T. 1991. Retroviral-mediated gene therapy for the treatment of hepatocellular carcinoma: an innovative approach for cancer therapy. *Proceedings of the National Academy of Sciences of the United States of America,* 88**,** 8039.

ISHII, T., OKAHATA, Y. & SATO, T. 2000. Facile preparation of a fluorescence-labeled plasmid. *Chemistry Letters,* 29**,** 386-387.

JANES, K., CALVO, P. & ALONSO, M. 2001. Polysaccharide colloidal particles as delivery systems for macromolecules. *Advanced Drug Delivery Reviews,* 47**,** 83-97.

JORDAN, C., GUZMAN, M. & NOBLE, M. 2006. Cancer stem cells. *The New England journal of medicine,* 355**,** 1253.

KIANG, T., WEN, J., LIM, H. & LEONG, K. 2004. The effect of the degree of chitosan deacetylation on the efficiency of gene transfection. *Biomaterials,* 25**,** 5293-5301.

KÖPING-HÖGGÅRD, M., MEL'NIKOVA, Y., VÅRUM, K., LINDMAN, B. & ARTURSSON, P. 2002. Relationship between the physical shape and the efficiency of oligomeric chitosan as a gene delivery system in vitro and in vivo. *The Journal of Gene Medicine,* 5**,** 130-141.

KÖPING-HÖGGÅRD, M., VÅRUM, K., ISSA, M., DANIELSEN, S., CHRISTENSEN, B., STOKKE, B. & ARTURSSON, P. 2004. Improved chitosan-mediated gene delivery based on easily dissociated chitosan polyplexes of highly defined chitosan oligomers. *Gene Therapy,* 11**,** 1441-1452.

LANE, D., CHEOK, C. & LAIN, S. 2010. p53-based Cancer Therapy. *Cold Spring Harbor perspectives in biology*.

LEDERBERG, J. 1963. Biological future of man. *Man and his Future***,** 263–73.

LIU, H. & GAO, C. 2008. Preparation and properties of ionically cross-linked chitosan nanoparticles. *Polymers for Advanced Technologies,* 20**,** 613-619.

LUO, J., SOLIMINI, N. & ELLEDGE, S. 2009. Principles of cancer therapy: oncogene and non-oncogene addiction. *Cell,* 136**,** 823-837.

LUSCOMBE, N., LASKOWSKI, R. & THORNTON, J. 2001. Amino acid-base interactions: a three-dimensional analysis of protein-DNA interactions at an atomic level. *Nucleic Acids Research,* 29**,** 2860.

MACDONALD, F., FORD, C. & CASSON, A. 2004. *Molecular biology of cancer*, BIOS Scientific Publ.

MAO, S., SUN, W. & KISSEL, T. 2009. Chitosan-based formulations for delivery of DNA and siRNA. *Advanced Drug Delivery Reviews*.

MELINO, G. & VAUX, D. 2010. Cell death. 1-12; 232-238; 253-255.

MENDELSOHN, J., HOWLEY, P., ISRAEL, M. & LIOTTA, L. 2008. *The molecular basis of cancer*, WB Saunders Philadelphia, PA.

MERLO, L. M. F., PEPPER, J. W., REID, B. J. & MALEY, C. C. 2006. Cancer as an evolutionary and ecological process. *Nat Rev Cancer,* 6**,** 924-935.

MONDAL, K. & GUPTA, M. 2006. The affinity concept in bioseparation: evolving paradigms and expanding range of applications. *Biomolecular engineering,* 23**,** 59-76.

MORILLE, M., PASSIRANI, C., VONARBOURG, A., CLAVREUL, A. & BENOIT, J. 2008. Progress in developing cationic vectors for non-viral systemic gene therapy against cancer. *Biomaterials,* 29**,** 3477-3496.

MOSQUEIRA, V., LEGRAND, P., GULIK, A., BOURDON, O., GREF, R., LABARRE, D. & BARRATT, G. 2001. Relationship between complement activation, cellular uptake and surface physicochemical aspects of novel PEG-modified nanocapsules. *Biomaterials,* 22**,** 2967-2979.

MÜLLER, W. 1986. Fractionation of DNA restriction fragments with ion-exchangers for high-performance liquid chromatography. *European Journal of Biochemistry,* 155**,** 203-212.

OLGA, V. C., ANTON, V. L., VALERY, G. A., INGA, C., EVERS, B. M., SHILLA, C., TODD, C. P. & RINAT, O. E. 2008. Composition of PLGA and PEI/DNA nanoparticles improves ultrasound-mediated gene delivery in solid tumors in vivo. *Cancer letters,* 261**,** 215-225.

OLIVIER, M., PETITJEAN, A., MARCEL, V., PETRE, A., MOUNAWAR, M., PLYMOTH, A., DE FROMENTEL, C. & HAINAUT, P. 2008. Recent advances in p53 research: an interdisciplinary perspective. *Cancer gene therapy,* 16**,** 1-12.

OW, D., NISSOM, P., PHILP, R., OH, S. & YAP, M. 2006. Global transcriptional analysis of metabolic burden due to plasmid maintenance in Escherichia coli DH5 [alpha] during batch fermentation. *Enzyme and Microbial Technology,* 39**,** 391-398.

PARK, T. G., JEONG, J. H. & KIM, S. W. 2006. Current status of polymeric gene delivery systems. *Advanced Drug Delivery Reviews,* 58**,** 467-486.

PARVEEN, S. & SAHOO, S. 2008. Polymeric nanoparticles for cancer therapy. *Journal of drug targeting,* 16**,** 108-123.

PATHAK, A., PATNAIK, S. & GUPTA, K. 2009. Recent trends in non-viral vector-mediated gene delivery. *Biotechnology Journal,* 4**,** 1559-1572.

PEER, D., KARP, J., HONG, S., FAROKHZAD, O., MARGALIT, R. & LANGER, R. 2007. Nanocarriers as an emerging platform for cancer therapy. *Nature nanotechnology,* 2**,** 751-760.

PELENGARIS, S. & KHAN, M. 2006. *The molecular biology of cancer*, Wiley-Blackwell.

PRABHA, S., ZHOU, W., PANYAM, J. & LABHASETWAR, V. 2002. Size-dependency of nanoparticle-mediated gene transfection: studies with fractionated nanoparticles. *International journal of pharmaceutics,* 244**,** 105-115.

QIAO, W., WANG, B., WANG, Y., YANG, L., ZHANG, Y. & SHAO, P. 2010. Cancer Therapy Based on Nanomaterials and Nanocarrier Systems.

QUAAK, S. G. L., DEN BERG, J. H. V., OOSTERHUIS, K., BEIJNEN, J. H., HAANEN, J. B. A. G. & NUIJEN, B. 2009. DNA tattoo vaccination: Effect on plasmid purity and transfection efficiency of different topoisoforms. *Journal of Controlled Release,* 139**,** 153-159.

REIS, C., NEUFELD, R., VILELA, S., RIBEIRO, A. & VEIGA, F. 2006. Review and current status of emulsion/dispersion technology using an internal gelation process for the design of alginate particles. *Journal of microencapsulation,* 23**,** 245-257.

REYA, T., MORRISON, S., CLARKE, M. & WEISSMAN, I. 2001. Stem cells, cancer, and cancer stem cells. *Nature,* 414**,** 105-111.

RICHARDI, J. 2009. One-dimensional assemblies of charged nanoparticles in water: A simulation study. *The Journal of Chemical Physics,* 130**,** 044701.

ROTHENBERG, M. & CLARKE, M. F. 2009. Cancer Stem Cells. *In:* ROBERT, L., JOHN, G., BRIGID, H., DOUGLAS, M., ROGER, P., THOMAS, E. D., JAMES, T. & SIR IAN, W. (eds.) *Essentials of Stem Cell Biology (Second Edition).* San Diego: Academic Press.

SCHLEEF, M. 2001. *Plasmids for therapy and vaccination*, Vch Verlagsgesellschaft Mbh.

SCHLICK, T., OLSON, W., WESTCOTT, T. & GREENBERG, J. 2004. On higher buckling transitions in supercoiled DNA. *Biopolymers,* 34**,** 565-597.

SEEMAN, N., ROSENBERG, J. & RICH, A. 1976. Sequence-specific recognition of double helical nucleic acids by proteins. *Proceedings of the National Academy of Sciences,* 73**,** 804.

SHAMLOU, P. 2003. Scaleable processes for the manufacture of therapeutic quantities of plasmid DNA. *Biotechnology and applied biochemistry,* 37**,** 207-218.

SOUSA, F., MATOS, T., PRAZERES, D. & QUEIROZ, J. 2007. Specific recognition of supercoiled plasmid DNA in arginine affinity chromatography. *Analytical biochemistry*.

SOUSA, F., PRAZERES, D. & QUEIROZ, J. 2008a. Affinity chromatography approaches to overcome the challenges of purifying plasmid DNA. *Trends in Biotechnology,* 26**,** 518-525.

SOUSA, F., PRAZERES, D. & QUEIROZ, J. 2008b. Improvement of transfection efficiency by using supercoiled plasmid DNA purified with arginine affinity chromatography. *The Journal of Gene Medicine,* 11**,** 79-88.

SOUSA, F., PRAZERES, D. & QUEIROZ, J. 2009. Binding and elution strategy for improved performance of arginine affinity chromatography in supercoiled plasmid DNA purification. *Biomedical Chromatography,* 23**,** 160-165.

SOUSA, F., PRAZERES, D. M. F. & QUEIROZ, J. A. 2008c. Affinity chromatography approaches to overcome the challenges of purifying plasmid DNA. *Trends in Biotechnology,* 26**,** 518-525.

STRATTON, M., CAMPBELL, P. & FUTREAL, P. 2009. The cancer genome. *Nature,* 458**,** 719-724.

TAN, S., KHOR, E., TAN, T. & WONG, S. 1998. The degree of deacetylation of chitosan: advocating the first derivative UV-spectrophotometry method of determination. *Talanta,* 45**,** 713-719.

TATUM, E. 1967. *Molecular biologym nucleic acids, and the future of medicine. In: Lyght, C.E., ed. Reflections on Research and the Future of Medicine,* New York, MacGraw-Hill.

TU, S., SUN, Y., CUI, J., ZOU, B., LIN, M., GU, Q., JIANG, S., KUNG, H., KORNELUK, R. & WONG, B. 2010. Tumor suppressor XIAP-Associated factor 1 (XAF1) cooperates with tumor necrosis factor-related apoptosis-inducing ligand to suppress colon cancer growth and trigger tumor regression. *Cancer*.

URTHALER, J., BUCHINGER, W. & NECINA, R. 2005. Improved downstream process for the production of plasmid DNA for gene therapy. *ACTA BIOCHIMICA POLONICA-ENGLISH EDITION-,* 52**,** 703.

VISVADER, J. & LINDEMAN, G. 2008. Cancer stem cells in solid tumours: accumulating evidence and unresolved questions. *Nature Reviews Cancer,* 8**,** 755-768.

VOGELSTEIN, B. & KINZLER, K. 2004. Cancer genes and the pathways they control. *Nature medicine,* 10**,** 789-799.

VOLOGODSKII, A., LEVENE, S., KLENIN, K., FRANK-KAMENETSKII, M. & COZZARELLI, N. 1992. Conformational and thermodynamic properties of supercoiled DNA. *Journal of molecular biology,* 227**,** 1224-1243.

VOUSDEN, K. & PRIVES, C. 2009. Blinded by the light: the growing complexity of p53. *Cell,* 137**,** 413-431.

WEINSTEIN, I. & JOE, A. 2006. Mechanisms of disease: oncogene addiction—a rationale for molecular targeting in cancer therapy. *Nature Clinical Practice Oncology,* 3**,** 448-457.

WILLIAMS, J., CARNES, A. & HODGSON, C. 2009. Plasmid DNA vaccine vector design: impact on efficacy, safety and upstream production. *Biotechnology advances,* 27**,** 353-370.

YANG, L., CHEN, L., ZENG, R., LI, C., QIAO, R., HU, L. & LI, Z. 2010. Synthesis, nanosizing and in vitro drug release of a novel anti-HIV polymeric prodrug: Chitosan-O-isopropyl-5'-O-d4T monophosphate conjugate. *Bioorganic & medicinal chemistry,* 18**,** 117-123.

ZAMBETTI, G. P. 2005. *The p53 Tumor Supressor Pathway and Cancer,* New York, Springer.

ZHANG, H., OH, M., ALLEN, C. & KUMACHEVA, E. 2004. Monodisperse chitosan nanoparticles for mucosal drug delivery. *Biomacromolecules,* 5**,** 2461-2468.

ZHAO, X., YU, S., WU, F., MAO, Z. & YU, C. 2006. Transfection of primary chondrocytes using chitosan-pEGFP nanoparticles. *Journal of Controlled Release,* 112**,** 223-228.

ZHIVOTOVSKY, B. & ORRENIUS, S. 2003. Defects in the apoptotic machinery of cancer cells: role in drug resistance. *Seminars in Cancer Biology,* 13**,** 125-134.

Appendices 1

PDF#39-1894: QM=Blank(B); d=Diffractometer; I=Film/Visual
Chitosan
(C6 H11 N O4)x
Radiation=CuKa Lambda=1.5418 Filter=Ni
Calibration= 2T=13.612-37.933 I/Ic(RIR)=
Ref: Ogawa, K., Hirano, S., Miyanishi, T., Yui, T., Watanabe, T.
Macromolecules, v17 p973 (1984)
Orthorhombic - (Unknown) Z=8 mp=
CELL: 8.24 x 16.48 x 10.39 <90.0 x 90.0 x 90.0>P.S=o?0 (?)
Density(c)=1.520 Density(m)=1.440 Mwt=0.00 Vol=1410.91
F(20)=1.7(0.178,66/0)
Ref: Ibid.

Strong Lines: 5.83/X 4.37/X 4.17/X 3.72/X 2.98/7 3.86/5 3.48/5 3.17/5 2.64/5 2.62/5

2-Theta	d(?)	I(f)	(h k l)	Theta	1/(2d)	2pi/d	n^2
13.612	6.5000	10.0	(0 2 1)	6.806	0.0769	0.9666	
13.612	6.5000	10.0	(1 0 1)	6.806	0.0769	0.9666	
15.185	5.8300	100.0	(1 2 0)	7.592	0.0858	1.0777	
16.971	5.2200	10.0	(0 0 2)	8.486	0.0958	1.2037	
17.688	5.0100	10.0	(1 2 1)	8.844	0.0998	1.2541	
20.305	4.3700	100.0	(0 2 2)	10.152	0.1144	1.4378	
20.305	4.3700	100.0	(1 0 2)	10.152	0.1144	1.4378	
21.290	4.1700	100.0	(2 0 0)	10.645	0.1199	1.5068	
21.290	4.1700	100.0	(0 4 0)	10.645	0.1199	1.5068	
23.022	3.8600	50.0	(1 2 2)	11.511	0.1295	1.6278	
23.901	3.7200	100.0	(1 4 0)	11.950	0.1344	1.6890	
23.901	3.7200	100.0	(2 2 0)	11.950	0.1344	1.6890	
25.576	3.4800	50.0	(1 4 1)	12.788	0.1437	1.8055	
25.576	3.4800	50.0	(2 2 1)	12.788	0.1437	1.8055	
26.188	3.4000	10.0	(0 1 3)	13.094	0.1471	1.8480	
27.946	3.1900	20.0	(2 0 2)	13.973	0.1567	1.9697	
27.946	3.1900	20.0	(0 4 2)	13.973	0.1567	1.9697	
28.126	3.1700	50.0	(0 2 3)	14.063	0.1577	1.9821	
28.126	3.1700	50.0	(1 0 3)	14.063	0.1577	1.9821	
29.960	2.9800	70.0	(1 2 3)	14.980	0.1678	2.1085	
31.936	2.8000	20.0	(2 4 1)	15.968	0.1786	2.2440	
33.928	2.6400	50.0	(3 2 0)	16.964	0.1894	2.3800	
33.928	2.6400	50.0	(1 5 2)	16.964	0.1894	2.3800	
34.195	2.6200	50.0	(3 0 1)	17.098	0.1908	2.3982	
34.195	2.6200	50.0	(0 6 1)	17.098	0.1908	2.3982	
35.307	2.5400	20.0	(2 4 2)	17.654	0.1969	2.4737	
35.743	2.5100	20.0	(1 4 3)	17.872	0.1992	2.5033	
35.743	2.5100	20.0	(2 2 3)	17.872	0.1992	2.5033	
36.342	2.4700	50.0	(0 2 4)	18.171	0.2024	2.5438	
36.342	2.4700	50.0	(1 0 4)	18.171	0.2024	2.5438	
37.933	2.3700	10.0	(0 3 4)	18.966	0.2110	2.6511	
37.933	2.3700	10.0	(1 2 4)	18.966	0.2110	2.6511	